CHARACTERIZATION OF INTRAVENOUS IMMUNOGLOBULIN-MEDIATED FUNCTIONAL CHANGES IN INNATE IMMUNE CELLS

A THESIS SUBMITTED TO
THE GRADUATE SCHOOL OF NATURAL AND APPLIED SCIENCES
OF
MIDDLE EAST TECHNICAL UNIVERSITY

BY

BÜŞRANUR GEÇKİN

IN PARTIAL FULFILLMENT OF THE REQUIREMENTS
FOR
THE DEGREE OF MASTER OF SCIENCE
IN
BIOLOGY

SEPTEMBER 2019

Approval of the thesis:

CHARACTERIZATION OF INTRAVENOUS IMMUNOGLOBULIN-MEDIATED FUNCTIONAL CHANGES IN INNATE IMMUNE CELLS

submitted by **BÜŞRANUR GEÇKİN** in partial fulfillment of the requirements for the degree of **Master of Science in Biology Department, Middle East Technical University** by,

Prof. Dr. Halil Kalıpçılar
Dean, Graduate School of **Natural and Applied Sciences** _____

Prof. Dr. Ayşegül Gözen
Head of Department, **Biology** _____

Prof. Dr. Mayda Gürsel
Supervisor, **Biology, METU** _____

Examining Committee Members:

Prof. Dr. Can Naci Kocabaş
Internal Medical Sciences, Muğla Sıtkı Koçman University _____

Prof. Dr. Mayda Gürsel
Biology, METU _____

Assoc. Prof. Dr. Çağdaş Devrim Son
Biological Sciences, METU _____

Date: 06.09.2019

I hereby declare that all information in this document has been obtained and presented in accordance with academic rules and ethical conduct. I also declare that, as required by these rules and conduct, I have fully cited and referenced all material and results that are not original to this work.

Name, Surname: Büşranur Geçkin

Signature:

ABSTRACT

CHARACTERIZATION OF INTRAVENOUS IMMUNOGLOBULIN-MEDIATED FUNCTIONAL CHANGES IN INNATE IMMUNE CELLS

Geçkin, Büşranur
Master of Science, Biology
Supervisor: Prof. Dr. Mayda Gürsel

September 2019, 89 pages

Intravenous Immunoglobulin (IVIg) is mainly composed of IgG derived from pooled plasma of healthy individuals and used to treat variety of immune diseases. Low dose administration can activate the immune system in case of immunodeficiencies, while high doses suppress immune responses in autoimmune/autoinflammatory conditions. The mechanisms underlying this disparate effect is poorly understood. Herein, we examined the effects of IVIg treatment on the functionality of specific innate immune cell populations in the absence or presence of various immune activators and investigated whether IVIg can induce trained immunity or not.

In this context, we examined the effects of IVIg on neutrophils. Our results showed that high dose of IVIg suppresses PMA-induced NET-formation and TLR7/8 ligand-mediated IL-8-production. Conversely, in healthy neutrophils, IVIg stimulated ROS-production, NET-formation and IL-8-production in response to bacterial and fungal ligands. Similarly, we analysed how IVIg treatment altered responses to TLR-mediated immune activation in IVIg co-treated hPBMCs. Results showed that IVIg synergized with most TLR-mediated signalling pathways at lower doses but demonstrated a suppressive effect at the highest dose, especially when co-administered with endosomal TLR agonists.

In the second part of the thesis, we explored the possible role of IVIg in inducing trained immunity in monocytes. For this purpose, we trained THP1-Dual cells with IVIg parallel to other reprogramming controls (LPS and PGN). Functional assays based on ROS-production, secondary pro-inflammatory cytokine secretion and NF-κB activation showed that IVIg is a potent inducer of trained immunity, capable of increasing recall responses to bacterial, fungal and/or viral ligands.

Keywords: IVIg, immunodeficiencies, autoimmunity, neutrophil functions, trained immunity

ÖZ

DOĞAL BAĞIŞIKLIK HÜCRELERİNDE İNTRAVENÖZ İMMÜNGLOBULİN-ARACILI FONKSİYONEL DEĞİŞİMLERİN KARAKTERİZASYONU

Geçkin, Büşranur
Yüksek Lisans, Biyoloji
Tez Danışmanı: Prof. Dr. Mayda Gürsel

Eylül 2019, 89 sayfa

İntravenöz İmmünglobulin (İVİg) sağlıklı bireylerin plazmalarından elde edilen IgG'den oluşmakta ve çeşitli immün hastalıkları tedavi etmekte kullanılmaktadır. İmmün yetmezliklerde düşük doz kullanımı immün sistemi aktive edebilirken, otoimmün/otoenflammatuvar durumlarda yüksek dozlar immün yanıtları baskılamaktadır. Bu farklı etkisinin altında yatan mekanizmalar yeterince anlaşılamamıştır. Bu noktada, çeşitli immün aktivatörlerinin varlığında ve yokluğunda İVİg'in spesifik doğal bağışıklık hücrelerinin fonksiyonları üzerine etkilerini inceledik ve İVİg'in eğitilmiş immüniteyi tetikleyip tetikleyemeyeceğini araştırdık.

Bu bağlamda, İVİg'in nötrofiller üzerine etkilerini inceledik. Sonuçlarımız, yüksek doz İVİg'in PMA-aracılı NET oluşumunu ve TLR7/8 ligand-aracılı IL-8 üretimini baskıladığını göstermiştir. Bunun aksine, İVİg sağlıklı nötrofillerde bakteriyel ve mantarsı ligandlarına karşı ROS üretimini, NET oluşumunu ve IL-8 üretimini uyarmıştır. Benzer bir şekilde, İVİg uygulamasının insan PBMClerinde TLR-aracılı immün aktivasyonunu nasıl değiştirdiğini analiz ettik. Sonuçlar, İVİg'in birçok TLR-aracılı sinyal yolaklarıyla düşük dozda sinerjik çalıştığını fakat en yüksek dozda, özellikle endozomal TLR agonistleriyle birlikte uygulandığında, baskılayıcı olduğunu göstermiştir.

Tezin ikinci kısmında, İVİg'in monositlerde eğitilmiş immüniteyi tetiklemede muhtemel rolünü tetkik ettik. Bu amaçla, THP1-Dual hücrelerini İVİg ve beraberinde diğer yeniden programlama kontrolleriyle (LPS ve PGN) eğittik. ROS üretimi, ikincil pro-enflammatuvar sitokin salınımı ve NF-κB aktivasyonu bazındaki fonksiyonel çalışmalar, İVİg'in potansiyel eğitilmiş immünite tetikleyicisi olduğunu ve bakteriyel, mantarsı ve/veya viral ligandlara karşı anımsatıcı yanıtları artırabilme kapasitesine sahip olduğunu göstermiştir.

Anahtar Kelimeler: İVİg, immün yetmezlikler, otoimmünite, nötrofil fonksiyonları, eğitilmiş immünite

To my little sister

ACKNOWLEDGEMENTS

First and the most, I would like to express my gratitude to my dear supervisor Prof. Dr. Mayda Gürsel. She is the kindest and wisest guide I could have ever asked for and I cannot explain how lucky I am to be her student. Her scientific enthusiasm and excitement always gave me courage to improve as a researcher. She is more than a supervisor to me and she will always be.

I also want to thank the members of thesis examining committee; Prof. Dr. Can Naci Kocabaş and Assoc. Prof. Dr. Çağdaş Devrim Son for their participation, suggestions and comments.

I would like to thank my lab mates for being a family more than lab mates and supporting me whenever I needed. First, I want to say “thank you” to Başak Kayaoğlu as both my friend and mentor, teaching me everything and helping me even with the littlest problems. I would like to thank Naz Yılmaz for being a ball of sunshine and lifting my mood whenever I feel down and gloomy for whatever reason. I also want to say that I love our chemistry when I work with Başak and Naz as PID group, learning and getting tired together will always remain as precious memories. I also would like to thank İhsan Cihan Ayanoğlu for his endless patience both when teaching me things and advising me as a big brother. His knowledge on almost everything amazes me every time even if I know him for a quiet long time. He also helped me when I write my thesis even while he was writing his own. Also, I would like to say that I appreciate all the support and help that I received from Emre Mert İpekoğlu as he also gave me a hand when I needed in this thesis writing period. I would like to thank the other Emre (Dünüroğlu) firstly for being my adoptive brother and all the good moments we shared while working in the lab.

Also, I would like to thank my dear friend and new lab mate İlayda Baydemir for her tremendous support whenever and wherever I needed. She was always there when I seek for a helping hand. Here I am saying, I love you sis.

I would like to thank my other lab members; Hatice Asena Şanlı, Yağmur Aydın, İsmail Cem Yılmaz and our former member Esin Alpdündar Bulut for all the times they brought a smile to my face even with the littlest things.

I also want to thank Prof. Dr. İhsan Gürsel for always look after me and to thank IG group members, especially Göksu Gökberk Kaya for being a sweet friend.

Last but not the least, I would like to thank my father for being supportive to what I want to do in this life even when he does not really want and my little sister for being my strength to carry on and do better things.

TABLE OF CONTENTS

LIST OF TABLES

TABLES

LIST OF FIGURES

FIGURES

LIST OF ABBREVIATIONS

ACK	Ammonium-Chloride-Potassium
AIM2	Absent in Melanoma 2
ALP	Alkaline Phosphatase
BCG	Bacillus Calmette-Guérin
BSA	Bovine Serum Albumin
CD	Cluster of Differentiation
cGAS	Cyclic GMP-AMP Synthase
CLR	C-type Lectin Receptor
CpG	Unmethylated Cytosine-Phosphate-Guanosine Motifs
DAMP	Damage Associated Molecular Pattern
DC	Dendritic Cell
DHR123	Dihydrorhodamine 123
DPBS	Dulbecco's Phosphate-Buffered Saline
EDTA	Ethylenediaminetetraacetic Acid
ELISA	Enzyme Linked Immunosorbent Assay
FBS	Fetal Bovine Serum
Fab	Fragment, Antigen-Binding
Fc	Fragment, Crystallizable
FcγR	Fc-gamma Receptor
FSC	Forward Scatter

HEPES	4-(2-hydroxyethyl)-1-Piperazineethanesulfonic Acid)
HKCA	Heat Killed *Candida albicans*
hPBMC	Human Peripheral Blood Mononuclear Cells
HRP	Horseradish Peroxidase
IFN	Interferon
Ig	Immunoglobulin
IL	Interleukin
IP-10	Interferon Gamma-Induced Protein 10
IRF	Interferon Regulatory Factor
IVIg	Intravenous Immunoglobulin
LPS	Lipopolysaccharide
MAPK	Mitogen-Activated Protein Kinase
MFI	Mean Fluorescent Intensity
MHC	Major Histocompatibility Complex
MyD88	Myleoid Differentiation Factor 88
NET	Neutrophil Extracellular Trap
NF-κB	Nuclear Factor kappa B
NK	Natural Killer
NLR	Nucleotide-Binding Oligomerization Domain like Receptor
NOD	Nucleotide-Binding and Oligomerization Domain
ODN	Oligodeoxynucleotide
PAMP	Pathogen Associated Molecular Pattern

PBS	Phosphate Buffer Saline
pDC	Plasmacytoid Dendritic Cell
PGN	Peptidoglycan
PKC	Protein Kinase C
PMA	Phorbol 1-Myristate 13-Acetate
PMN	Polymorphonuclear
PNPP	Para-Nitrophenyl Pyro-Phosphate
polyI:C	Polyriboinosinic Polyribocytidylic Acid
PYHIN	Pyrin and Hin
PRR	Pattern Recognition Receptor
R848	Resiquimod
RIG-I	Retinoic Acid-Induced Gene-I
RLR	Retinoic Acid-Induced Gene-I like Receptor
ROS	Reactive Oxygen Species
RPMI	Roswell Park Memorial Institute
SEAP	Secreted Embryonic Alkaline Phosphatase
SSC	Side Scatter
STING	Stimulator of Interferon Genes
Syk	Spleen Tyrosine Kinase
THP1	Tohoku Hospital Pediatrics 1
TLR	Toll-Like Receptor
TNF	Tumor Necrosis Factor

CHAPTER 1

INTRODUCTION

1.1. Immune System

The immune system consists of a complex network of cells, tissues, organs, and effector molecules that collectively constitute body's defense system against pathogens. This integrated system of host defense is subdivided into two arms: innate and adaptive immunity. Innate immunity has the capacity to react to a wide range of pathogens and is characterized by short-term, immediate responses which are not specific to individual pathogens. Cells of the innate immune system act first-line in defense and include dendritic cells, polymorphonuclear phagocytes (neutrophils, eosinophils and basophils), monocytes, macrophages, mast cells, natural killer (NK) cells, NK-T cells and innate lymphoid cells. The response generated by innate immune cells that are triggered either by pathogen associated molecular patterns (PAMPs) or damage associated molecular patterns (DAMPs) that are recognized through the pattern recognition receptors (PRRs) expressed by these cells (Kawai & Akira, 2009).

Conversely, adaptive immunity develops in response to a specific pathogen. This type of immunity has immunological memory which enables establishment of more effective recall responses upon re-infection and provides long-term protection. Adaptive immunity is directed against antigens and is highly specific. Antigens are recognized by distinct receptors on T and B cells which are generated by somatic gene rearrangements (Han et al., 2007). Antigen recognition through B cell receptors trigger antibody production to generate humoral immunity. Antigen presenting cells (APCs) take part in the process to present peptides derived from antigens in the context of MHC Class I or Class II to cytotoxic T cells and helper T cells, respectively. Antigen-activated T and B cells proliferate and differentiate into effector cells. Specifically, B

cells differentiate into antibody secreting plasma cells, whereas activated cytotoxic T cells recognize and kill virally infected cells. Depending on the type of pathogen exposed and the nature of ensuing innate immune responses, antigen experienced helper T cells differentiate into distinct subclasses and provide help to other immune cells.

1.1.1. Immune Cells

Leukocytes, or white blood cells, originate from hematopoietic stem cells in the bone marrow. Hematopoietic stem cells differentiate into lymphoid or myeloid progenitors. The common lymphoid progenitors generate B, T and NK cells, whereas the myeloid progenitors give rise to monocytes, granulocytes (neutrophils, eosinophils and basophils) and dendritic cells (DCs).

Neutrophils

Neutrophils are classified as granulocytes or polymorphonuclear leukocytes, owing to their dense cytoplasm granules and their oddly shaped nuclei. They are the most abundant white blood cell type in the circulation and are short-lived. Although neutrophils are highly abundant in blood, they are recruited into tissues only in the case of infection and/or inflammation. For such an event to happen, there must be signals coming from the injured tissue in the form of cytokines and chemokines. In infected tissues, neutrophils function to clear pathogens through their specialized effector functions, including phagocytosis, Reactive Oxygen Species (ROS) production, and/or NETosis. Neutrophils take up the pathogens and produce a variety of toxic ROS that collectively exert bactericidal activity. Depending on the pathogen type and/or the nature of the inflammatory environment, these cells can also generate neutrophil extracellular traps (NETs) to prevent spread of infection. NETs are defined as extruded chromatin fibers carrying granule-derived antimicrobial peptides and enzymes. This characteristic form of cell death is known as NETosis (Kaplan & Radic, 2012).

Monocytes, Macrophages and Dendritic Cells

Peripheral blood mononuclear cells (PBMCs) are generally defined as the fraction of blood enriched in monocytes, dendritic cells and lymphocytes (T, B and NK cells) following their separation using density gradient centrifugation. These cells have round shape of nuclei and they are important for cytokine response, especially, monocytes produce pro-inflammatory cytokines and dendritic cells are important for type I interferon generation (Turner, Nedjai, Hurst, & Pennington, 2014).

Monocytes are the largest leukocyte type in blood and are phagocytic in nature. These cells circulate in blood until signals from inflamed tissues recruit them to the site of injury. Once they enter into the tissue, they maturate into macrophages. Both monocytes and macrophages are capable of engulfing pathogens, yet macrophages are the ones mainly performing this task since most of the infections are seen in tissues. In addition to their phagocytic activities, monocytes and macrophages express a wide range of PRRs so that they can recognize and respond to pathogens and other danger signals. Macrophages constantly sample their environment and can function as APCs (Monie, 2017). Another important role of macrophages is that they act like scavengers and clear cell debris and dead cells, thereby maintain homeostasis (Murphy, 2012). Monocytes and macrophages contribute to inflammation through production of pro-inflammatory cytokines such as TNFα, IL-6 and IL-1β (Mirjam & Broos, 2019).

Dendritic cells (DCs) mediate innate immune responses and are pivotal in triggering adaptive immune responses as they are considered as excellent antigen presenters. There are three major types of DCs. Two of them are considered as conventional DCs (cDCs which are CD1c+ and CD141+) and plasmacytoid DCs (pDCs). CD1c+ DCs are capable of secreting interleukin-12 (IL-12), tumor necrosis factor α (TNFα), IL-10 and IL-8 in response to several types of PAMPs, whereas CD141+ DCs express high levels of TLR3, secrete IL-12p70 and IFN-β, and induce T helper 1 cell responses. Aside from cDCs, pDCs are the most potent type I interferon (IFN) producers in response to viral infections when compared to other cell types. They

express high levels of TLR7 and TLR9 which makes them remarkably suited to respond to viral and self-nucleic acids (Shang et al., 2017).

1.1.2. Innate Immunity and Pattern Recognition Receptors (PRRs)

The cells of innate immune system express a wide range of PRRs on their cell surface, in endosomes or in the cytoplasm, which collectively enable the recognition of pathogen and/or damage associated molecular signatures to initiate an inflammatory response (Janeway, 1992). Based on their protein domain homologies, PRRs can be classified into distinct families consisting of Toll-Like Receptors (TLRs), C-type Lectin Receptors (CLRs), Nucleotide-binding Oligomerization Domain (NOD)-Like Receptors (NLRs), RIG-I-Like Receptors (RLRs), PYHIN (Pyrin and HIN) family receptors and cytosolic dsDNA/cyclic di-nucleotide sensors (Broz & Monack, 2013).

TLRs are type I transmembrane proteins that possess leucine-rich repeats on their ectodomains and are expressed in many cell types including, macrophages, neutrophils and DCs (Pasare & Medzhitov, 2005). There are 10 TLRs defined in humans (TLR1-TLR10) and 12 in mouse (TLR1-9 and TLR11-TLR13). Depending on their function, TLRs are expressed either on the cell surface or within intracellular compartments such as endosomes. In humans, TLR1, 2, 4, 5, 6 and 10 are found on the cell surface whereas TLR3, 7, 8 and 9 are found in endosomes (Dowling & Mansell, 2016; Kawasaki & Kawai, 2014). TLRs are capable of recognizing proteins, lipids, lipoproteins and nucleic acids derived from bacteria, viruses, parasites and fungi. For instance, cell surface TLRs (e.g. TLR4 recognizes lipopolysaccharide (LPS); outer membrane component of gram-negative bacteria) are responsible for recognition of microbial cell wall components whereas, endosomal TLRs (TLR7/8 recognizes dsRNA) recognize nucleic acids derived from microbes (Kawai & Akira, 2010). Ligand recognition by TLRs initiates MyD88 and/or TRIF-mediated signaling, resulting in activation of NF-κB and/or IRF3/IRF7 transcription factors which mediate

expression of either pro-inflammatory cytokine or type I interferon production, respectively (Wu & Chen, 2014).

Table 1.1. *TLRs and their ligands*

(Adapted from (Savva & Roger, 2013))

Receptor	Sub-cellular expression	Adaptor molecule	Ligand	Origin
TLR1 (with TLR2)	Cell membrane	MyD88/TIRAP	Triacyl lipopeptides Soluble factors	Bacteria, mycobacteria *Neisseria meningitidis*
TLR2 (with TLR1 or TLR6)	Cell membrane	MyD88/TIRAP	Lipoproteins, lipopeptides Lipoteichoic acid Peptidoglycan Lipoarabinomannan Phenol-soluble modulin, porins Atypical LPS Glycoinositolphospholipids, glycolipids Beta-glucan, mannan Core and NS3 proteins, dUTPase, glycoproteins HSP70	Various pathogens Gram-positive bacteria Bacteria Mycobacteria *Staphylococcus epidermidis, Neisseria* *Leptospira interrogans, Porphyromonas gingivalis* *Trypanozoma, Toxoplasma, Plasmodium* Fungi Hepatitis virus, Epstein–Barr virus, Cytomegalovirus Host
TLR3	Endolysosomal	TRIF	Double-stranded RNA	Viruses
TLR4	Cell membrane and endolysosomal	MyD88/TIRAP, TRIF/TRAM	LPS O-linked mannan Taxol Fusion and envelope protein HSP60 HMGB1, HSP70, fibronectin, fibrinogen	Gram-negative bacteria Fungi Plants Respiratory syncytial virus, mouse mammary tumor virus *Chlamydia pneumoniae* Host
TLR5	Cell membrane	MyD88	Flagellin	Flagellated bacteria
TLR6 (with TLR2)	Cell membrane	MyD88/TIRAP	Diacyl lipopeptides, lipoteichoic acid, β-glucan	*Mycoplasma*, Gram-positive bacteria, fungi
TLR7	Endolysosomal	MyD88	Single-stranded RNA Imidazoquinoline, loxoribine, bropirimine	Viruses, bacteria Synthetic compounds
TLR8	Endolysosomal	MyD88	Single-stranded RNA Imidazoquinoline	Viruses, bacteria Synthetic compounds
TLR9	Endolysosomal	MyD88	CpG-containing DNA Homozoin	Bacteria, viruses, fungi *Plasmodium falciparum*
TLR10 (±TLR1 or TLR2)	Cell membrane	MyD88	Lipopeptides (prediction)	
TLR11	Endolysosomal	MyD88	Flagellin	Flagellated bacteria
TLR12	Endolysosomal	MyD88	Profilin	Apicomplexan parasites
TLR13	Endolysosomal	MyD88	23S RNA	Bacteria

Another transmembrane protein family of PRRs include the CLRs that recognize pathogen-derived carbohydrates (Hoving, Wilson, & Brown, 2014). Based on their

signaling potential, CLRs are divided into three groups, consisting of CLRs that contain Immunoreceptor Tyrosine-based Activation Motif (ITAM) domain and Syk-coupled activation, inhibitory CLRs with Immunoreceptor Tyrosine-based Inhibition Motif (ITIM) domains and CLRs a group of CLRs lacking typical signaling motifs such as DC-SIGN (Sancho & Reis e Sousa, 2012). These receptors play a critical role in defense against fungal ligands. For example, β-glucans (especially β-1,3-glucans) are recognized by Dectin-1, whereas mannans and mannoproteins are recognized by macrophage Mannose Receptor (MR), Macrophage-inducible C-type Lectin (Mincle), Dectin-2&3 (recognize specifically α-mannans) and Dendritic Cell-specific ICAM3-grabbing non-integrin (DC-SIGN) (Tang, Lin, Langdon, Tao, & Zhang, 2018).

NLR family of pattern recognition receptors such as NOD1 and NOD2 reside in the cytoplasm and specifically recognize fragments of bacterial peptidoglycan to activate NF-κB-dependent pro-inflammatory cytokine production. Other members such as the NLRP3 recognize various PAMPs or DAMPs and form distinct inflammasomes that play essential roles in immune protection against bacterial, viral, fungal and parasitic infections (Broz & Monack, 2013).

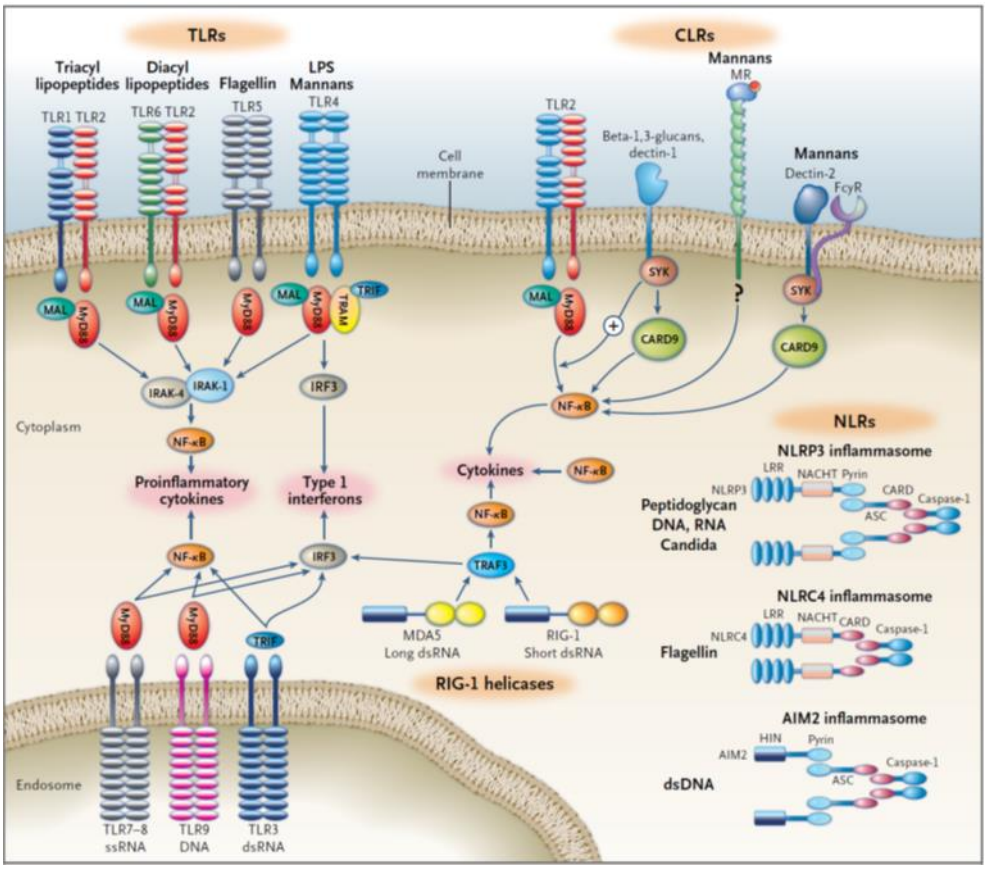

Figure 1.1. Membrane-bound and cytosolic PRRs, their ligands and signaling pathways

(Adapted from (Netea & Van Der Meer, 2011))

Nucleic Acid Sensors

Endosomal recognition of RNA occurs through TLR7/8 (dsRNA) and TLR3 (ssRNA), which recruit the adaptor proteins Myeloid Differentiation Primary Response Protein (MyD88) and TIR domain-containing Adaptor Inducing Interferon β (TRIF), respectively, leading to IRF3/IRF7-dependent type I IFN production (Roers, Hiller, & Hornung, 2016; Schlee & Hartmann, 2016). Apart from endosomal recognition, RNA can also be detected by certain other sensors found in the cytosol. Cytosolic RNA is recognized by RLR family members RIG-I and MDA5, which sense short dsRNA with 5' triphosphate caps and long dsRNA molecules, respectively. Both sensors

interact with an adaptor protein known as Mitochondrial Antiviral Signaling Protein (MAVS) to initiate downstream IFN signaling (Reikine, Nguyen, & Modis, 2014).

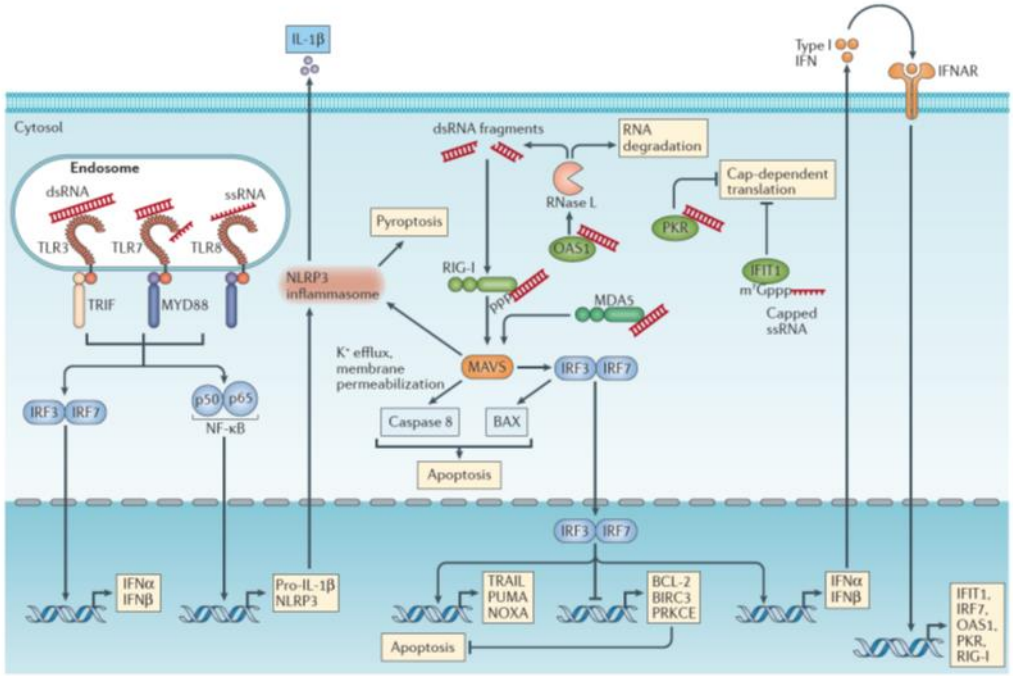

Figure 1.2. RNA sensing pathways

(Adapted from (Schlee & Hartmann, 2016))

Similar to RNA, there are many receptors and sensors that recognize DNA. TLR9 is specialized to recognize unmethylated CpG-rich DNA in endosomes. For example, synthetic oligonucleotides enriched in CpG dinucleotides (ODNs) are recognized by TLR9 and initiate MyD88-dependent signaling. However, outcome of this signaling can be differ depending on the class of CpG ODN. Specifically, D class (also called A class) CpG ODN supports IRF7-dependent type I interferon production, whereas K class (also called B class) ODN triggers NF-κB-dependent pro-inflammatory cytokine release upon stimulation (Gursel, Gursel, Mostowski, & Klinman, 2006). Although K

ODNs trigger short-term increase in IFNα/β responses in pDCs, D ODNs show persistent stimulation of IFNα/β production (Steinhagen et al., 2012).

For cytosolic DNA, various sensors have been defined, including Absent in Melanoma 2 (AIM2) and IFN-γ Inducible Protein 16 (IFI16) as members of PHYIN family which triggers inflammasome activation (Roers et al., 2016). Furthermore, RNA polymerase III can act as a cytosolic DNA sensor by transcribing AT-rich DNA into 5' triphosphorylated RNA which subsequently activates RIG-I-dependent signaling. Apart from these sensors, the central cytosolic dsDNA sensor has recently been defined to involve the enzyme cyclic GMP-AMP synthetase (cGAS) (Sun, Wu, Du, Chen, & Chen, 2013; Wu et al., 2013). cGAS-mediated recognition of cytosolic dsDNA results in generation of a secondary messenger 2'3'-cGAMP (cyclic [G(2',5')pA(3',5')p]), which then binds to the Stimulator of Interferon Genes (STING). Binding of 2'3'-cGAMP to STING activates it and leads to recruitment of TBK1 and IRF3. Signaling through the cGAS/STING/TBK1/IRF3 axis culminates in type I IFN production as a result of translocation of active phosphorylated IRF3 dimers into the nucleus (Tao, Zhou, & Jiang, 2016).

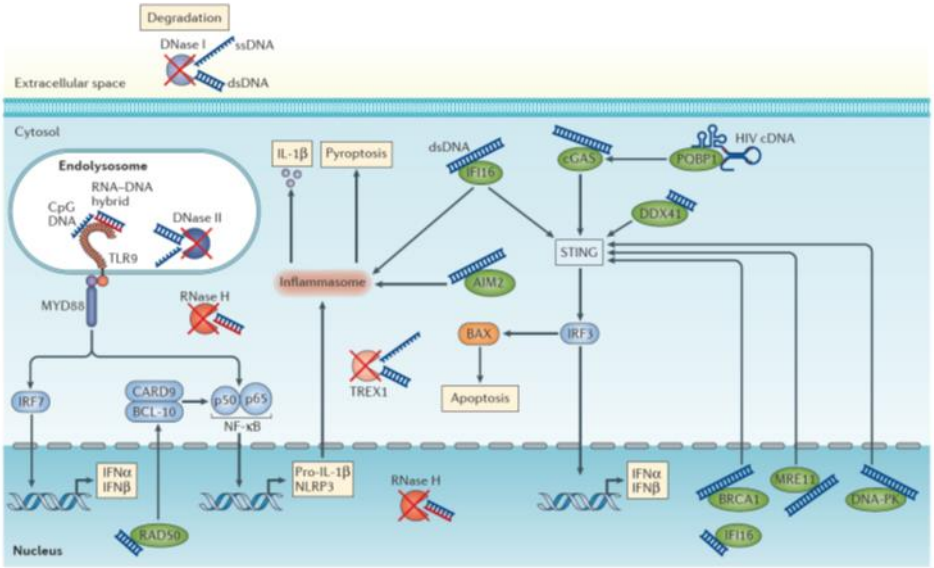

Figure 1.3. DNA sensing pathways

(Adapted from (Schlee & Hartmann, 2016)).

1.2. Immunoglobulins

In 1890, Emil von Behring (1854-1917) and Shibasaburo Kitasato (1852-1931) injected heat-treated diphtheria toxin to guinea pigs and showed that immunized animals were resistant to lethal doses of the bacteria. They also demonstrated that an animal was cured from diphtheria when injected with serum of an immunized animal. They reported that a substance in immunized sera was responsible for this immuneprotection and immunotherapy (Behring & Kitasato, 1890; Kantha, 1991). They named this agent as antitoxin, which was named as antibody later on. Emil von Behring was awarded with the first Nobel Prize in Medicine for his work on serum therapy in 1901 ("The Nobel Prize in Physiology or Medicine 1901 - NobelPrize.org," n.d.).

Then, in 1939, it was demonstrated that the antibody activity corresponded to the γ-globulin fraction of serum proteins following electrophoretic separation. Hence, antibodies were also called as γ-globulins (Tiselius & Kabat, 1939). Later on, it was demonstrated that molecules other than antibodies could be found in the γ-globulin fraction. Therefore, the term immunoglobulin (Ig) was adopted to discriminate antibodies from other molecules that are present in the γ-fraction (Fahey, 1965).

Immunoglobulins (Igs) are glycoprotein molecules consisting of two light (~23kDa) and two heavy chains (50-70 kDa), both of which contain one N-terminal variable domain and one or more (usually three) C-terminal constant domains. These chains are held together with inter-chain disulfide bonds and also intra-chain disulfide bonds are present within each polypeptide chain (Williams & Barclay, 1988). Antibodies include a hinge region between the first and second constant domains of the heavy chain, which provides flexibility to the molecule. Hinge region provides the classical 'Y' shape to antibody molecules (Brekke, Michaelsen, & Sandlie, 1995).

Earliest studies to elucidate the structure and functions of immunoglobulins were conducted by proteolytic cleavage using the enzyme papain. Papain digests Igs at hinge region below the inter-chain disulfide bond and produces three fragments. Two

of these fragments are identical and are composed of combined light chain and some portion of the heavy chain. These fragments were named as Fab fragments due to their ability to bind to an antigen. The other fragment was the remaining heavy chain portion and was named as the Fc fragment because it was easily crystallized. Fc fragment is not capable of recognizing antigens but it is responsible for the effector function of immunoglobulins (Porter, 1973). Rodney R. Porter and Gerald M. Edelman were jointly awarded with the Nobel Prize in Physiology or Medicine for their pioneering work on the chemical structure of antibodies in 1972 ("The Nobel Prize in Physiology or Medicine 1972," n.d.).

Comparison of amino acid sequences of variable regions revealed that the highest variability resided in three regions called as hypervariable or complementarity determining regions (CDRs) (Stewart, 2012). Variable regions were encoded by V(D)J segments belonging to immunoglobulin multigene family. Random assembly of V(D)J segments by a process known as somatic recombination generates the initial germ-line encoded diversity. Loss of several nucleotides during gene rearrangements and addition of N nucleotides by terminal deoxynucleotidyl transferase further increases the diversity (Bassing, Swat, & Alt, 2002; Little, Matthews, Oettinger, Roth, & Schatz, 2014; Tonegawa, 1983). Upon antigen recognition, variable domain genes undergo somatic hypermutation (SHM) at a rate of 10^{-3} changes per base pair in each cell cycle. SHM increases immunoglobulin diversity and enables affinity maturation of antibodies (Dorner, Foster, Farner, & Lipsky, 1998; Li, Woo, Iglesias-Ussel, Ronai, & Scharff, 2004; Rada, Ehrenstein, Neuberger, & Milstein, 1998). General structure of an antibody molecule is presented in Figure 1.4.

General effector functions of immunoglobulins include fixation of complement and binding to different cells to modulate their function. Effector functions, biological properties and functional locations of immunoglobulins depend on the class of the Igs. The immunoglobulins can be categorized under five classes/isotypes based on their heavy chains: IgG (γ chain), IgM (μ chain), IgA(α chain), IgD (δ chain) and IgE (ε chain) (Sondermann, Pincetic, Maamary, Lammens, & Ravetch, 2013).

Naïve B cells express only monomeric membrane bound IgM and start to express IgD isotype when they mature (Chen & Cerutti, 2011; Grönwall, Vas, & Silverman, 2012). Membrane bound IgD and IgM function in B-cell maturation and activation (Geisberger, Lamers, & Achatz, 2006). Upon activation, B cells first secrete pentameric IgM and monomeric IgD. Although the role of secreted IgD is poorly understood, it has been shown that IgD can bind to specific bacterial proteins in a variable region independent manner (Riesbeck & Nordström, 2006). Secreted pentameric IgMs are associated with primary immune responses. Although IgM molecules have low affinity, they have high avidity due to their pentameric structure. This ability makes IgM extremely efficient in opsonization of antigens and complement fixation (Boes, 2000).

Following infection or immunization, naïve B cells switch from expressing IgD and IgM to IgA, IgG or IgE by replacing CH regions through DNA recombination process specifically named as class switching recombination. Class switching improves pathogen elimination ability of Igs and changes their effector functions. This process is achieved by the help of CD4+ helper T-cells (Maizels, 2005; Stavnezer & Schrader, 2014).

Although IgA does not exhibit complement fixation as an effector function, it is critical for mucosal immunity (Woof & Mestecky, 2015). Polymeric IgA is more potent than its monomeric form (Stubbe, Berdoz, Kraehenbuhl, & Corthésy, 2000). In addition, secretory IgA can initiate immune responses in intestinal tissue by promoting antigen uptake by dendritic cells (Corthésy, 2007).

IgE has the lowest serum concentration among all Ig classes and yet it is a very potent Ig class. IgE can bind to Fcε receptors on mast cells, eosinophils and basophils with very high affinity and play critical roles in allergic responses (Galli & Tsai, 2012; Gould & Sutton, 2008).

IgG is the most abundantly found immunoglobulin class in human serum and is further divided into four subclasses in humans: IgG1, IgG2, IgG3, IgG4. These subclasses

were numbered based on their rank in terms of their serum levels. Although these subclasses show ~90% amino acid sequence similarity with each other, they exhibit different effector functions and antigen binding preferences. Excepting IgG4, all IgG subtypes have complement fixation function (Vidarsson, Dekkers, & Rispens, 2014).

Soluble and membrane bound antigens mainly induce IgG1 production and IgG1 deficiency results in recurring infections (JEFFERIS & KUMARARATNE, 2008). Capsular polysaccharide-based antigens of bacterial origin induce IgG2 responses. Although IgG2 is the main anti-carbohydrate antibody, IgG1 and IgG3 can compensate for IgG2 deficiency (Vidarsson et al., 1998). IgG3 has the highest complement fixation potency among all IgG subtypes and has the shortest half-life, possibly due to its highly inflammatory nature. Responses to viral infections and red blood cells components (observed in pregnancies and transfusions) are mainly dominated by IgG1 and IgG3 responses (Brouwers et al., 1988; Ferrante, Beard, & Feldman, 1990; Mawas, Wiener, Williamson, & Rodeck, 2009). In addition to IgE, allergens can also induce IgG4 production (Nouri-Aria et al., 2004). Furthermore, high IgG4 titers are observed in asymptomatic helminthic and parasitic infections (Atmadja et al., 1995).

In summary, immunoglobulins form a highly heterogeneous population with different functions and localizations to mainly eliminate the invading pathogens.

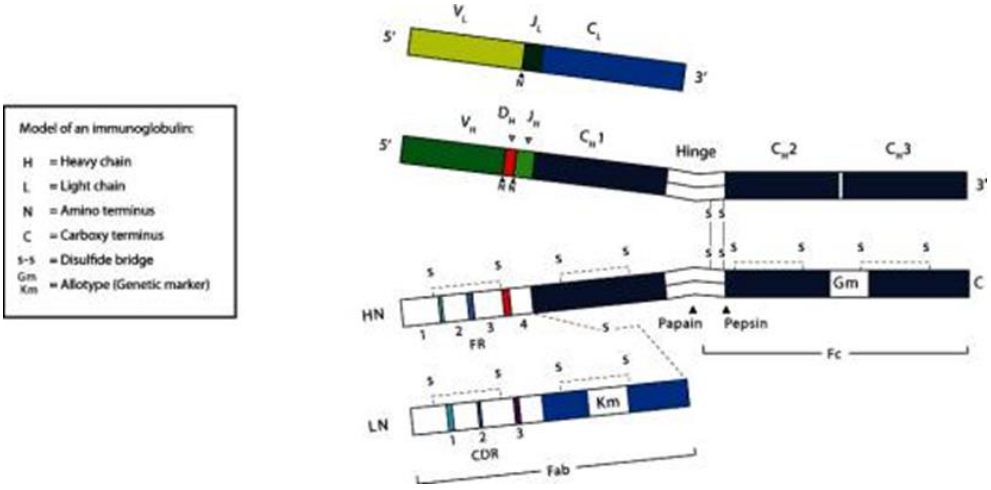

Figure 1.4. General structure of Immunoglobulin G

(Adapted from (Schroeder & Cavacini, 2010))

1.2.1. Mechanism of Actions of Intravenous Immunoglobulin (IVIg)

One of the striking features of Immunoglobulin G when introduced intravenously, is that it may display differential effects depending on the therapy dosage. Furthermore, its opposing effects in the context of autoinflammatory diseases versus immunodeficiencies, complicates development of a general mechanistic approach (Kerr et al., 2014). In this section, various mode of actions of IVIg will be briefly examined.

1.2.1.1. IVIg in Autoimmunity and Autoinflammation

Variability of the Fab regions of the immunoglobulins enables them to react and neutralize the immunomodulatory molecules such as cytokines, chemokines and receptors resulting in decrease of inflammatory responses (Gupta et al., 2001). Moreover, it has been reported that *in vitro* and in animal models, these anti-cytokine/receptor antibodies present in IVIg preparations stimulate the secretion of anti-inflammatory cytokines i.e. IL-10 and IL-1RA (Galeotti, Kaveri, & Bayry, 2017).

Not only they are effective in neutralizing secreted pro-inflammatory cytokines via their Fab fragments, but they also include anti-idiotype antibodies (i.e. antibodies blocking self-reactive antibodies) that are effective *in vivo* in autoimmune disease models (Blank et al., 2007).

Although the Fab portion has a significant effect on dissipating inflammation, the Fc region also play indispensable roles. Fc region of the IgG molecules may bind to the complement system proteins such as C3a, C3b,C4b and this binding obstructs the complement uptake, resulting in reduction in inflammatory response (Basta, 2008). Furthermore, FcRn (neonatal FcR) saturation by Fc portion of the IVIg might cause shortening of the half-life of the auto-antibodies since FcRn plays a critical role in the IgG degradation by preventing binding of the auto-antibody to its target (Nimmerjahn & Ravetch, 2008). IVIg also blocks immune-complex binding to FcγR expressed on innate immune cells, thereby prevents activation (Qureshi et al., 2017). Lastly, it has been shown that immunomodulatory activity of IVIg largely depends on a small percentage of immunoglobulins enriched in terminally-sialylated Fc glycans (Kaneko, Nimmerjahn, & Ravetch, 2006). According to this model, the anti-inflammatory sialylated Fcs in IVIg binds to specific receptors on macrophages such as SIGN-R1, stimulating the release of soluble mediators which then interact with inhibitory FcγRIIB receptors. This milieu of effector macrophages creates a competition between activatory and inhibitory molecules, and shift the balance towards inhibition (Shimoni, Bulvik, & Froom, 2013).

1.2.1.2. IVIg in Immunodeficiencies

In contrast to autoimmune and autoinflammatory disorders, IVIg is used at a lower dose in treatment of immunodeficiencies (Garcia-Lloret, McGhee, & Chatila, 2008). How IVIg complements functional defects in primary immune deficiencies is poorly understood and available data is highly conflicting depending on the gene defect, complexity of the disease and whether the effects have been studied on human subjects

or *in vitro* (Gelfand, Ochs, & Shearer, 2013). One type of immunodeficiency known as common variable immunodeficiency (CVID), is characterized by low antibody levels, arising from defective B-cell responses. Low dose IVIg signals B-cells to proliferate and induces the production of immunoglobulins from the B-cells of the CVID patients in a T-cell independent manner (Bayry et al., 2011). Moreover, intravenous IVIg infusion activates the dendritic cells of CVID patients, and upregulates of co-stimulatory and MHC molecules expression in these cells (Bayry et al., 2003). In the case of patients with severe combined immunodeficiency (SCID), IVIg replacement is initiated immediately after diagnosis to prevent infections and continued even after bone-marrow transplantation, until sufficient reconstitution of the immune system, although the mechanism of action in this context remains poorly defined (Albin & Cunningham-Rundles, 2014). Similarly, in Chronic Granulomatous Disease (CGD) patients with defective nicotinamide dinucleotide phosphate (NADPH) oxidase activity affecting basic neutrophil functions (Dinauer, 2016), IVIg is administered to improve symptoms and increase survival rates of patients. Yet again, the mechanism of action of IVIg in this disease remains unresolved (Álvarez-Cardona, Rodríguez-Lozano, Blancas-Galicia, Rivas-Larrauri, & Yamazaki-Nakashimada, 2012).

1.2.1.3. IVIg in Infections

Use of IVIg in primary immunodeficiencies revealed that infection rates were significantly reduced during therapy. Specifically, bacterial infection rates decrease significantly in B-cell chronic lymphocytic leukemia, Kawasaki disease, graft-versus-host disease following IVIg administration (Orange et al., 2006). For most immunodeficiencies, the rationale for IVIg administration is based on the low levels of immunoglobulins found in such patients. In fact, for this reason, IVIg therapy is also called as “immunoglobulin replacement” and routinely used in treatment of these diseases. IVIg administration is believed to increase the level of immunoglobulins and

therefore benefit clearance of bacterial infection (Krivan et al., 2017). In the case of fungal infections, there are reports stating that IVIg can help clearance of *Candida* infections in neutropenic patients (Casadevall & Pirofski, 2001). Furthermore, IVIg treatment was shown to be clinically beneficial in various inflammatory conditions related to fungal infections (Elluru, Kaveri, & Bayry, 2015). Despite the number of clinical reports on the beneficial role of IVIg treatment in immunodeficiencies and prevention of infections, the mechanism of action of this important therapeutic remains unclear, except for one publication stating that IVIg can enhance neutrophil functions (Jang, Hidalgo, & Frenette, 2012) and therefore can contribute to clearance of pathogens.

1.3. Trained Immunity

For many years, we have been taught that innate immunity is primitive and lacks specificity, and therefore, it fails to establish immune memory. However, recent advancements revealed that persistent (weeks to months) immunomodulation in innate immune cells reflect a type of innate immune memory known as “trained immunity”.

Trained immunity is a phenomenon proposed for the first time in 2011 by Netea and his colleagues based on the observation that plants and invertebrates which classically lack adaptive immune responses are protected against re-infection with pathogens (Netea, Quintin, & Van Der Meer, 2011). In 2012, Netea’s Laboratory experimentally showed that mice lacking T and B cells can resist re-infection with *Candida albicans*, following primary *C. albicans* infection which predominantly affects monocytes and macrophages in the absence of adaptive immune cells. Their findings showed that non-lethal *C. albicans* infection protected mice against secondary infection (Quintin et al., 2012). In 1934, a similar phenomenon had been observed in Swedish infants vaccinated with Bacillus Calmette–Guérin (BCG), where vaccination aided survival against neonatal sepsis (Netea & van der Meer, 2017). Although this clinic observation

remained unilluminated back then, now we know that this vaccine reprograms innate immune cells to augment their responsiveness to other pathogens.

Certain PRR ligands and signaling pathways can establish trained immunity in innate immune cells of particular hematopoietic lineage. So far, majority of stimulants known to induce reprogramming were defined as PRR agonists, and therefore, innate immune cells that express a wide range of PRRs tend to undergo reprogramming process when exposed to some of these ligands. Type of innate immune cells particularly susceptible to innate reprogramming include monocytes/macrophages and NK cells but not neutrophils since these cells are short-lived and highly differentiated (Netea, 2013). When monocytes are trained, they generally enlarge, secrete higher levels of secondary cytokines and increase ROS production (Bekkering et al., 2016). Although most of the trained immunity studies involved monocytes/macrophages, NK cells also display characteristics of innate immune memory. Evidence suggests that Cytomegalovirus (CMV) infection reprograms NK cells such that they can rapidly degranulate and produce cytokines during re-infections (Netea et al., 2016; Sun, Beilke, & Lanier, 2009).

The most potent inducer of trained immunity is known to be β-glucan (Quintin et al., 2012). This Dectin-1 ligand triggers Raf-1/Akt dependent signaling pathway to induce reprogramming. As a result, H3K4 modifications (H3K4me1, H3K4me3, H2K27Ac and H3K9me2) take place which then lead to enhanced cytokine production and metabolic rearrangements (Quintin, Cheng, van der Meer, & Netea, 2014). Additionally, there are several other ligands capable of inducing reprogramming in monocytes/macrophages other than β-glucans as shown in Table 1.2. Among these inducers, BCG vaccine elicits reprogramming through its component muramyl dipeptide (MDP; fragment of peptidoglycan) (Ifrim et al., 2014)) which activates NOD2-dependent signaling. Conversely, LPS can cause immune tolerance under certain conditions through MAPK-dependent pathway (Netea et al., 2016). It is now known that adaptor proteins and/or transcription factors in the downstream signaling pathways of PRR receptors play are crucial in induction of trained immunity.

Table 1.2. *Innate immune reprogramming mechanisms described for certain type of immune cells*

(Adapted from (Netea et al., 2016))

Innate immune cell types	**Primary challenge**	**Type of memory**	**Pathway involved**	**Mechanism**
Monocytes & Macrophages	LPS	Tolerance/trained immunity	TLR4/MAPK-dependent ATF7-dependent	Epigenetic changes: latent enhancers (H3K4me1). Other modifications (H3K4me3, H2K27me, H3K9me2)
Monocytes & Macrophages	β-glucan, *Candida* infection, BCG vaccination	Trained immunity	Dectin-1/Raf1/Akt-dependent STAT1-dependent NOD2-dependent	Epigenetic changes (H3K4me1, H3K4me3, H2K27Ac, H3K9me2) Metabolic rewiring
NK cells	Hepten-induced influenza A, vaccinia virus, HIV-1 infection	Antigen-specific	Not described	CXCR6-dependent NKG2D-dependent
NK cells	CMV infection	Antigen-dependent	Atg3-mediated mitophagy	BNIP3/BNIP3L-dependent
NK cells	CMV infection	Trained immunity	Stable down-regulation of adaptors and transcription factor (e.g. Syk, PLZF)	Epigenetic modification of gene promotors DNA methylation

In addition to epigenetic changes, metabolic profiles of the cells also change upon training. Similar to changes observed in immune responsiveness, certain metabolic pathways are also upregulated. In the resting state, monocytes and macrophages meet their energy needs by oxidative phosphorylation but switch to aerobic glycolysis when stimulated (a process known as the Warburg effect) (Netea & van der Meer, 2017). In this context, β-glucan induced activation of Dectin-1/Akt/mTOR/HIF-1α pathway results in a metabolic switch from oxidative phosphorylation to glycolysis (Cheng et al., 2014). BCG vaccine similarly supports an increase in aerobic glycolysis but also augments oxidative phosphorylation and glutamine metabolism (van der Heijden et al., 2018).

Other than the ligands which are reported as trained immunity inducers, the potential of Immunoglobulin G was also investigated in a recent study (van Splunter et al., 2018). Bovine milk, milk proteins and milk derived Immunoglobulin G was tested for reprogramming induction in human monocytes. The results showed that bovine IgG can induce trained immunity in human macrophages through activation of the MAPK pathway via engagement of FcγRII, inducing epigenetic modifications on IL-6 and TNF-α promoters, leading to NF-κB-dependent immune activation (van Splunter et al., 2018). In light of this information, we questioned whether IVIg can induce innate immune reprogramming in monocytes.

1.4. Aim of the Study

Intravenous Immunoglobulin (IVIg) is a therapeutic composed of pooled human Immunoglobulin G that has been used to treat a wide variety of immune diseases/disorders in the clinic. Initially, it was used in Ig replacement and was administered to the patients with Ig deficiency. However, later on, its use expanded to involve inflammatory/autoimmune diseases. The mechanism underlying the opposing effects of IVIg (augmentation of defective responses in immunodeficiencies versus suppression of autoinflammation/autoimmunity) is still under examination and is

known to be strictly dependent on the administered dose. While there is no consensus on mechanism(s) that account for the therapeutic effects of IVIg, at least its immune modulatory effects are thought to depend on the interaction between the Fc portion of IVIg with the Fcγ receptors expressed on the surface of macrophages, B-cells, natural killer (NK) cells, plasma cells, and platelets (Nagelkerke & Kuijpers, 2015). Herein, we aimed to examine the effects of IVIg treatment on specific innate immune cell populations to delineate changes in their functionality and immune responsiveness directed by IVIg in the absence or presence of various immune activators. To achieve this goal, we first adapted five different working concentrations IVIg (0, 0.2, 1, 5 and 25 mg/ml) based on the information stating that the highest dose of Ig administration corresponds to a plasma dose of at least 15 mg/ml (Issekutz, Rowter, & MacMillan, 2011). We reasoned that these concentrations would be able to mimic the low and high doses used for immunodeficiencies an autoinflammatory/autoimmune conditions in the clinic, respectively. Using this approach, we first examined the effect of IVIg on neutrophil functions (ROS production, NET formation and IL-8 production) activated in response to LPS, Zymosan and R848 as model bacterial, fungal and viral ligands, respectively. Similarly, we examined the effect of IVIg on TLR ligand induced pro-inflammatory cytokine production from human peripheral blood mononuclear cells.

Another aim of this study was to investigate whether IVIg is capable of inducing trained immunity. For this purpose, we used THP1-Dual monocytes to see if Ig can improve the responsiveness to secondary stimulants. We used two other agents to induce trained immunity, LPS and PGN that are known to induce innate immune reprogramming/tolerance (Ifrim et al., 2014) in comparison to IVIg. To analyse trained immunity profile, we imaged the cells under a light microscope to evaluate possible morphological changes, measured secondary ROS production and pro-inflammatory cytokine secretion in response to activation through bacterial, fungal and viral ligands. To further confirm the validity of pro-inflammatory cytokine secretion-based assessment, we also measured the extent of NF-κB activation in trained/stimulated THP1-Dual cells.

CHAPTER 2

MATERIALS & METHODS

2.1. Materials

2.1.1. Primary Cells and Cell Lines

Blood from healthy volunteers was collected into EDTA-coated tubes and used as the source of primary cells (i.e. polymorphonuclear phagocytic cells (PMNs) and/or peripheral blood mononuclear cells (PBMCs)). EDTA coated 10 ml vacutainers used for blood collection were purchased from BD Bioscience (USA). Blood-sampling was carried out at METU Medical Center using standard medical protocols.

Human acute monocytic leukemia cell line, THP1-Dual wild type was purchased from Invivogen ((thpd-nfis), USA). These cells express inducible luciferase and secreted embryonic alkaline phosphatase (SEAP) upon activation of IRF3/IRF9 or NF-κB, respectively. These cells were chosen for training experiments because they are known to express broad range of pattern recognition receptors (PRRs) and are monocytic in nature. Reporter activity of THP1-Dual cells makes investigation of NF-κB pathway activity easier and quicker as it can be measured directly from the cell culture supernatant.

2.1.2. Cell Culture Media, Solutions and Buffers

RPMI 1640 growth medium with L-Glutamine was obtained from Biological Industries (BI, Israel) and was supplemented with heat inactivated Fetal Bovine Serum (FBS; 5-10%), 50 U/ml penicillin, 50 μg/ml streptomycin, 0.1 mM nonessential amino acids, 1 mM sodium pyruvate and 10 mM HEPES. Complete recipe of cell culture medium was included in Appendix A.

For imaging of Neutrophil Extracellular Traps (NET), FBS was subjected to further heat inactivation at 65°C for 40-60 minutes to ensure inactivation of DNase. For this assay, DNase inactivated FBS was used at a final concentration of 2%. Antibiotics used in culture medium of THP1-Dual cell line were obtained from Invivogen (USA) and included Normocin (cat. #ant-nr), Zeocin (cat. #ant-zn) and Blasticidin (cat. #ant-bl). Cell culture grade water and Dulbecco's Phosphate Buffered Saline (DPBS) were purchased from BI (Israel).

Ficoll-Hypaque density-gradient separation medium used in isolation of PBMCs was from Capricorn Scientific (Germany) (Lymphocyte Separation Medium, density 1.077 g/ml (cat. #LSM-A)), Homemade Ammonium-Chloride-Potassium (ACK) buffer (Appendix A) or Pharm Lyse buffer (cat. #555899) from BD Biosciences (USA) was used to eliminate remaining red blood cells in the isolated cell pellet.

2.1.3. Chemicals and Reagents

Dextran from *Leuconostoc mesenteroides* (cat. #D4876-50G) used in PMN isolation was from Sigma-Aldrich (Germany). Fluorescent nucleic acid stains Syto16 Green (cat. #S7578) and Sytox Orange (cat. #S11368) were purchased from Thermo Scientific (USA). Dihydrorhodamine 123 (DHR123, cat. #109244-58-8), a probe for detection of cytosolic Reactive Oxygen Species (ROS), was from Cayman Chemical (USA). QUANTI-Blue (cat. #rep-qb2) was purchased from Invivogen (USA).

Unlabeled monoclonal antibodies used for capture and detection in Enzyme-Linked Immunosorbent Assay (ELISA) were obtained from Mabtech (Sweeden), Biolegend (USA) or BD Biosciences (see Table 2.1.). Other ELISA components were Streptavidin-Alkaline Phosphatase (ALP) conjugate (Mabtech), Avidin-HorseRadish Peroxidase (HRP) conjugate (BD Biosciences), 3, 3', 5, 5' tetramethyl benzidine (TMB) solution A and B (Biolegend, cat. #34064), and *p*-Nitrophenyl Phosphate disodium salt (*p*NPP, cat. #4264-83-9) was obtained from VWR Life Sciences

(Ireland). 2N sulfuric acid used as stop solution in HRP conjugated ELISA was prepared from 95-97% stock sulfuric acid (Merck, Germany).

Table 2.1. *Capture and detection antibodies used in ELISA*

Cytokine	**Company**	**Kit**	**Cat. #**
TNFα	Mabtech, Sweeden	Human TNFα ELISA development kit (ALP)	3512-1A-20
IL-1β	Mabtech, Sweeden	Human IL-1β ELISA development kit (ALP)	3416-1A-20
IL-6	Biolegend, USA	Purified anti-human antibody for capture/ biotinylated antibody for detection	501102/501202
IP-10	BD Bioscience, USA	BD OptEIA Human IP-10 ELISA Set	550926
IL-8	Endogen, USA	Purified anti-human antibody for capture/ biotinylated antibody for detection	M801/M802b

2.1.4. Ligands and Training Agents

Human Intravenous Immunoglobulin (IVIg; 5g/50ml), Kiovig was from Baxter (USA), and was a kind gift from Prof. Dr. İsmail Reisli, Necmettin Erbakan University, Meram Faculty of Medicine. IVIg was used to treat PMNs and PBMCs

and to train THP1-Dual cells. Other agents used in training experiments were Lipopolysaccharide (LPS) from Sigma Aldrich (Germany) and Peptidoglycan (PGN) from Invivogen (USA, cat. #tlrl-pgnb3).

PRR ligands used to stimulate cells for induction of ROS production, NET formation and cytokine release were described in Table 2.2.

Table 2.2. *Descriptions and working concentrations of ligands used in cellular activation*

Ligand	**Description**	**Working concentration**	**Company**	**Cat. #**
PMA	phorbol 12-myristate 13-acetate	50 ng/ml	Invivogen, USA	tlrl-pma
LPS from *E. coli*	Gram (-) bacteria outer membrane component	1 µg/ml	Sigma-Aldrich, USA	L2630-10MG
Zymosan	Cell wall preparation of *S. cerevisiae*	10 µg/ml	Invivogen, USA	tlrl-zyn
Flagellin	Bacterial flagella component	1 µg/ml	Invivogen, USA	tlrlepstfla-5
K3 (CpG:ODN)	20-mer atcgactctcgagcgttctc	1 µM	Alpha DNA, Canada	---
Poly I:C (HMW)	Long synthetic analog of dsRNA	10 µg/ml	Invivogen, USA	tlrl-pic-5
Resiquimod (R848)	Imidazoquinoline compound	5 µg/ml	Invivogen, USA	tlrl-r848
Heat killed *Candida albicans*	Heat killed *Candida albicans*	2.5 *Candida albicans*/cell	Invivogen, USA	tlrl-hkca

2.2. Methods

2.2.1. Cell Culture and Maintenance

2.2.1.1. Isolation of Peripheral Blood Mononuclear Cells (PBMCs) and Polymorphonuclear Phagocytes (PMNs) from Whole Blood

Blood samples were collected from healthy donors into EDTA coated 10 ml vacutainers (BD Biosciences, USA). Samples were diluted 1:1 with DPBS to adjust the density for better separation. Diluted blood samples were carefully layered on lymphocyte separation medium at 1.5:1 ratio (V/V). Tubes were centrifuged at 1800 rpm for 30 minutes with the break set to "off" to prevent mixing of separated layers during deceleration. The cloudy layer between separation media and the plasma corresponding to PBMCs was collected with a sterile Pasteur pipet and transferred into another falcon tube. As such collected cells were washed twice with wash medium (RPMI 1640 with 2% FBS) and centrifuged at 300g for 10 minutes at RT. Cell pellet was re-suspended in 1 ml of regular complete medium (RPMI 1640 with 10% FBS).

For neutrophil enrichment, the density-gradient medium residing above the red blood cell/granulocyte pellet was carefully aspirated, and the pellet was resuspended in a volume of DPBS equivalent to the initial volume of blood. Next, the suspension was mixed with an equal volume of 3% dextran-saline solution (prepared by dissolving dextran in DPBS). Tubes were placed vertically for dextran induced red blood cell aggregation and gravitational sedimentation. Approximately 20 minutes later, erythrocyte-poor top fraction containing PMNs were collected and washed in DPBS at 300g for 10 minutes at +4°C. Red blood cell contamination in the pellet was eliminated by the addition of 2-3 ml of lysis buffer (ACK or Pharm Lyse Buffer). After 2-3 minutes of lysis buffer treatment, reaction was stopped by diluting the buffer with cold DPBS. Cells were washed with 10 ml of cold DPBS once more and centrifuged at the same conditions as stated above. The pellet was re-suspended in 1 ml of either regular complete medium or medium containing 2% DNase inactivated FBS for use in further assays.

Isolated primary cells were counted using a Novocyte 2060R flow cytometer (ACEA Biosciences, USA). Forward Scatter (FSC) and Side Scatter (SSC) of the cells were examined to confirm the success and purity of PBMC and/or neutrophil separation.

2.2.1.2. Cell Line Maintenance

THP1-Dual wild type cells were maintained in filtered T25 flasks starting at a concentration of 500,000 cells/ml and passaged before the the cell density reached $2x10^6$ cells/ml (approximately every 3 days). Regular complete medium additionally contained Normocin (100 µg/ml) to prevent mycoplasma, bacteria and fungi contamination and Zeocin (100 µg/ml) & Blasticidin (10 µg/ml) to maintain selection pressure of the reporters. The cells were discarded after 20^{th} passage.

2.2.2. *In vitro* IVIg Treatment and Stimulations

2.2.2.1. IVIg Treatment for PMNs and PBMCs

Four different concentrations of IVIg (0.2, 1, 5, 25 mg/ml, diluted in DPBS) were used to treat different cell types either prior to stimulation or simultaneously depending on the type of assay. PMNs were pre-treated with IVIg for 45 minutes for cytosolic ROS detection and NET imaging experiments. For cytokine secretion measurements, cells were treated with the same doses of IVIg in the absence or presence of various PRR ligand simultaneously overnight (16-18 hours) or for a period of 24 hours.

2.2.2.2. Cell Stimulations

To detect cytosolic ROS in PMNs, cells were distributed to eppendorf tubes at a concentration of 250,000 cells/tube in regular complete medium. After 45 minutes of IVIg treatment in 5% CO_2 incubator at 37°C, the cells were exposed to LPS or Zymosan for 45 minutes or PMA for 15 minutes (Table 2.2.).

For NETosis assays, neutrophils were re-suspended in 2% DNase inactivated FBS containing culture medium. The cells were distributed into 96-well plates at a concentration of 40,000 cells/well and were stimulated as described above but for a period of 4 hours of incubation.

Neutrophil stimulation for cytokine quantification by ELISA was performed using 500,000 cells/well in a 96-well plate. IVIg and stimulants were introduced to cells simultaneously and incubation duration was 16-18 hours.

Stimulation of PBMCs (400,000 cells/well) was achieved using several TLR ligands (Table 2.2.) in the absence or presence of IVIg for 24 hours.

Table 2.3. summarizes the sub-cellular locations, identities of the cognate receptors and signal transduction pathways activated in response to the used ligands.

Table 2.3. *TLR ligands used in the experiments, their receptors and the ensuing signaling pathways that are activated*

Ligand	**Target PRR**	**Pathway**	**Location of PRR**
LPS from *E. coli*	TLR4	NF-κB, IRF3	Cell surface
Zymosan	TLR1/2, Dectin-1	NF-κB	Cell surface
Flagellin	TLR5	NF-κB	Cell surface
K3 (CpG:ODN)	TLR9	NF-κB, IRF7	Endosome
Poly I:C (HMW)	TLR3	NF-κB, IRF3	Endosome

Table 2.3 cont'd. *TLR ligands used in the experiments, their receptors and the ensuing signalling pathways that are activated*

Ligand	Target PRR	Pathway	Location of PRR
Resiquimod (R848)	TLR7/8	IRF7	Endosome

2.2.2.3. Training Experiments

THP1-Dual wild type cells were treated with different training agents, including IVIg (0.2, 1, 5, and 25 mg/ml), LPS (0.2, 1 and 5 µg/ml) or PGN (0.5, 2.5, and 12.5 µg/ml). Cells were seeded in 6-well plates at a density of $1x10^6$/well in 10% FBS RPMI 1640 containing Normocin (100 µg/ml). Training agents were added into wells as mentioned. After 24 hours of incubation, cells were washed with warm DPBS and centrifuged at 300g for 10 minutes (RT). Following fresh culture medium replenishment and a period of 3 days of rest, the cells were collected and counted using a flow cytometer (NovoCyte by ACEA (USA)). Cells were layered into 96-well plate at a final density of 100,000 cells/well. As such trained or untrained cells (kept in RPMI medium alone) were then exposed to secondary stimulation with bacterial (LPS), viral (R848) or fungal (Zymosan, opsonized HKCA) agonists for a period of 24 hours (see *Figure 2.1.).* Following this incubation period, cell culture media were collected for cytokine quantification and SEAP activity measurement, and the cells were stained with DHR123 for cytosolic ROS measurement.

Heat killed *Candida albicans* (HKCA) was used after opsonization. Opsonized HKCA was prepared by mixing the suspension of fungi with fresh human serum at a 1:1 ratio and incubating at 37°C for 30 minutes on a heat block. An additional 20 minutes incubation at 65°C was done carried out to inactivate enzymes and complement components in serum.

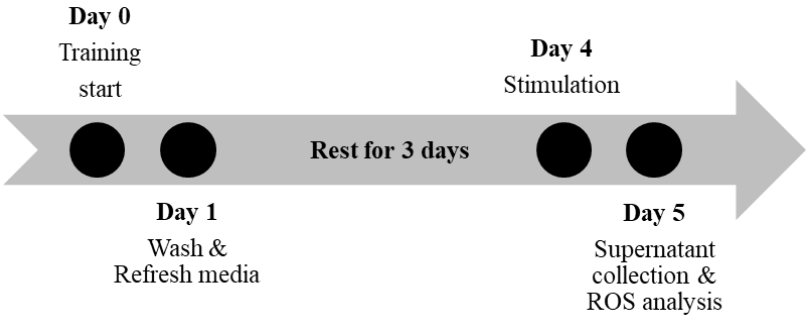

Figure 2.1. Schematic overview of trained immunity protocol

For morphological observation of cells at training period, they were imaged using JuLi Smart fluorescent cell analyzer under white light (NanoEnTek, Korea) with 4X magnification at Day 1 and Day 4.

2.2.3. Cytosolic ROS Detection by DHR123 Staining

DHR123 (1:1000, diluted in cell culture grade water) was directly added onto PMNs after stimulation and incubated for 15 minutes at 37°C. Once the incubation was completed, samples were transferred on ice to inhibit further ROS production. The cells were then immediately analysed by flow cytometry using the BL1 fluorescence channel equipped with a 530/30 nm emission channel. Mean Fluorescent Intensity (MFI) and percentage of DHR123 positive cells were assessed from histogram and dot plots using the NovoExpress flow cytometer software.

ROS detection in trained THP1-Dual cells was performed after sampling of supernatants. The cells were treated with cold DPBS to detach any adherent cells from the wells. After 10 minutes incubation in cold DPBS at +4°C, cells were collected and transferred into eppendorf tubes. The cells were centrifuged at 300g for 10 minutes and re-suspended in 2% FBS RPMI 1640. DHR123 was added onto cells and analysed as described above.

2.2.4. Neutrophil Extracellular Trap Imaging by Fluorescent Microscopy

Extracellular traps released from neutrophils were imaged on Floid Cell Imaging Station (Thermo Scientific, USA) under 20X magnification. Cells were stained with one cell membrane permeable dye, Syto16 Green (1:1500 diluted), and one membrane impermeable dye Sytox Orange (1:5000 diluted). Using these two dyes together allows for visualization of external sticky DNA material around the cells and the dead ones which appear red, while labeling the live ones as green. Images were taken under green channel at 488/518 nm excitation/emission for Syto16 Green and red channel at 547/570 nm for Sytox Orange.

2.2.5. Enzyme-Linked Immunosorbent Assay for Cytokine Quantification

Supernatants that were collected after cellular stimulations were stored at -20°C until ELISA was performed. Thermo Scientific (USA) semi-hydrophobic Polysorp (cat. #43145) or hydrophilic Maxisorp (cat. #442404) plates were used for this procedure. Surface of wells were coated with 50 µl of capture antibody solution at a specific final concentration (Table 2.4.) either in DPBS for Mabtech antibodies or sodium bicarbonate coating buffer (pH:9.5; Appendix A) for Biolegend and BD Biosciences antibodies. The plates were left for overnight (16-18 hours) coating at +4°C. The second day, capture antibody was removed and 200 µl blocking buffer containing 1% BSA in PBS (Appendix A) was added to each well. After 2 hours of incubation at RT on a rocker, the plates were washed by soaking into ELISA wash buffer containing 0.05% Tween20 (Appendix A) for four times with 3 minutes of incubation duration. After plates were air-dried, samples (diluted 1:5 ratio for IP-10 and IL-6 detection) and serially diluted (12 2-fold dilutions) recombinant protein to construct a standard curve were added into wells and left for 2 hours of incubation at RT on rocker. The plates were washed again as previously described. Biotin conjugated detection antibodies were adjusted to their specific working concentrations (Table 2.4.) in T-cell buffer (Appendix A) and was added at a volume of 50 µl/well for overnight

incubation at +4°C. On the third day, the biotinylated antibody was removed and the plates were washed. Streptavidin-ALP or Avidin-HRP conjugates were prepared at 1:1000 dilution in T-cell buffer and added at a volume of 50 µl/well followed by incubation for 1 hour or 30 minutes for Streptavidin-ALP or Avidin-HRP, respectively. After washing of the plates as previously described and additionally washing in distilled water once, substrates were added to the wells and color development was measured on a Multiskan FC Microplate Photometer (Thermo Fisher Scientific, USA) device. OD recordings of Streptavidin-ALP conjugate treated samples were measured at 405 nm wavelength every 15 minutes at first hour and at 30 minutes time intervals after that. Time point where the highest concentration of standards reached saturation was chosen for quantification of unknowns. In Avidin-HRP conjugate treated samples, color development was stopped with 2N sulfuric acid and OD values were recorded at 450 and 570 nm. Final absorbance of samples was calculated by subtracting absorbance (570) from absorbance (450). Quantification of cytokine concentrations was based on the recombinant cytokine-based standard curves that were generated using a 4-parameter logistic curve fit.

Table 2.4. *Working concentrations of antibodies, type of conjugates and substrates used to quantify corresponding cytokines*

Cytokine	**Working concentration of capture antibody**	**Working concentration of detection antibody**	**Conjugated protein-enzyme complex**	**Substrate**
IL-6	2 µg/ml	0.5 µg/ml	Avidin-HRP	TMB solution*
TNF-α	2 µg/ml	1 µg/ml	Streptavidin-ALP	*p*NPP
IL-1β	2 µg/ml	1 µg/ml	Streptavidin-ALP	*p*NPP
IP-10	500X	1000x	Streptavidin-ALP	*p*NPP
IL-8	1 µg/ml	0.5 µg/ml	Streptavidin-ALP	*p*NPP

*3, 3', 5, 5' tetramethyl benzidine (TMB) solution is prepared by mixing Solution A and B (1:1).

2.2.6. Examination of NF-κB Activation in THP1-Dual Cells

These cells release SEAP upon activation of NF-κB and luciferase upon activation of the IRF pathway. QUANTI-Blue powder was dissolved according to instructions of the company and it was used for SEAP detection in the supernatant. 30 µl sample supernatant was mixed with 170 µl of QUANTI-Blue solution in 96-well tissue culture plates. Multiskan FC Microplate Photometer (Thermo Fisher Scientific, USA) was used to measure optical density at 645nm and the data was analyzed in terms of optical density (OD).

2.2.7. Cell Viability

PMNs were stained with Syto16 Green (1:1500) and Sytox Orange (1:5000) dyes to distinguish dead and live cells. Samples were imaged on Floid Cell Imaging Station (Thermo Scientific, USA) as previously described in Section 2.2.4.

2.2.8. Statistical Analysis

Graphpad Prism 8 was used to construct graphs and analyze the data statistically. Mann-Whitney U and Kruskal-Wallis followed by Dunnet's Multiple comparison test were used to analyze the data, * $p<0.05$, ** $p<0.01$, *** $p<0001$.

CHAPTER 3

RESULTS & DISCUSSION

Intravenous Immunoglobulin (IVIg) derived from the plasma of healthy individuals, has been used in the treatment of immunodeficiencies and more recently, in treatment of inflammatory and autoimmune diseases. Although the use of a single therapeutic agent to treat deficient versus over-active immune system associated disorders seem paradoxical, these opposing effects depend on the dose that is administered. In general, relatively low doses are preferred for immune deficiencies to activate the immune system, whereas high dose Ig has been used for inflammatory/autoimmune diseases to suppress the over-active immune system (Lünemann, Nimmerjahn, & Dalakas, 2015). The mechanism by which IVIg exerts its therapeutic effects, is not completely understood. In this context, neutrophils represent the major cell population pivotal in protection against bacterial infections and play a key role in inflammatory and autoimmune diseases. Knowledge on whether IVIg alters neutrophil and innate immune cell functions is incomplete. Therefore, we first aimed to assess the effect of IVIg treatment on major neutrophil functions including, ROS production, cytokine secretion and neutrophil extracellular trap formation. Next, we also analyzed how IVIg treatment altered responses to TLR-mediated immune activation in human peripheral blood mononuclear cells.

3.1. Determination of the Effect of IVIg Treatment on Peripheral Blood Polymorphonuclear Cell Functions

3.1.1. Effect of Stand-Alone IVIg Treatment on ROS Production from Unprimed Neutrophils

Evidence suggests that IVIg improves ROS production in TNF-primed human neutrophils (Higurashi et al., 2012). To test whether IVIg altered ROS production in

unprimed neutrophils, the therapeutic agent was introduced to purified cells at four different concentrations to mimic both low and high dose treatments used in the clinic. The highest dose of treatment is approximately 1-2 g/kg per day which causes elevation in the plasma IgG to at least 15 mg/ml (Issekutz, Rowter, & MacMillan, 2011). Considering this, working concentrations for *in vitro* immunoglobulin treatment were adapted as 0.2, 1, 5 and 25 mg/ml. Formation of reactive oxygen species in IVIg treated neutrophils was assessed using the ROS-reactive dye (DHR123) and flow cytometry. Results showed that, lower concentrations of IVIg (0.2 and 1 mg/ml) had no impact on neutrophil-mediated ROS production, whereas the mean fluorescence intensity of DHR123 slightly increased in 5 and 25 mg/ml IVIg treated samples where the 25 mg/ml dose yielded statistically significant difference compared to cells with no IVIg treatment (Figure 3.1 a and b).

a.

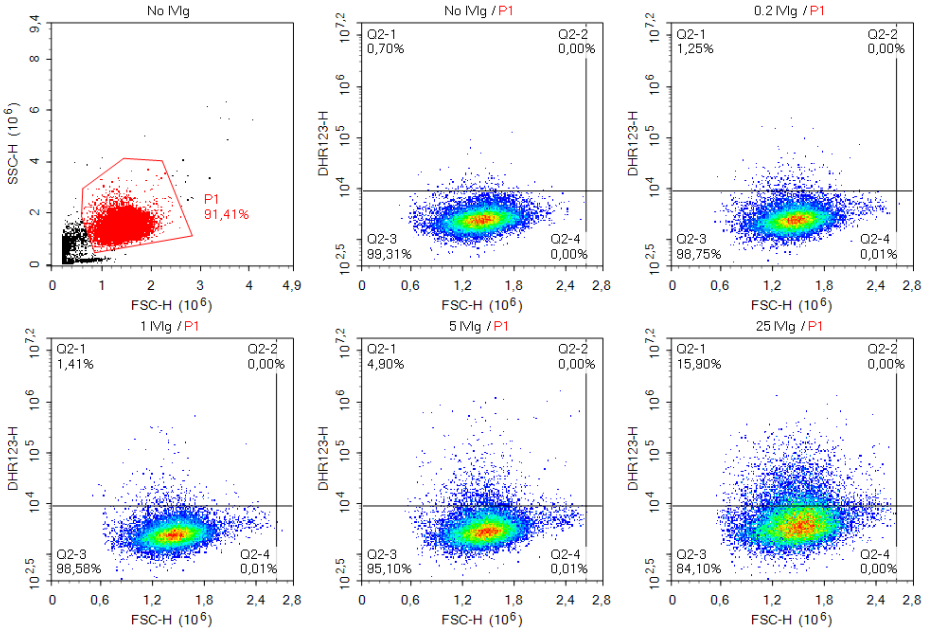

b.

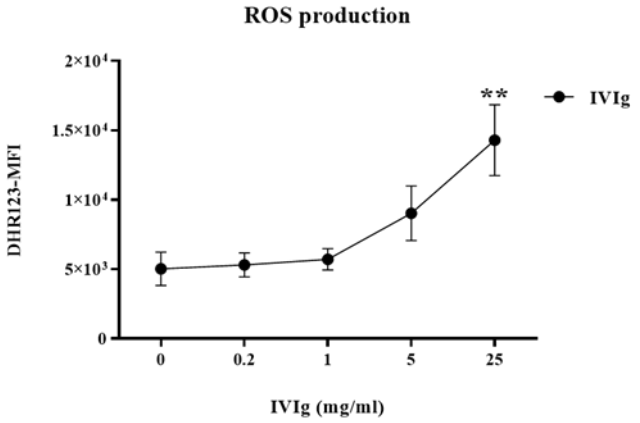

Figure 3.1. IVIg induced ROS production in healthy neutrophils

Neutrophils (250,000/tube) were stimulated with the indicated concentrations of IVIg for 45 min at 37°C. ROS reactive dye DHR123 was added onto cells during the last 15 min of incubation (1:1000). (a) Representative Flow cytometry density plots of ROS production in healthy peripheral blood neutrophils in the presence or absence of different IVIg concentrations. (b) Average MFI quantification of IVIg induced ROS production.

The data are presented as MFI ± S.E.M (n=7) and were analyzed by Mann-Whitney U test (**p<0.01).

This result suggests that high dose IVIg primes neutrophils for cytosolic ROS production even in the absence of any other activating ligands. It is likely that such an effect might be mediated through the activating FcγRIII receptors on neutrophils (Schwab & Nimmerjahn, 2013).

3.1.2. Effect of IVIg Treatment on ROS Production from TLR Ligand or PMA-Activated Neutrophils

Activating versus suppressor effects of IVIg are known to vary depending on its concentration. However, we hypothesized that not only the concentration but also the types of ligands that the host might be exposed to could modulate the outcome of IVIg administration. For instance, IVIg is known to augment the clearance of fungal

infections in case of primary immune deficiencies (Elluru et al., 2015), suggesting that anti-fungal innate defense signaling pathway(s) and IVIg might synergize. For this reason, a fungal ligand, Zymosan, was chosen along with a bacterial ligand, LPS, and PMA as neutrophil activators and IVIg was introduced at various doses to gain insight into how IVIg might modulate various signal transduction pathways. When the response of neutrophils to the TLR4 ligand alone versus together with increasing concentrations of IVIg were compared, there was no statistically significant difference between groups in terms of ROS production (Figure 3.2b). In contrast, TLR2/Dectin-1 ligand Zymosan triggered ~5- and 7-fold higher ROS production in the presence of 5 and 25 mg/ml IVIg, respectively, compared to Zymosan alone -induced ROS (Figures 3.2a and 3.2b, $p<0.05$). Interestingly, IVIg treatment had a dose-dependent suppressive effect and significantly decreased PMA-induced ROS production at a concentration of 25 mg/ml (Figure 3.2b).

a.

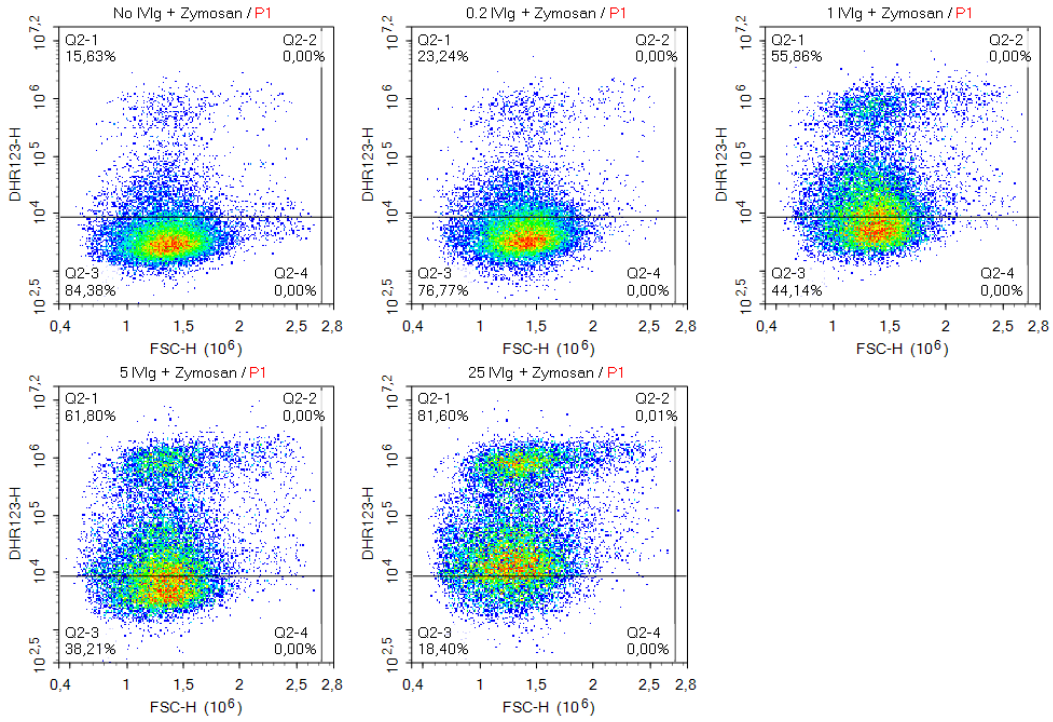

b.

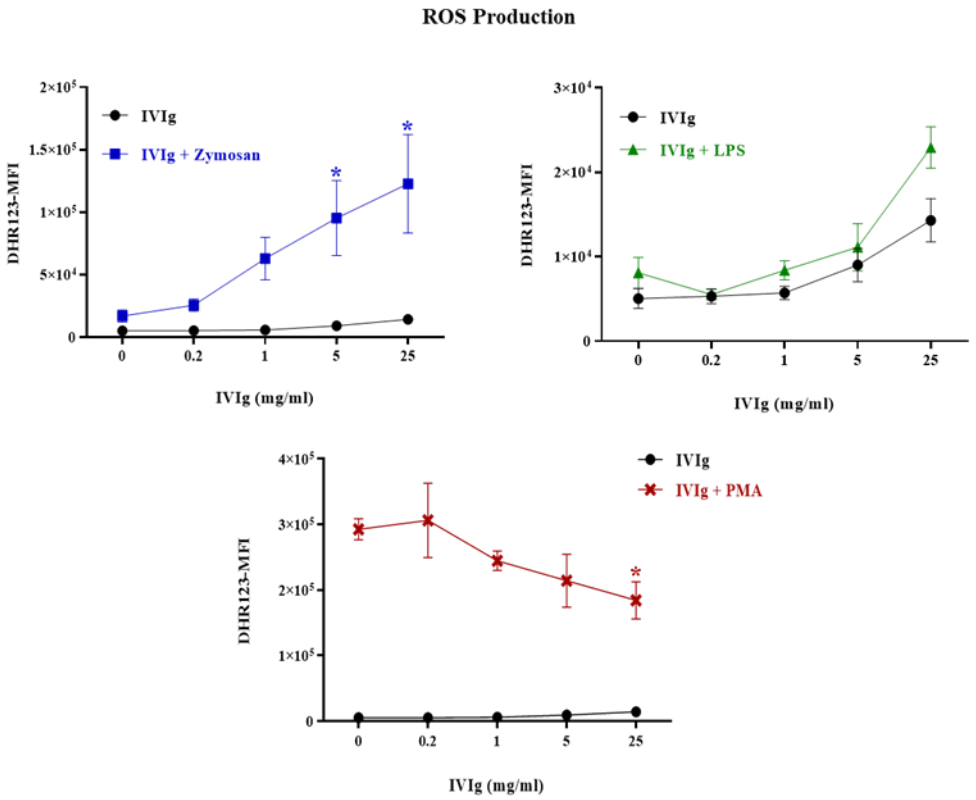

Figure 3.2. ROS production in Zymosan, LPS or PMA-activated neutrophils in the absence or presence of IVIg treatment

Neutrophils (250,000/tube) were stimulated with optimal concentrations of LPS, Zymosan or PMA in the absence or presence of IVIg for 45 or 15 min (PMA) at 37°C. ROS reactive dye DHR123 was added onto cells during the last 15 min of incubation (1:1000). (a) Representative flow cytometry density plots of ROS production in Zymosan-activated with or without IVIg treatment (b) Average MFI quantification of ROS production from Zymosan, LPS or PMA-activated neutrophils.

The data are presented as MFI ± S.E.M (Zymosan stimulation, n=5; LPS stimulation, n=3; PMA stimulation, n=4). Statistical analysis was based on Mann-Whitney U test (*$p<0.05$).

These results suggest that IVIg might synergize with TLR2/Dectin-1 signaling pathway, has no effect on TLR4-mediated activation but could interfere with the Protein Kinase C signaling pathway.

3.1.3. IVIg Treatment Has Opposing Effects on NET Formation Depending on the Dose and Type of Stimulant

NETosis is a regulated form of neutrophil cell death that is strongly associated with ROS production (Kaplan & Radic, 2012). Since IVIg treatment resulted in elevated levels of ROS in neutrophils (Figure 3.1), we, next, aimed to determine the effect of IVIg on NET formation. Results showed that 5 and 25 mg/ml IVIg alone triggered neutrophil extracellular trap formation (Figure 3.3a) and the process synergized with LPS and Zymosan-induced NETosis (Figures 3.3b and 3.3c). Consistent with the suppression of PMA-induced ROS production in the presence of high dose of immunoglobulin, 25 mg/ml IVIg also exerted a suppressive effect on NET formation triggered by PMA. In Figure 3.3d, it can clearly be seen that PMA-induced death was significantly lower in 5 and 25 mg/ml IVIg treated samples.

These results suggest that, IVIg treatment might augment clearance of bacterial and fungal infections through enhanced neutrophil extracellular trap formation in the presence of such ligands. In contrast, high dose IVIg might curtail ROS production and NETosis for potent neutrophil activators as exemplified by PMA.

a.

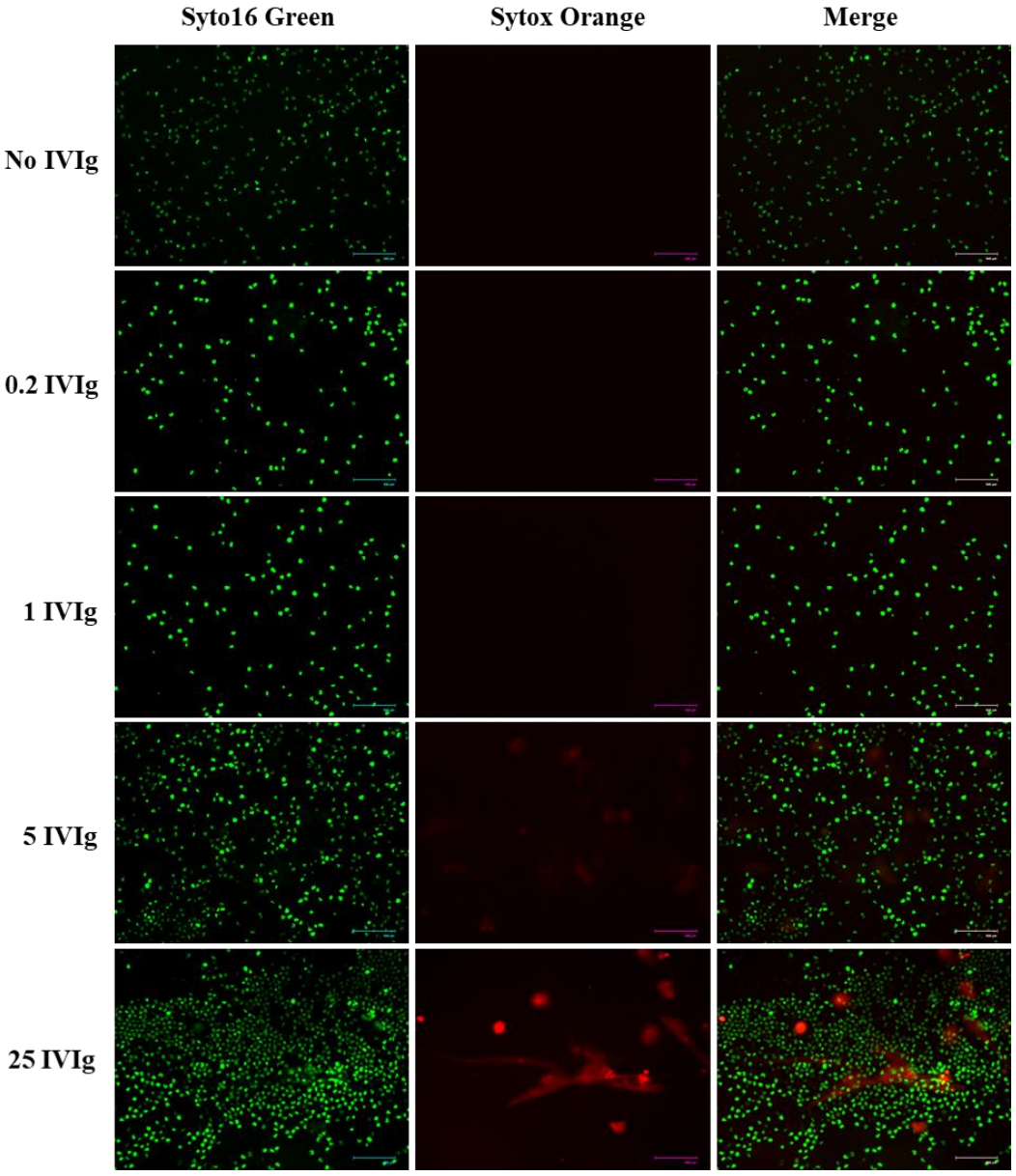
Syto16 Green
Sytox Orange
Merge
No IVIg
0.2 IVIg
1 IVIg
5 IVIg
25 IVIg

b.

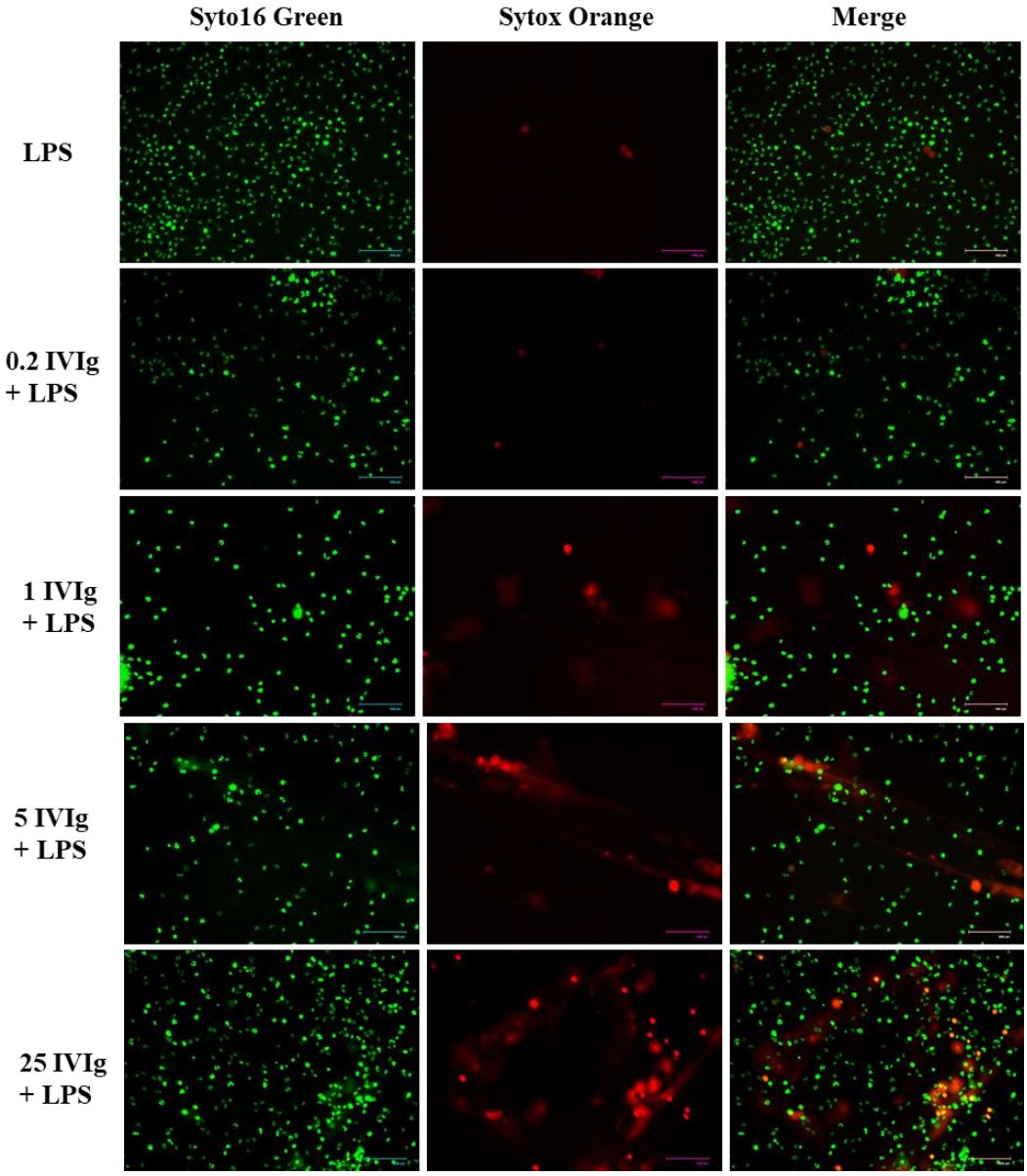
Syto16 Green
Sytox Orange
Merge
LPS
0.2 IVIg + LPS
1 IVIg + LPS
5 IVIg + LPS
25 IVIg + LPS

c.

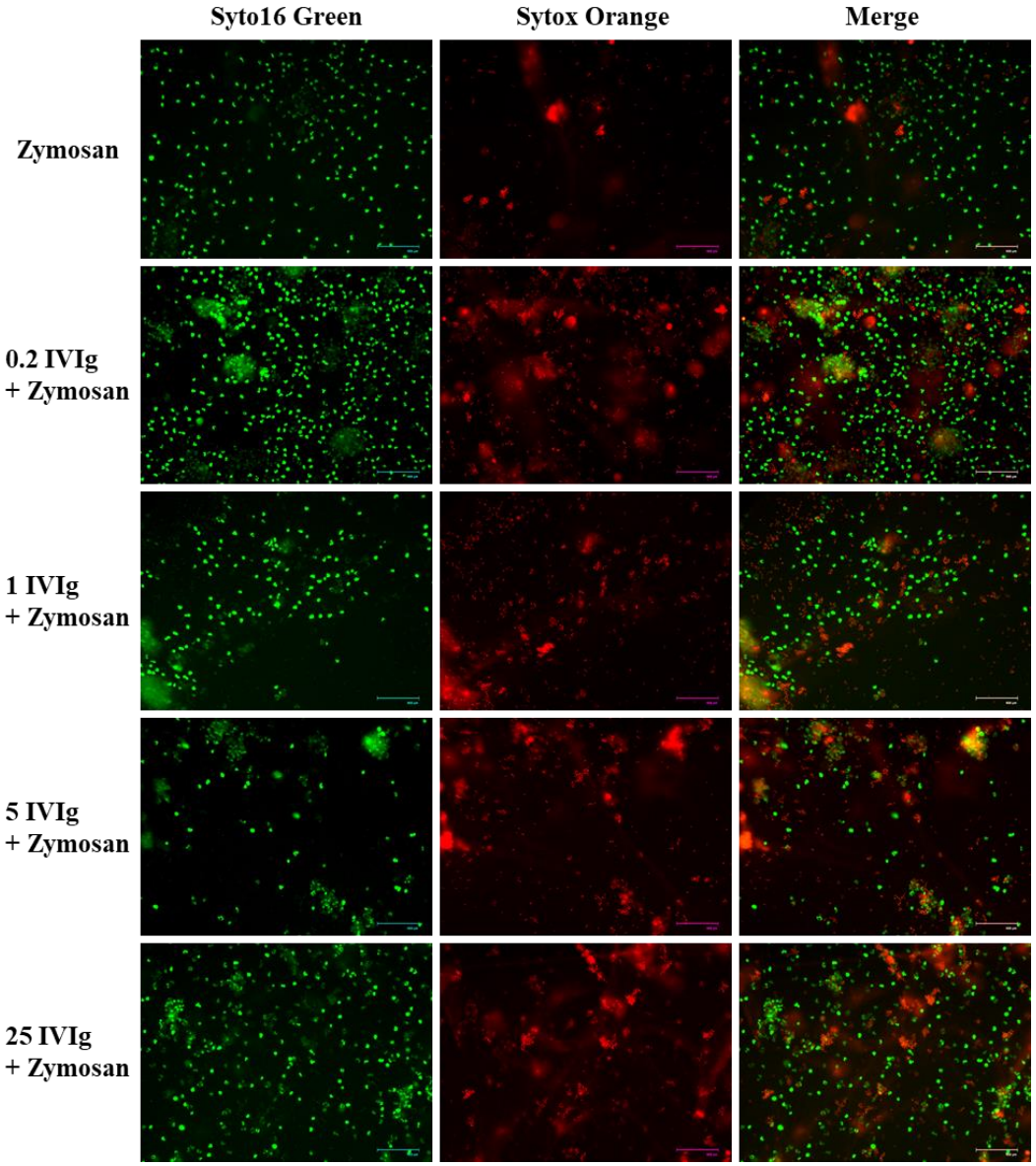
Syto16 Green
Sytox Orange
Merge
Zymosan
0.2 IVIg
+ Zymosan
1 IVIg
+ Zymosan
5 IVIg
+ Zymosan
25 IVIg
+ Zymosan

d.

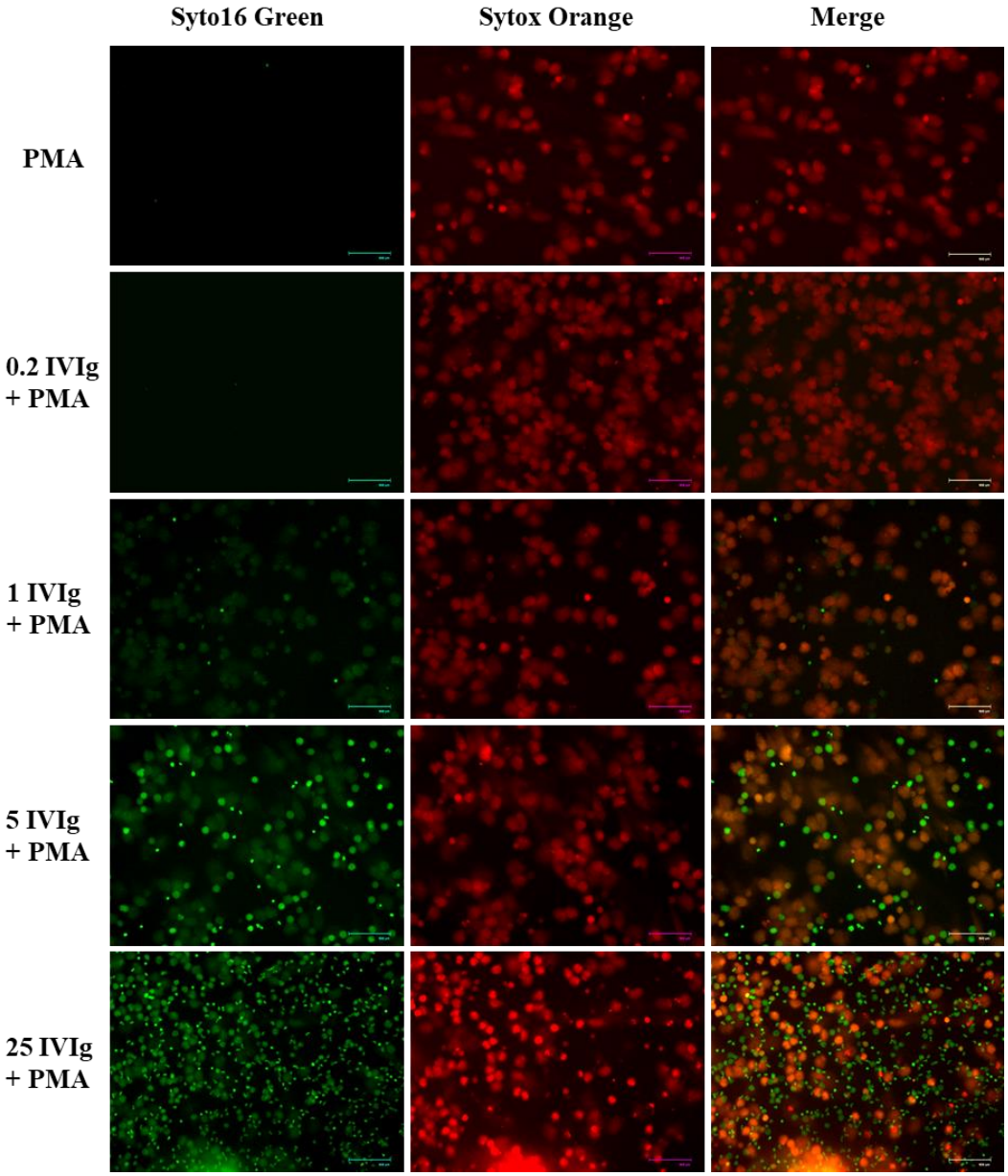

Figure 3.3. Syto16 Green and Sytox Orange stained fluorescent microscopy images of NETosis induced by IVIg, LPS, Zymosan and PMA

3.1.4. IVIg Regulates Cytokine Release from Neutrophils

Subsequent to the results mentioned above, we wanted to analyze the effect of IVIg treatment on cytokine release from activated neutrophils. To mimic the situation during fungal, bacterial and viral infections, the impact of IVIg on Zymosan, LPS and R848 activated neutrophils was investigated as model agonists of TLR2/Dectin-1, TLR4 and TLR7/8, respectively. PMA was excluded from these experiments as it causes rapid cell death in neutrophils through NETosis, precluding its use from experiments where an incubation period of 16-18 h is required for cytokine determination. The signature neutrophil cytokine, IL-8, levels were assessed by ELISA from activated neutrophil culture supernatants.

As can be seen from Figure 3.4, IVIg alone induced no significant cytokine production at any dose compared to unstimulated controls. LPS and Zymosan alone caused 2.9- and 3.3-fold increase in IL-8 production over basal levels. In the presence of 0.2, 1, 5 and 25 mg/ml IVIg, LPS and Zymosan-induced IL-8 production further increased 2.0, 4.5, 10.4, 19.1 and 3.9, 4.3, 5.9, 7.8-fold, respectively (Figure 3.4). R848 itself caused 55-fold increase in IL-8 secretion. R848-induced IL-8, increased by ~1.80 and 2-fold with low dose IVIg (0.2 and 1 mg/ml), whereas highest dose of IVIg (25 mg/ml), suppressed cytokine production 1.8-fold, when compared to R848 treatment alone.

To confirm that these results represented the outcome of cellular activation and was independent of cell death, viability of neutrophils were also determined using Syto16 Green and Sytox Orange staining for live/dead cell discrimination. Observation under the fluorescence microscope showed that majority of neutrophils were viable after overnight stimulation (Figure C.1).

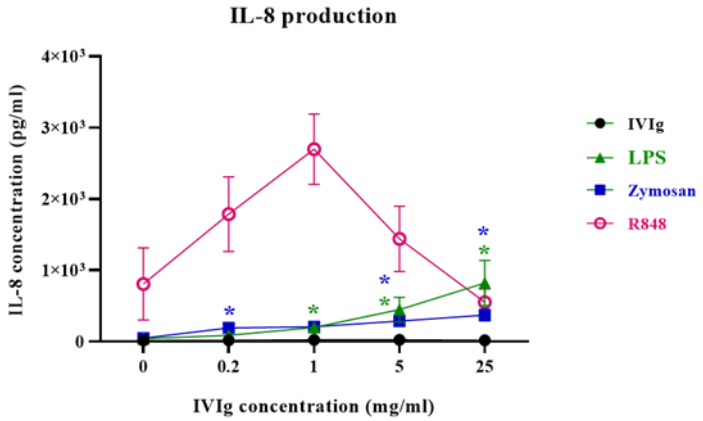

Figure 3.4. Cytokine production upon stimulation with Zymosan, LPS and R848 in the absence or presence of IVIg treatment

Neutrophils (500.000/well) were treated with 0, 0.2, 1, 5 and 25 mg/ml IVIg and stimulated with LPS, Zymosan and R848 for 16-18 h. Cell culture supernatants were collected and cytokine production was quantified by ELISA.

The data are presented as average cytokine concentration ± S.E.M (n=4), and were analyzed by Mann-Whitney U test (*$p<0.05$).

In summary, these results suggest that IVIg synergizes with TLR2/Dectin-1 and TLR4 signaling pathway and therefore might facilitate the clearance of fungal and bacterial pathogens. For TLR 7/8 activation, the final outcome depends on IVIg concentration: low dose IVIg modestly supports cytokine production, whereas high dose demonstrates a suppressive function. This observation is consistent with the immunomodulatory activity of high dose IVIg in inflammatory/autoimmune diseases, wherein evidence of TLR7/8-mediated immunopathology is plenty (Farrugia & Baron, 2017).

3.2. Differential Regulation of TLR-Mediated Cytokine Productions by IVIg Treatment in Human Peripheral Blood Mononuclear Cells

Evidence suggests that pre-incubation of hPBMCs with IVIg, reduces LPS-mediated IL-6 production (Andersson, Skansén-Saphir, Sparrelid, & Andersson, 1996). Considering this, we wanted to assess the impact of IVIg treatment on TLR-mediated cytokine production from peripheral blood mononuclear cells. For this purpose, freshly isolated human PBMCs were stimulated with cell surface and endosomal TLR ligands in the absence or presence of different concentrations of IVIg. LPS (TLR4), Zymosan (TLR2), Flagellin (TLR5) were used as cell surface TLR ligands, whereas R848 (TLR7/8), poly I:C (TLR3) and CpG ODN (TLR9) were employed to initiate signaling thorough endosomal TLRs. Release of pro-inflammatory cytokines from treated cells (IL-6, TNF-α and IL-1β) were quantified by ELISA, 24 h after stimulation of hPBMCs (Figure 3.5). IVIg treatment did not alter IL-6 secretion significantly in response to TLR4 or TLR2 ligands, whereas TLR5-mediated IL-6 production was enhanced in the presence of 5 and 25 mg/ml IVIg ~7.3 and 26.4 -fold, respectively compared to corresponding IVIg only treated groups (Figure 3.5a, $p<0.05$). In contrast, TNF-α and IL-1β secretion was strikingly augmented in the presence of IVIg in Zymosan stimulated hPBMCs, where even the lowest Ig concentrations (0.2 and 1 mg/ml) yielded significant improvement (Figure 3.5b, $^{**}p<0.01$, $^{***}p<0.001$). Zymosan induced TNF-α showed 3.2, 4.6 and 5.3 -fold increase in the presence of 0.2, 1, 5 mg/ml Ig respectively, compared to Zymosan alone stimulated samples. These results suggest that IVIg synergize with TLR2-mediated signaling and might explain the mechanism by which low-dose IVIg administration aids to suppress symptoms related to fungal infections in several primary immunodeficiencies (Lanternier et al., 2013). Our results further show that IVIg, boosted Flagellin-induced TNFα production by ~4 to 5 -fold with the highest concentrations of the therapeutic agent. Analysis of IL-1β production revealed that LPS-induced cytokine release was elevated up to 2 -fold, whereas the Fungal ligand Zymosan-mediated IL-1β secretion was 1.9, 4, 7.7 and 6.7-fold higher in the presence of 0.2, 1, 5 and 25 mg/ml IVIg, respectively (Figure

3.5c). These results suggest that in general, IVIg treatment synergize with cell-surface TLR ligands to stimulate higher levels of TNFα and IL-1β production. Interestingly, for the endosomal TLR ligands, IVIg treatment resulted in divergent outcomes. For example, highest concentration of IVIg decreased R848 (TLR7/8) induced IL-6 production by ~1.4 fold when compared to other Ig concentrations. While TNF-α production in R848 stimulated cells remained unchanged through all concentrations of IVIg, IL-1β secretion increased significantly with 5 and 25 mg/ml IVIg increased (2.8 and 2.3 -fold, respectively; Figure 3.5c, $p<0.01$).

Pro-inflammatory cytokine production depends largely on NF-κB activation. However, endosomal TLR signaling (TLR3, TLR7/8 and TLR9) also leads to the activation IRF3/7 transcription factors, resulting in type I IFN and Interferon gamma-induced protein 10 (IP-10) production. Therefore, to assess endosomal TLR-mediated immune activation, IP-10 production was also investigated. IVIg alone increased IP-10 production significantly at 1 and 5 mg/ml concentrations compared to untreated cells (Figure 3.5d, $p<0.05$, $p<0.001$), whereas this effect was abolished at 25 mg/ml. As expected, cell-surface TLR agonists did not trigger substantial IP-10 production by themselves yet IVIg synergized with these ligands in the presence of lower doses.

When endosomal TLR ligand-mediated IP-10 responses were analyzed, co-incubation with lower concentrations of IVIg augmented IP-10 secretion, whereas 25 mg/ml, suppressed cytokine production. Specifically, stimulation with CpG ODN (TLR9 agonist) synergized with 0.2 and 1 mg/ml IVIg in terms of IP-10 production, whereas high dose Ig (5 and 25 mg/ml) demonstrated a suppressive effect and this suppression was significant in poly I:C and R848-induced cytokine production in 25 mg/ml IVIg treated hPBMCs (Figure 3.5d, $p<0.01$, $p<0.001$).

a.

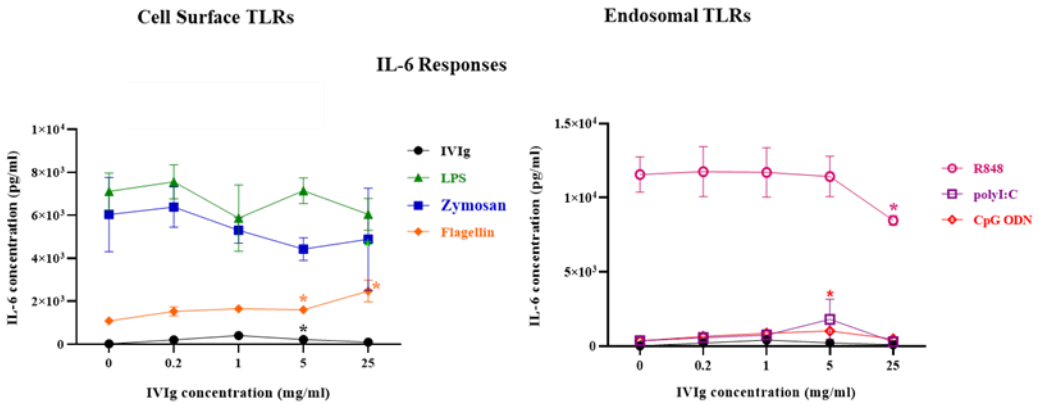
Cell Surface TLRs
Endosomal TLRs
IL-6 Responses
IL-6 concentration (pg/ml)
IVIg concentration (mg/ml)
IVIg
LPS
Zymosan
Flagellin
R848
polyI:C
CpG ODN

b.

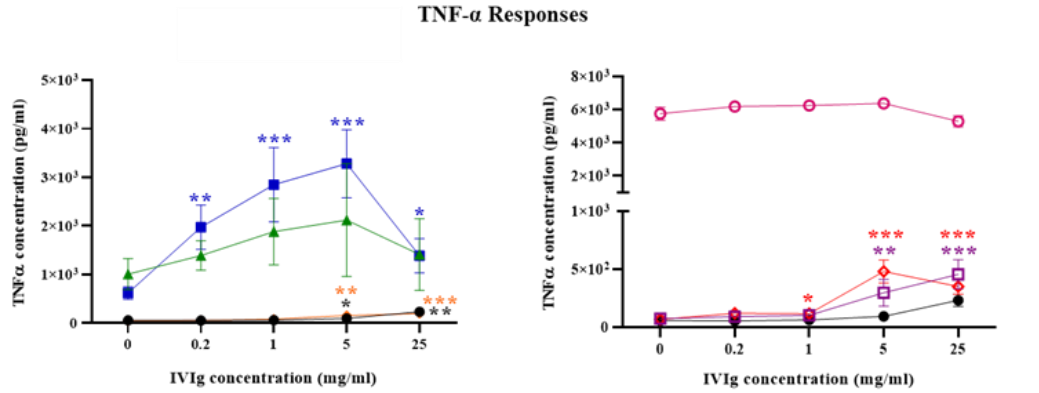
TNF-α Responses
TNFα concentration (pg/ml)
IVIg concentration (mg/ml)

c.

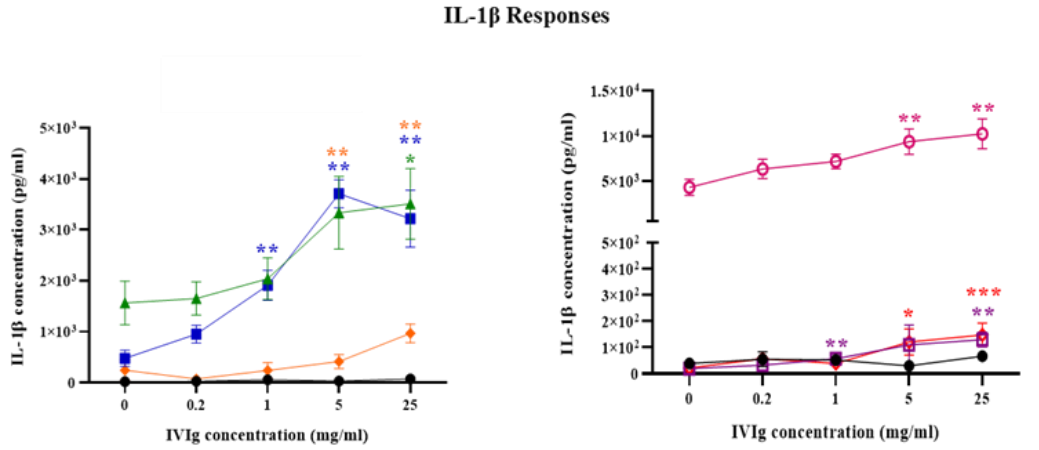
IL-1β Responses
IL-1β concentration (pg/ml)
IVIg concentration (mg/ml)

d.

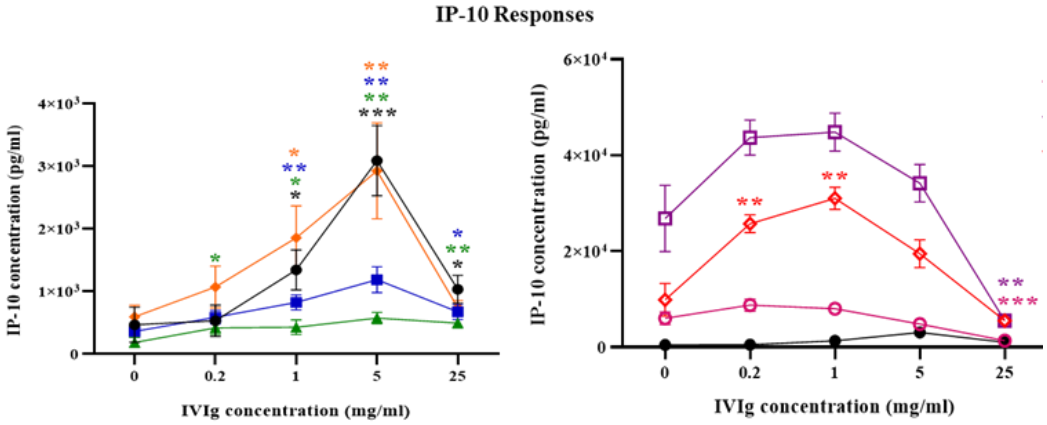

Figure 3.5. Effect of IVIg treatment on cytokine release from hPBMC upon stimulation with various TLR ligands

Peripheral blood mononuclear cells (400.000/well) were treated with 0.2, 1, 5 and 25 mg/ml IVIg and stimulated with LPS, Zymosan, Flagellin, R848, poly I:C or CpG ODN for 24 h. Cell culture supernatants were collected and cytokine production was quantified by ELISA.

The data are presented as average cytokine concentration ± S.E.M (n=4-10), and were analyzed by Mann-Whitney U test (*p<0.05, ** p<0.01, *** p<0.001).

In summary, our results showed that IVIg synergized with most TLR-mediated signaling pathways at lower doses but antagonized signaling at the highest dose. This suppressive effect was more pronounced in the case of endosomal TLR agonists.

These findings suggest that immunoglobulin replacement therapy may be of clinical benefit in prevention of fungal and bacterial infections in primary immune deficiencies and high dose IVIg therapy may suppress endosomal TLR dependent signal transduction that have been implicated in the pathogenesis of autoimmune diseases.

3.3. Induction of Trained Immunity in Human Monocytic Cells by IVIg

Trained immunity, also called “innate immune memory”, is a phenomenon in which organisms’ innate immune system can build resistance to re-infection. This type of

innate immune cell training is known to be induced by the Dectin-1 ligand, β-glucan (Netea et al., 2016). Other than β-glucan, there are many other inducers of trained immunity that act through other receptors such as NOD2 by which BCG vaccine induces memory in innate cells (Mourits, Wijkmans, Joosten, & Netea, 2018). Recently, bovine milk-derived Immunoglobulin G was reported to stimulate training in human monocytes (van Splunter et al., 2018). Based on this finding, we next questioned whether IVIg could induce immune reprogramming in monocytic cells. To test this hypothesis, we have chosen to work with THP1-Dual cells because of their monocytic nature. Along with IVIg, LPS (known to induce reprogramming and/or tolerance (Rusek, Wala, Druszczyńska, & Fol, 2018)) and PGN (found in BCG vaccine which is known to induce training in monocytes through its muramyl dipeptide component (Ifrim et al., 2014)) were used as controls to stimulate reprogramming and/or tolerance. Similar to previous experiments, IVIg's training potential was tested using different concentrations of the therapeutic agent (0.2, 1, 5, 25 mg/ml). LPS (0.2, 1 and 5 µg/ml) and PGN (0.5, 2.5 and 12.5 µg/ml) were used as training controls. As it can be seen in training procedure scheme, The cells were first stimulated with the indicated concentrations of the ligands for a period of 24 h, washed and then rested for 3 days before the second stimulation (Figure 3.6a). Next, the cells trained with various concentrations of IVIg, LPS or PGN were imaged under a light microscope on Day 1 (right after 24 h of training), and on Day 4, when the rest period was terminated and prior to secondary stimulations (Figure D.1.). Microscopy images of THP1-Dual cells showed minor changes after training with IVIg and LPS when compared to untrained cells. However, highest concentration of PGN (12.5 µg/ml) induced a switch to macrophage-like elongated cells (Figure 3.6b). Based on published results, where trained cells were larger in size compared to untrained and/or tolerized cells (Ifrim et al., 2014), morphological inspection of PGN trained cells (highest concentration) suggested that the highest concentration of PGN was able to induce reprogramming in THP1-Dual monocytes.

a.

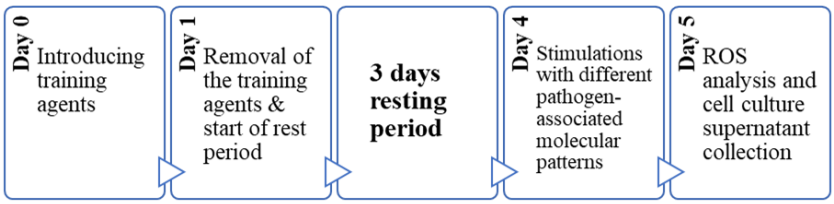
Day 0
Introducing training agents
Day 1
Removal of the training agents & start of rest period
3 days resting period
Day 4
Stimulations with different pathogen-associated molecular patterns
Day 5
ROS analysis and cell culture supernatant collection

b.

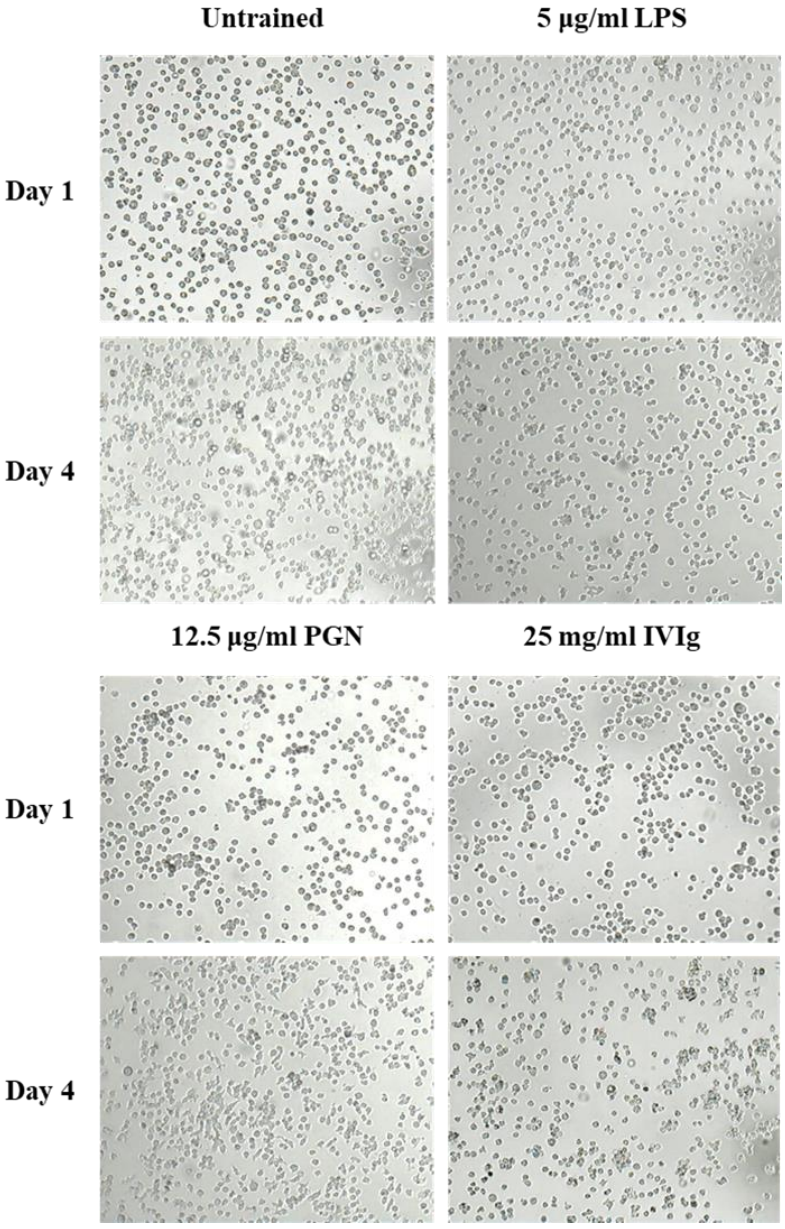
Untrained
5 µg/ml LPS
Day 1
Day 4
12.5 µg/ml PGN
25 mg/ml IVIg
Day 1
Day 4

Figure 3.6. Light microscopy images of wild type THP1-Dual cells trained with IVIg, LPS and PGN

(a) Overview of training procedure. (b) Microscopy images of trained THP1-Dual cells were taken 24 h after administration of training agents (Day 1) and 3 days after the rest period (Day 4). Images were taken under 4x magnification. Images of other training conditions can be found in Appendix D, Figure D.1.

LPS and IVIg training induced only minor changes in cell morphology (Figure 3.6b). Since a change in cellular morphology is a crude output of reprogramming and may require extended incubation (~7 days) for observable effects to fully manifest, we next assessed training potential of the ligands through measurement of ROS production and quantification of secondary cytokine secretion. Reactive oxygen species production and secondary cytokine responses were measured from cells or cell culture supernatant, respectively, after secondary ligand stimulation was performed. Secondary stimulants included bacterial (LPS), fungal (Zymosan and opsonized heat-killed *Candida albicans* (opsonized HKCA)) and viral (R848) ligands which were chosen considering the type of infections seen in clinical conditions in which IVIg is administered as a therapeutic.

3.3.1. Assessment of Reactive Oxygen Species (ROS) Production in THP1 Cells Following Training

To characterize functional changes in trained THP-1 cells, ROS production was assessed as a reporter of trained immunity (Bekkering et al., 2016). For this, cytosolic ROS levels of trained and untrained THP1-Dual cells were stimulated LPS, Zymosan, opsonized HKCA or R848. The cells were then analyzed by Flow cytometry following DHR123 staining after 24 h of ligand stimulation (Appendix B, Figure B.2.). Fold change in % DHR123 positive trained cells over untrained cells were analyzed as depicted in Figure 3.7. Each training condition (IVIg, LPS or PGN) was compared as a group to untrained cells using Kruskal-Wallis with Dunnet's multiple comparison test to determine statistical significance (Figure 3.7.). Among the tested training agents and conditions, IVIg (25 mg/ml), LPS (0.2 and 5 µg/ml) and PGN (12.5 µg/ml)

significantly augmented ROS production in unstimulated cells compared to untrained cells (Figure 3.7a). IVIg trained cells (25 mg/ml) generated ~10-fold more ROS in response to LPS, Zymosan and R848 stimulation ($p<0.05$, $p<0.01$, Figures 3.7b, c and e), suggesting that the highest dose of Ig reprogrammed THP1 monocytes to support their oxidative burst activity in response to bacteria and virus associated- but not to fungal-ligand, HKCA (Figure 3.7d). In LPS trained cells (5 µg/ml), cytosolic ROS accumulation was significantly higher following secondary stimulation with LPS, Zymosan, opsonized HKCA and R848 ($p<0.05$, $p<0.01$, Figures 3.7b, c, d and e). PGN training (12.5 µg/ml), similarly augmented ROS production in response to LPS and Zymosan ($p<0.05$, Figures 3.7b and c), had no significant effect on HKCA-induced ROS (Figure 3.7d). For R848 stimulated samples, only the lowest dose of PGN training (0.5 µg/ml) had a significant measurable effect ($p<0.01$, Figure 3.7e).

These results suggest that similar to the training controls (LPS and PGN), IVIg reprograms THP-1 monocytes to increase their responsiveness as demonstrated by the amplification of ROS production.

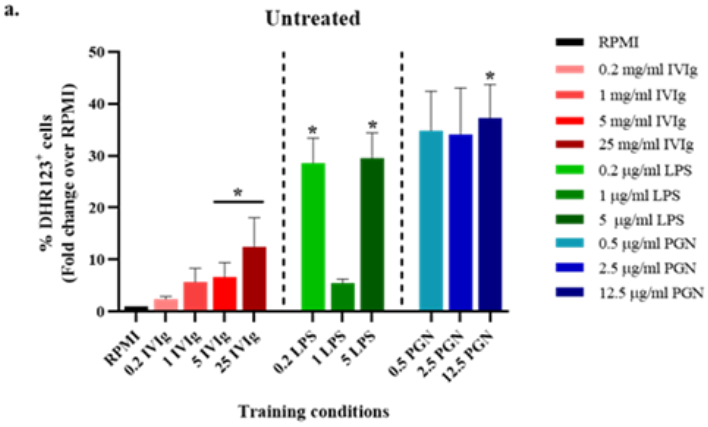

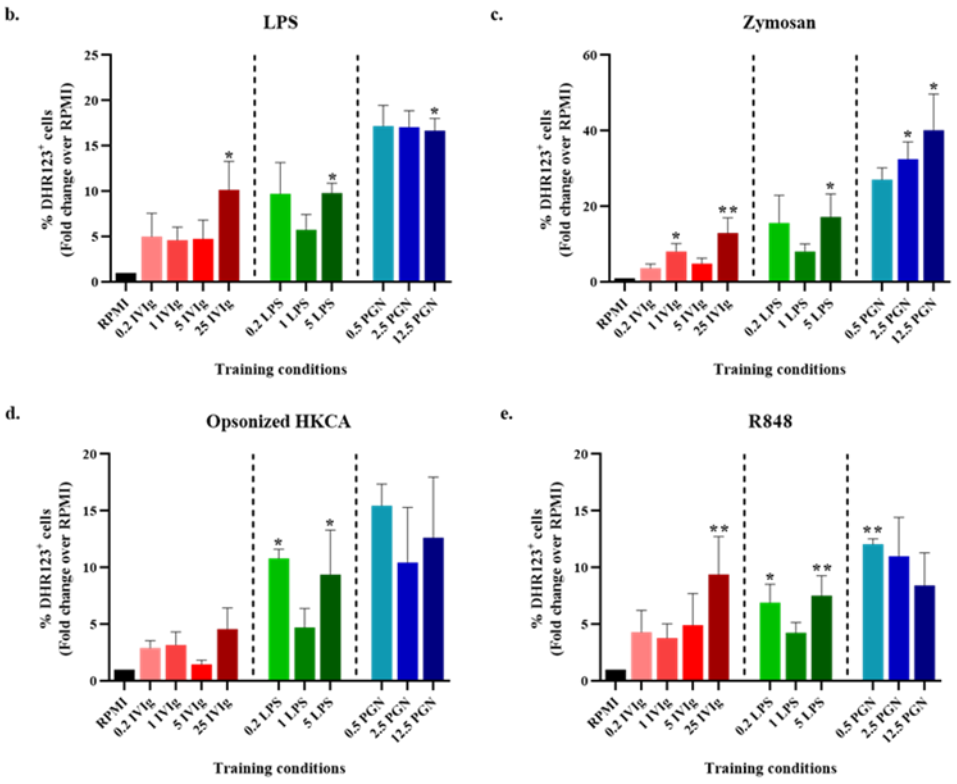

Figure 3.7. Fold-change in percentage of DHR123+ cells over RPMI trained THP1-Dual cells after secondary stimulation with PRR ligands

THP1-Dual cells (100,000/well) were stimulated for 24 h with LPS, Zymosan, opsonized HKCA and R848 (see Table 2.2. for ligand concentrations) after training with the indicated agents and concentrations. The cells were stained with DHR123 and analyzed via Flow cytometry at the end of the stimulation.

All training conditions were compared to RPMI training group statistically by Kruskal-Wallis test followed by Dunnet's multiple comparison test (n=2-5, *: $p<0.05$, **: $p<0.01$).

3.3.2. Pro-inflammatory Cytokine Secretion from Trained THP1 Cells in Response to Secondary Stimulation

Pro-inflammatory cytokine (TNFα, IL-6, IL-1β) recall responses, have been shown to be enhanced following training (Mourits et al., 2018). Therefore, as a third parameter to examine trained immunity profile, pro-inflammatory cytokine release from IVIg, LPS or PGN trained cells were determined from cell culture supernatants upon secondary stimulation with the previously mentioned PRR ligands by ELISA. Fold

change in released cytokine levels of trained cells over untrained cells (RPMI group) were calculated and analyzed by using Kruskal-Wallis with Dunnet's multiple comparison test (Figure 3.8, 3.9 and 3.10).

Analysis of TNFα recall responses revealed that training with IVIg, LPS or PGN had no impact on background levels (untreated samples, Figure 3.8a). However, training conditions affected the response to secondary ligand stimulation with variable outcomes. For example, LPS (5 µg/ml) and PGN (2.5 µg/ml) training caused a significant decrease in TNFα levels ($p<0.05$, $p<0.01$, Figure 3.8b), suggesting that these two training conditions tolerized the cells against LPS activation. IVIg trained cells produced similar levels of TNFα when compared to untrained cells (Figure 3.8b). None of the training conditions altered TNF response to Zymosan with respect to untrained cells (Figure 3.8c). IVIg training was the only condition supporting >10-fold increase in TNFα production in response to HKCA, although this increase was not statistically significant in comparison to untrained cells (Figure 3.8d). It is known that THP1 monocytes do not express high levels of Dectin-1 receptor in their undifferentiated state (Rogers, Williams, Feng, Lewis, & Wei, 2013). Therefore, responses to Zymosan and opsonized HKCA may be limited and secondary stimulation with these ligands might fail to reveal the training potential of the reprogramming agents. Interestingly, whereas IVIg (25 mg/ml) and LPS (5 µg/ml) training augmented responses to the viral ligand R848 3- and 2-fold, respectively, PGN training (2.5 and 12.5 µg/ml) tolerized the cells against this ligand ($p<0.05$, $p<0.01$, Figure 3.8e).

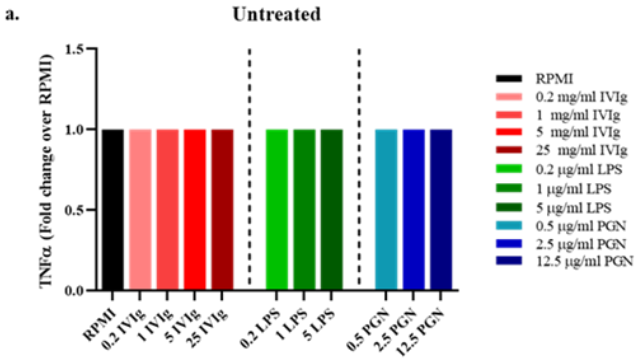

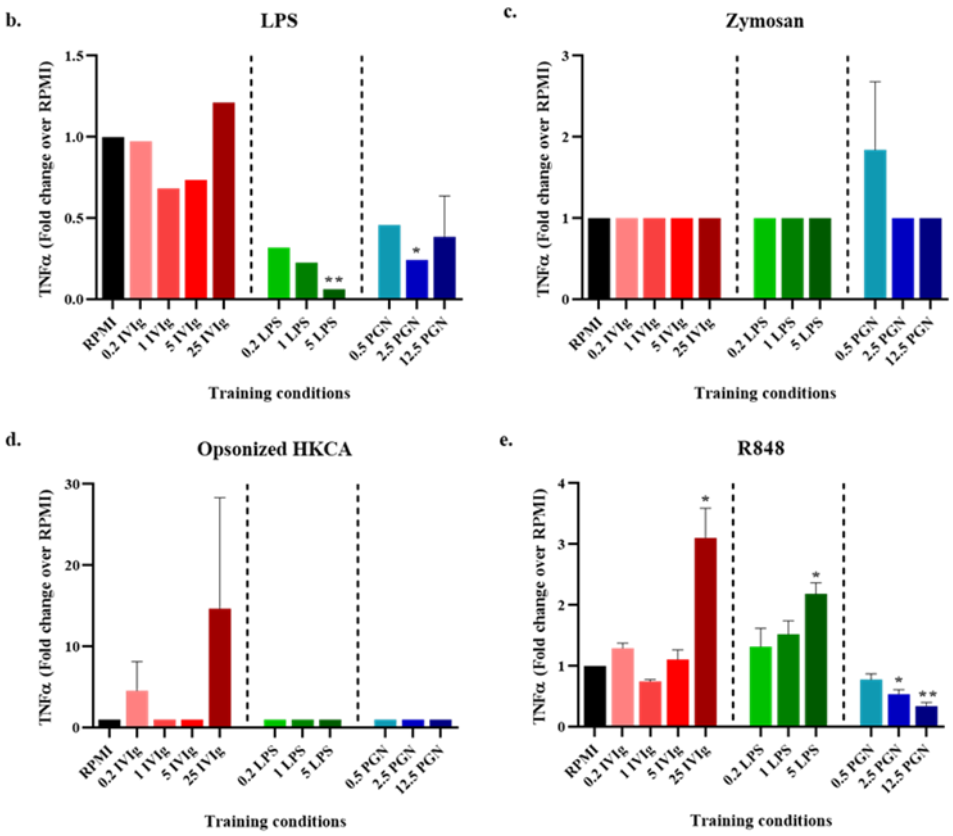

Figure 3.8. Fold change in TNFα production from trained cells over untrained cells in response to secondary PRR ligand stimulation

THP1-Dual cells (100.000/well) were stimulated for 24 h with LPS, Zymosan, opsonized HKCA and R848 (see Table 2.2. for ligand concentrations) after training with the indicated concentrations of IVIg, LPS and PGN. Cell culture supernatants were collected and cytokine levels were then quantified by ELISA.

All training conditions were compared to RPMI training group statistically by Kruskal-Wallis test followed by Dunnet's multiple comparison test (n=3-4, *: $p<0.05$, **: $p<0.01$, ***: $p<0.001$).

IL-6 production increased upon training with IVIg in response to secondary LPS stimulation. In Figure 3.9b, it can be seen that both 0.2 and 25 mg/ml IVIg, with the highest concentration being the most effective of them, showed significant increase in fold induction of IL-6 over untrained cells (~1.5- versus 2.5-fold, $p<0.05$ and $p<0.001$ respectively). PGN training also exerted positive effects on IL-6 production mediated by TLR4 such that 12.5 µg/ml PGN gave rise to significantly higher response (~2.5-

fold, p<0.01). In contrast, LPS training (5 µg/ml) had the opposite effect on LPS secondary stimulation-induced IL-6 production and statistically significantly decreased secretion (p<0.01. Figure 3.9b). Conversely, only PGN (12.5 µg/ml) exerted training effect on THP1-Dual cells and enhanced responsiveness to the fungal ligands (Zymosan and opsonized HKCA) when compared to other training conditions and untrained controls (p<0.01, Figure 3.9 c and d). Since R848 stimulation resulted in a very robust IL-6 response, any effect of training could not be determined above the maximum limit of detection in ELISA (Figure 3.9e).

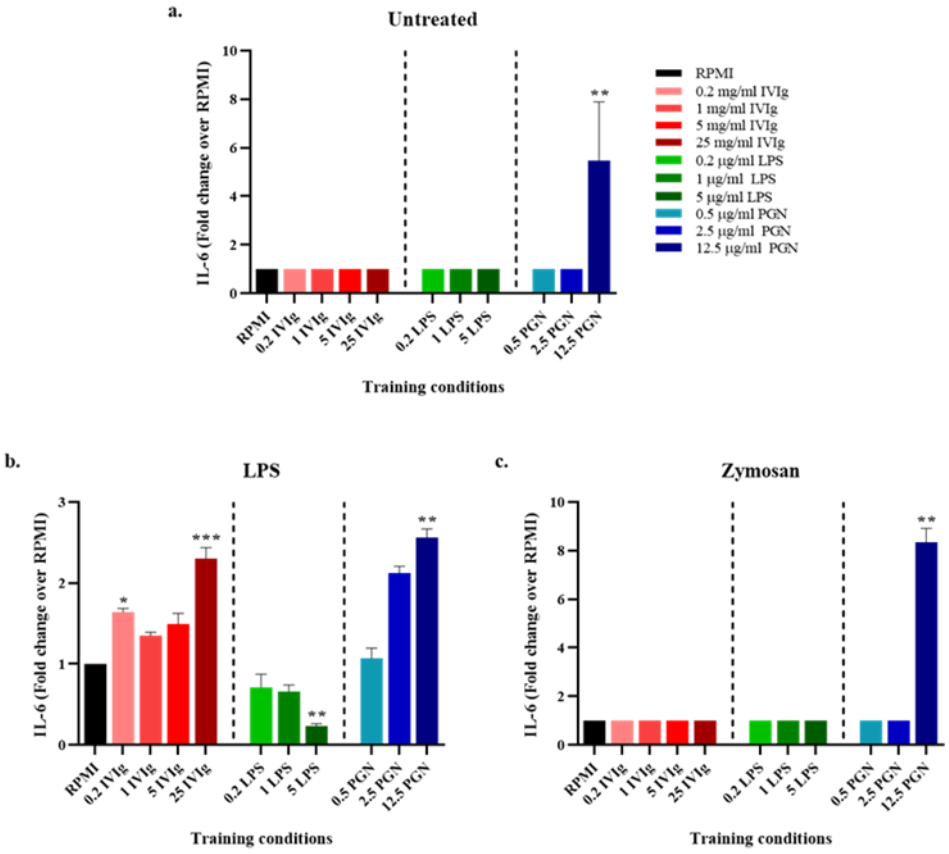

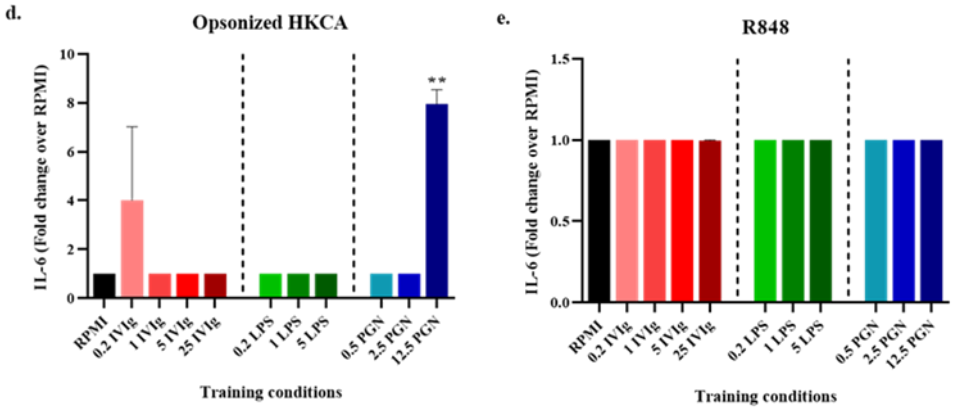

Figure 3.9. Fold change in IL-6 production from of trained cells over untrained cells in response to secondary PRR ligand stimulation

THP1-Dual cells (100.000/well) were stimulated for 24 h with LPS, Zymosan, opsonized HKCA and R848 (see Table 2.2. for ligand concentrations) after training with the indicated concentrations of IVIg, LPS and PGN. Cell culture supernatants were collected and cytokine levels were then quantified by ELISA.

All training conditions were compared to RPMI training group statistically by Kruskal-Wallis test followed by Dunnet's multiple comparison test (n=3-4, *: $p<0.05$, **: $p<0.01$, ***: $p<0.001$).

IL-1β was another pro-inflammatory cytokine which was analyzed to gain insight into training potential of the chosen ligands and concentrations. Similar to TNFα and IL-6 responses, IVIg enhanced IL-1β production in response to secondary LPS stimulation when used at its highest training concentration (25 mg/ml, $p<0.01$, Figure 3.10b), whereas LPS and PGN trained cells did not show significant changes (Figure 3.10b). 25 mg/ml IVIg trained cells demonstrated ~3-fold increase in IL-1β production in secondary R848 stimulated samples but this difference was not statistically significant (Figure 3.10 e). IL-1β release in response to R848 stimulation in PGN (12.5 µg/ml) trained cells was significantly suppressed ($p<0.001$, Figure 3.10e).

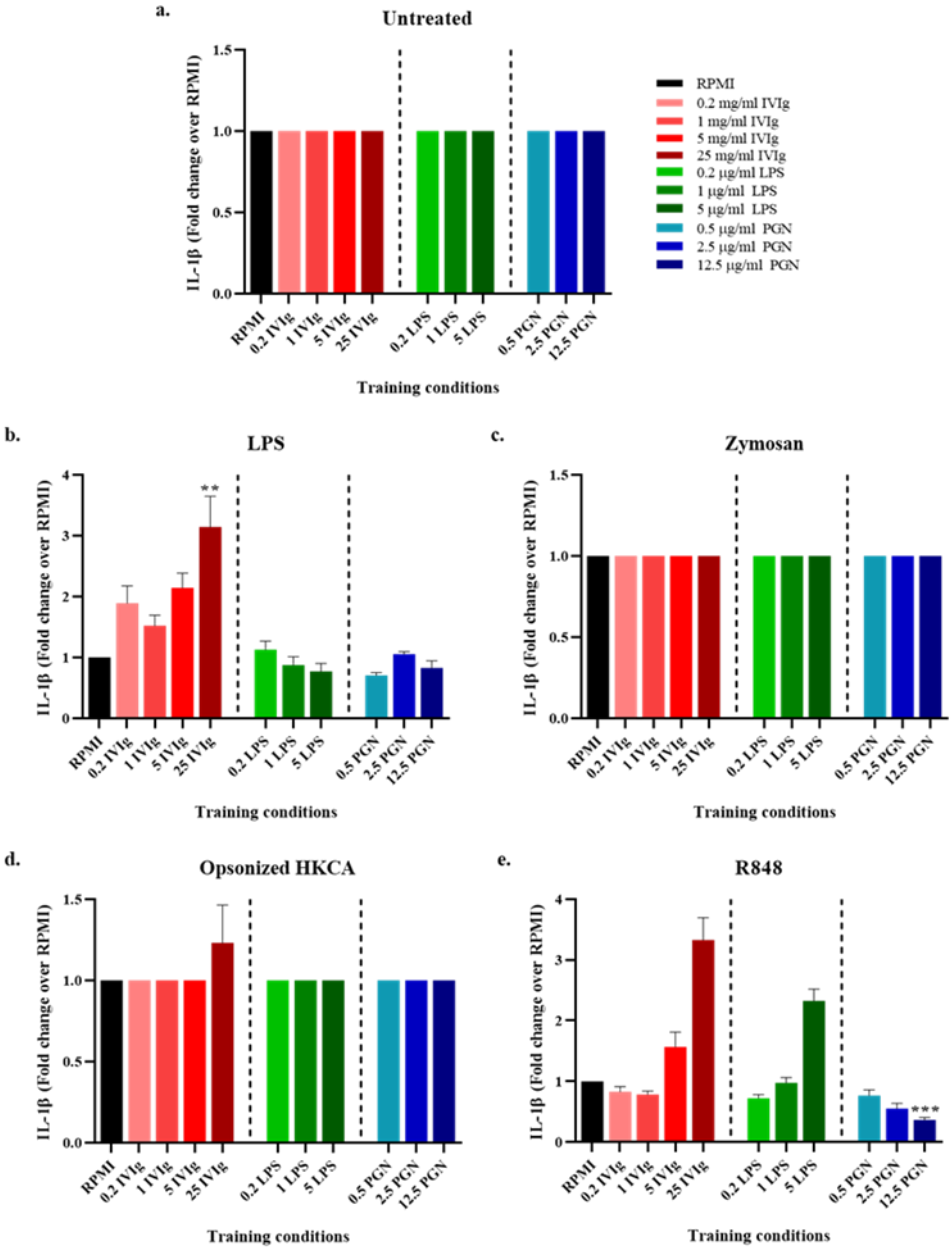

Figure 3.10. Fold change in IL-1β production from trained cells over untrained cells in response to secondary PRR ligand stimulation

THP1-Dual cells (100.000/well) were stimulated for 24 h with LPS, Zymosan, opsonized HKCA and R848 (see Table 2.2. for ligand concentrations) after training with the indicated concentrations of IVIg, LPS and PGN. Cell culture supernatants were collected and cytokine levels were then quantified by ELISA.

All training conditions were compared to RPMI training group statistically by Kruskal-Wallis test followed by Dunnet's multiple comparison test (n=3-4, *: $p<0.05$, **: $p<0.01$, ***: $p<0.001$).

3.3.3. Determination of NF-κB Activation in Trained THP1 Cells in Response to Secondary PRR Ligand Stimulation

Since TLR stimulation activates the canonical NF-κB pathway which leads to pro-inflammatory cytokine production (Liu, Zhang, Joo, & Sun, 2017), we also wanted to see how NF-κB activation in THP1-Dual cells changed in response to LPS, Zymosan, opsonized HKCA and R848 secondary stimulation following training. To further confirm the trained/tolerized responses that we observed in ELISA results, we utilized secreted embryonic alkaline phosphatase (SEAP) reporter property of the THP1-Dual cell line (Invivogen, USA). These cells produce SEAP and secrete it into cell culture medium upon TLR-mediated NF-κB activation. Secreted SEAP is then quantitated using the QUANTI-Blue reagent. In the presence of SEAP, the color of the detection reagent QUANTI-Blue changes from pink to purple/dark blue, which can be followed by measuring the optical density (OD) to quantify NF-κB inducible SEAP reporter activity. NF-κB activation in trained THP1 cells in response to secondary PRR ligand stimulations were quantitated and the results are presented in Figure 3.11. Findings suggest that the extent of NF-κB activation is in support of ELISA results, where a significant increase in NF-κB activation was observed in IVIg trained cells (25 mg/ml) in response to LPS and R848 ($p<0.05$, Figure 3.11b and e). Although Zymosan-induced cytokine levels of IVIg trained cells could not be measured, SEAP reporter activity implies that IVIg (25 mg/ml) training can increase NF-κB activation against this fungal ligand. Similar to IVIg, LPS and PGN seem to aid trained response to Zymosan ($p<0.05$, Figure 3.11c). LPS training suppressed NF-κB activity in response to secondary LPS stimulation but not the response to other ligands. It was also clear that PGN training (12.5 µg/ml) caused tolerance in response to R848 re-stimulation as deduced from reduced SEAP activity (Figure 3.11e).

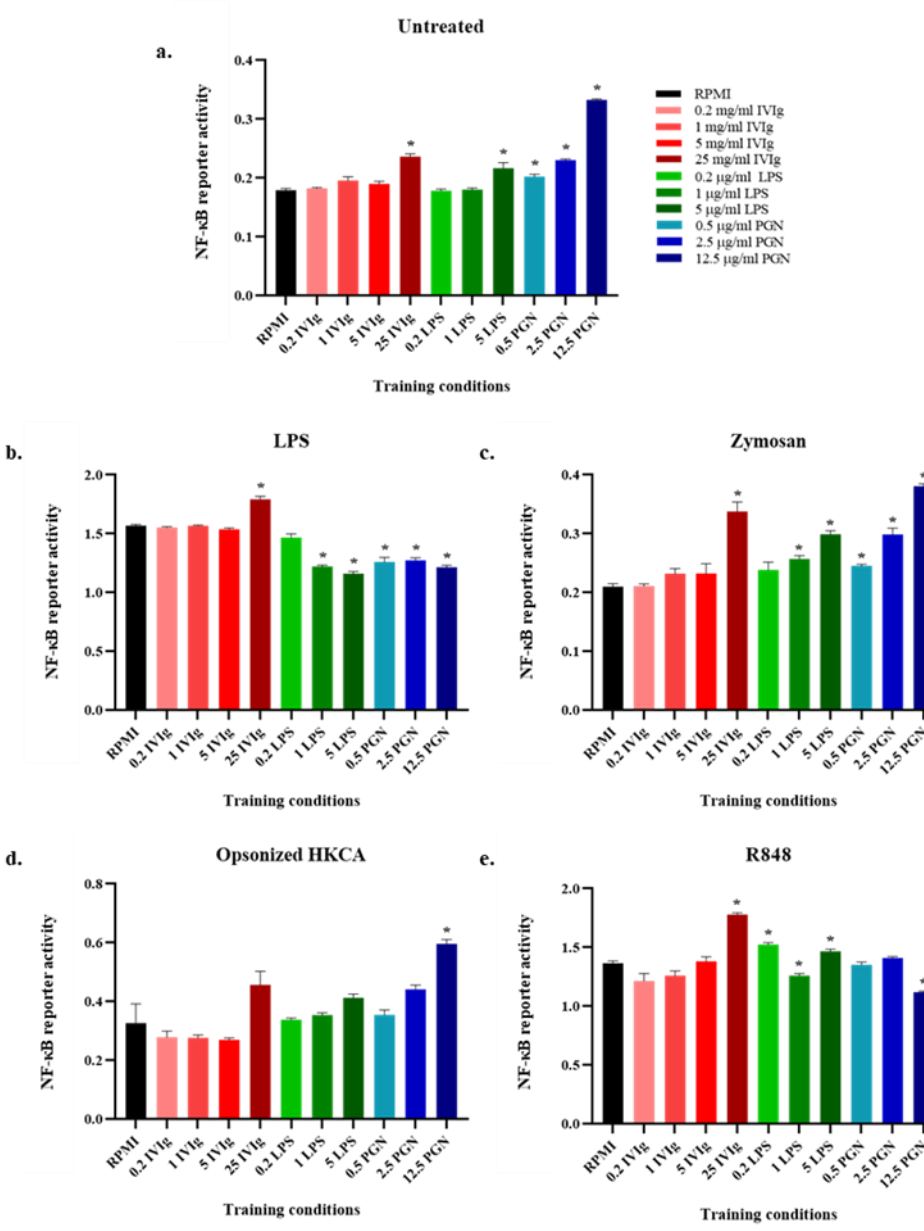

Figure 3.11. NF-κB inducible SEAP activity in response to secondary PRR ligand stimulation following training with different concentrations of IVIg, LPS, PGN.

THP1-Dual cells (100.000/well) were stimulated for 24 h with LPS, Zymosan, opsonized HKCA and R848 (see Table 2.2. for ligand concentrations) after training with the indicated agents and concentrations. Cell culture supernatants were collected and QUANTI-Blue reagent was used to detect SEAP in the supernatants. Optical Density (OD) was measured at 645 nm.

All training conditions were compared to RPMI training group statistically by Mann-Whitney U test (n=4, *: $p<0.05$).

In conclusion, based on the pro-inflammatory cytokine responses and SEAP-dependent NF-κB activity assay, our data suggest that IVIg can induce trained immunity towards LPS and R848 in undifferentiated THP1-Dual monocytes. LPS training tolerized the cells against LPS stimulation but not to R848 recall. These results are in line with literature findings where training through the TLR4/MAPK dependent pathway tolerize cells (Netea et al., 2016) but also indicate that the outcome is dependent on the signaling pathway the ligands act through. THP1-Dual cells were tolerized by LPS training in terms of cytokine release upon TLR4-mediated ligand stimulation but not against TLR7/8-mediated immune responses. While LPS training mainly causes tolerance, PGN training resulted in tolerance against LPS in terms of TNFα and IL-1β but not IL-6 response. However, PGN training caused a state of unresponsiveness to the viral TLR7/8 ligand. Our study shows for the first time that the mechanism underlying IVIg-induced enhancement of immune responses in patients with defective immunity may partly be dependent on IVIg's potential to exert reprogramming in innate immune cells and enhance recall responses to bacterial, fungal and/or viral ligands.

CHAPTER 4

CONCLUSIONS & FUTURE PERSPECTIVES

Intravenous Immunoglobulin (IVIg) was administered for immunoglobulin replacement to an immunodeficient patient for the first time in 1952 (Stiehm, 2013). Since then, IVIg was used to treat many primary immunodeficiencies, and later on, this therapeutic was adopted for treatment of inflammatory/autoimmune conditions. Outcome of IVIg treatment depends on the administered dose in such a way that low doses supplement immune deficiencies, whereas high doses suppress inflammation/autoimmunity. Until now, researchers have been trying to understand the mode of action of IVIg and there are several suggested mechanisms as discussed in Section 1.2.1. In this thesis, we focused on the effects of IVIg on different immune cell populations and aimed to propose a new mechanism that could account for the divergent therapeutic effects of IVIg treatment.

For this purpose, we first wanted to examine the effects of IVIg on neutrophil functions since whether IVIg alters neutrophil-mediated innate immune functions is still unclear. Therefore, we focused on the major neutrophil functions including ROS production, cytokine secretion and neutrophil extracellular trap formation (Section 3.1.).

To investigate IVIg mediated effect on neutrophils, we first utilized four different concentrations of IVIg to evaluate the dose dependent effect of stand-alone IVIg treatment on ROS production in neutrophils (Section 3.1.1.). We observed that the highest dose of Ig increased ROS production significantly. This suggests that IVIg can directly prime neutrophils and augment oxidative burst even in the absence of any other immune activators.

Based on these preliminary results, we next hypothesized that IVIg treatment would modulate the responsiveness of neutrophils to immune activators (Section 3.1.2.). Administration of this therapeutic is known to aid clearance of fungal infections (Elluru, Kaveri, & Bayry, 2015). Therefore, we examined cytosolic ROS levels in neutrophils stimulated with a model fungal ligand (Zymosan), a bacterial ligand (LPS) or PMA (PKC activator) with or without IVIg treatment. Results showed that Ig treatment (5 and 25 mg/ml) augmented ROS levels in response to Zymosan up to 7-fold. Conversely, LPS-stimulated ROS production was not affected, whereas IVIg suppressed ROS levels triggered by PMA. Overall, these findings suggest that IVIg can aid Dectin-1/TLR2 mediated ROS production but has the opposite effect on Protein Kinase C signaling pathway. Although our results also support the idea that IVIg does not alter TLR4-mediated activation, since LPS is a poor ROS inducer, this assay would not be ideal to derive such a conclusion.

Another important neutrophil function critical for pathogen clearance is NETosis-mediated neutrophil extracellular trap (NET) formation. ROS production is known to be strongly associated with NET formation (Kaplan & Radic, 2012). Therefore, to analyze this specific form of cell death, we stimulated the neutrophils with the ligands given above along with four different concentrations of Ig (Section 3.1.3). Results expectedly correlated with the ROS data as Zymosan-induced NET formation was augmented in the presence of IVIg. LPS-induced NET formation was also enhanced in the presence of IVIg, suggesting that Ig administration can aid clearance of not only fungal but also bacterial infections through NETosis. Conversely, IVIg suppressed NET formation induced by the potent neutrophil activator PMA. These results indicate that IVIg can augment neutrophil responses to Dectin-1/TLR2 and TLR4 agonists but exhibit suppressive effects when introduced simultaneously with a PKC activator.

To gain further insight into how IVIg impacts neutrophil functions, we also assessed its effect on cytokine release from Zymosan, LPS or R848 activated neutrophils to mimic conditions relevant in fungal, bacterial or viral infections, respectively (Section 3.1.4.). IVIg dose dependently increased IL-8 production in response to Zymosan and

LPS stimulation whereas R848 (TLR7/8) mediated cytokine production decreased in the presence of the highest Ig concentration.

Collectively, these results indicate that IVIg can synergize with Dectin-1/TLR2 and TLR4 signaling pathways in the presence of low dose Ig and help clearance of fungal and bacterial pathogens, whereas high doses show suppressive effects as it was observed in TLR7/8-mediated cytokine production. TLR7/8 mediated inflammatory responses contribute to pathogenesis of certain autoimmune diseases such as systemic lupus erythematosus, our data suggest that high dose IVIg would ameliorate inflammation in this setting.

Next, we also analyzed how IVIg treatment altered responses to TLR-mediated immune activation in human peripheral blood mononuclear cells (hPBMCs). Evidence suggests that pre-incubation of hPBMCs with IVIg reduces LPS-mediated IL-6 production (Andersson, Skansén-Saphir, Sparrelid, & Andersson, 1996). Equipped with this knowledge, we examined the effect of Ig treatment on TLR-mediated cytokine production from hPBMCs (Section 3.2.). Consistent with the neutrophil data, hPBMCs treated with low doses of IVIg showed elevated pro-inflammatory cytokine production in TLR2-agonist activated cells. TLR4 and TLR5-mediated pro-inflammatory cytokine production was similarly increased with IVIg co-treatment, suggesting that in general, IVIg synergizes with cell surface TLR ligands in terms of TNFα and IL-1β production. Interestingly, IVIg treatment showed differential effects on endosomal TLR ligand-mediated responses. TLR7/8-mediated IL-6 response decreased with the highest concentration of Ig, while IL-1β secretion increased with the two highest concentrations and TNF-α responses remained unchanged in the presence of IVIg. In addition to pro-inflammatory cytokine production via NF-κB activation, we also examined IP-10 secretion as a reporter of IRF3/7 transcription factor activation, based on the knowledge that endosomal TLRs trigger type I IFN and IP-10 production. Whereas lower IVIg concentrations increased IP-10 production in response to endosomal TLR ligands, high dose Ig suppressed cytokine production especially in the case of TLR7/8 ligand dependent activation (R848).

These findings suggest that low dose immunoglobulin therapy can help to prevent and clear fungal, bacterial and/or viral infections and high doses may suppress endosomal TLR-dependent signaling that may have implications in the treatment of autoimmune diseases.

In the second part of this thesis, based on the evidence showing that bovine milk-derived IgG can induce innate immune reprogramming in human monocytes (van Splunter et al., 2018), we hypothesized that IVIg could similarly act as an inducer of trained immunity. To test for this hypothesis, we analyzed changes in cell morphology, ROS production and pro-inflammatory cytokine release as well as NF-κB activity in IVIg trained THP1-Dual cells following secondary stimulation with various ligands. As training controls, LPS and PGN which are known to induce training/tolerance (Ifrim et al., 2014; Rusek, Wala, Druszczyńska, & Fol, 2018) were chosen (Section 3.3.).

Morphological analysis of THP1-Dual cells was inconclusive in the case of IVIg or LPS training, whereas PGN trained cells acquired macrophage-like elongated shapes at the end of the resting period of training.

For secondary stimulations, bacterial (LPS), fungal (Zymosan and opsonized HKCA) and viral (R848) mimetic ligand were used to replicate the type of infections observed in the clinic intended for IVIg therapy. To delineate how training affected cellular functions, ROS production was assessed as one of the reporter assays. When ROS levels of trained and untrained cells were compared, IVIg (25 mg/ml) enhanced secondary ROS production in THP1-Dual cells in response to LPS, Zymosan and R848 similar to training controls (LPS and PGN) (Section 3.3.1.).

As a second readout of trained immunity, pro-inflammatory cytokine (TNF-α, IL-6, IL-1β) recall responses previously reported to be enhanced following training (Mourits et al., 2018), were analyzed (Section 3.3.2.). TNF-α responses of IVIg trained cells were remarkably enhanced in response to TLR7/8 agonist (R848) stimulation, whereas PGN induced tolerance against the same ligand. Moreover, IVIg was the only

training agent that could exert ~10 -fold increase in this cytokine in response to opsonized HKCA. Secondly, the highest concentration of PGN significantly increased secondary LPS, Zymosan and opsonized HKCA stimulated IL-6 responses, consistent with its training potential. IVIg (25 mg/ml) was the most efficient training agent against LPS while LPS training favored tolerance against secondary LPS stimulation. Lastly, secondary IL-1β production in response to LPS significantly increased in IVIg trained cells, whereas the other training agents failed to show such an effect. Similar to TNF-α responses, IL-1β production in PGN trained/R848-stimulated cells decreased significantly, indicating that PGN tolerized the cells against this viral ligand. To further support these results, we measured the levels of NF-κB-inducible SEAP secreted from THP1-Dual cells (Section 3.3.3.). NF-κB reporter activity showed that IVIg was the most potent training agent in secondary LPS stimulated cells, whereas the other two agents tolerized the cells. Zymosan-induced NF-κB activity was augmented under all training conditions. Finally, consistent with the results of cytokine production, IVIg exerted the highest training capacity in response to R848, while PGN tolerized the cells. In summary, results of reporter assays based on pro-inflammatory cytokine responses and NF-κB activity showed that IVIg treatment reprogrammed undifferentiated THP1-Dual cells to enhance their responsiveness to LPS and R848. Conversely, LPS training tolerized the cells against secondary LPS (TLR4) stimulation but not against R848 (TLR7/8). Interestingly, PGN training generated tolerance only against this viral PRR agonist mimetic. Overall, our data suggests that IVIg can induce innate reprogramming which may account for its infection-protective effects when used in patients with immunodeficiencies.

Our preliminary results might implicate that, IVIg can induce innate reprogramming through Fc receptors, most probably through the FcγRI (CD64) which is the only high-affinity Fc receptor in humans capable of binding to monomeric Ig (Bruhns et al., 2009). This possible signaling cascade triggered by interaction of IVIg and FcγRI

might cause epigenetic modifications through activation of Syk-dependent downstream pathways (Getahun & Cambier, 2015).

In the near future, we also intend to analyze possible metabolic changes (Warburg effect) in IVIg trained cells (Netea & van der Meer, 2017) as well as indicated epigenetic modifications in monocytes upon training (H3K4 modifications) (van der Heijden et al., 2018). To ensure that IVIg indeed induce trained immunity, we intend to inhibit critical downstream molecules of FcγRI (Syk and MAPK) to see whether the reprogramming in monocytes would remain intact or not. Furthermore, inhibition of histone methyltransferase and histone demethylase would give us a better understanding on how the possible epigenetic changes upon IVIg training affects the secondary responses of THP1-Dual cells. These preliminary findings on IVIg-trained THP1-Dual cells should be replicated using primary human monocytes to accurately conclude that IVIg can induce training in human monocytes in FcγRI dependent manner.

REFERENCES

Albin, S., & Cunningham-Rundles, C. (2014). An update on the use of immunoglobulin for the treatment of immunodeficiency disorders. *Immunotherapy*. https://doi.org/10.2217/imt.14.67

Álvarez-Cardona, A., Rodríguez-Lozano, A. L., Blancas-Galicia, L., Rivas-Larrauri, F. E., & Yamazaki-Nakashimada, M. A. (2012). Intravenous immunoglobulin treatment for macrophage activation syndrome complicating chronic granulomatous disease. *Journal of Clinical Immunology*. https://doi.org/10.1007/s10875-011-9616-5

Andersson, J., Skansén-Saphir, U., Sparrelid, E., & Andersson, U. (1996). Intravenous immune globulin affects cytokine production in T lymphocytes and monocytesjmacrophages. *Clinical & Experimental Immunology*. https://doi.org/10.1111/cei.1996.104.s1.10

Atmadja, A. K., Atkinson, R., Sartono, E., Partono, F., Yazdanbakhsh, M., & Maizels, R. M. (1995). Differential decline in filaria-specific igg1, igg4, and ige antibodies in brugia malayi-infected patients after diethylcarbamazine chemotherapy. *Journal of Infectious Diseases*, *172*(6), 1567–1572. https://doi.org/10.1093/infdis/172.6.1567

Bassing, C. H., Swat, W., & Alt, F. W. (2002). The mechanism and regulation of chromosomal V(D)J recombination. *Cell*, *109*(2 SUPPL. 1). https://doi.org/10.1016/S0092-8674(02)00675-X

Basta, M. (2008). Ambivalent effect of immunoglobulins on the complement system: Activation versus inhibition. *Molecular Immunology*. https://doi.org/10.1016/j.molimm.2008.07.012

Bayry, J., Fournier, E. M., Maddur, M. S., Vani, J., Wootla, B., Sibéril, S., … Kaveri, S. V. (2011). Intravenous immunoglobulin induces proliferation and immunoglobulin synthesis from B cells of patients with common variable immunodeficiency: A mechanism underlying the beneficial effect of IVIg in primary immunodeficiencies. *Journal of Autoimmunity*. https://doi.org/10.1016/j.jaut.2010.09.006

Bayry, J., Lacroix-Desmazes, S., Carbonneil, C., Misra, N., Donkova, V., Pashov, A.,

… Kaveri, S. V. (2003). Inhibition of maturation and function of dendritic cells by intravenous immunoglobulin. *Blood*. https://doi.org/10.1182/blood-2002-05-1447

Behring, & Kitasato. (1890). Ueber das Zustandekommen der Diphtherie-Immunität und der Tetanus-Immunität bei Thieren. *Deutsche Medizinische Wochenschrift*, *16*(49), 1113–1114. https://doi.org/10.1055/s-0029-1207589

Blank, M., Anafi, L., Zandman-Goddard, G., Krause, I., Goldman, S., Shalev, E., … Shoenfeld, Y. (2007). The efficacy of specific IVIG anti-idiotypic antibodies in antiphospholipid syndrome (APS): Trophoblast invasiveness and APS animal model. *International Immunology*. https://doi.org/10.1093/intimm/dxm052

Boes, M. (2000). Role of natural and immune IgM antibodies in immune responses. *Molecular Immunology*, *37*(18), 1141–1149. https://doi.org/10.1016/S0161-5890(01)00025-6

Brekke, O. H., Michaelsen, T. E., & Sandlie, I. (1995). The structural requirements for complement activation by IgG: does it hinge on the hinge? *Immunology Today*, *16*(2), 85–90. https://doi.org/10.1016/0167-5699(95)80094-8

Brouwers, H. A. A., Overbeeke, M. A. M., Ouwehand, W. H., Keuning, K., Van Ertbruggen, I., Van Leeuwen, E. F., … Engelfriet, C. P. (1988). Maternal antibodies against fetal blood group antigens A or B: Lytic activity of IgG subclasses in monocyte-driven cytotoxicity and correlation with ABO haemolytic disease of the newborn. *British Journal of Haematology*, *70*(4), 465–469. https://doi.org/10.1111/j.1365-2141.1988.tb02518.x

Casadevall, A., & Pirofski, L. (2001). Adjunctive Immune Therapy for Fungal Infections. *Clinical Infectious Diseases*. https://doi.org/10.1086/322710

Chen, K., & Cerutti, A. (2011). The function and regulation of immunoglobulin D. *Current Opinion in Immunology*, *23*(3), 345–352. https://doi.org/10.1016/j.coi.2011.01.006

Corthésy, B. (2007). Roundtrip Ticket for Secretory IgA: Role in Mucosal Homeostasis? *The Journal of Immunology*. https://doi.org/10.4049/jimmunol.178.1.27

Dinauer, M. C. (2016). Primary immune deficiencies with defects in neutrophil function. *Hematology*. https://doi.org/10.1182/asheducation-2016.1.43

Dorner, T., Foster, S. J., Farner, N. L., & Lipsky, P. E. (1998). Somatic hypermutation

of human immunoglobulin heavy chain genes: Targeting of RGYW motifs on both DNA strands. *European Journal of Immunology*, *28*(10), 3384–3396. https://doi.org/10.1002/(SICI)1521-4141(199810)28:10<3384::AID-IMMU3384>3.0.CO;2-T

Elluru, S. R., Kaveri, S. V., & Bayry, J. (2015). The protective role of immunoglobulins in fungal infections and inflammation. *Seminars in Immunopathology*. https://doi.org/10.1007/s00281-014-0466-0

Fahey, J. L. (1965). Antibodies and Immunoglobulins: I. Structure and Function. *JAMA: The Journal of the American Medical Association*, *194*(1), 71–74. https://doi.org/10.1001/jama.1965.03090140079020

Farrugia, M., & Baron, B. (2017). The Role of Toll-Like Receptors in Autoimmune Diseases through Failure of the Self-Recognition Mechanism. *International Journal of Inflammation*. https://doi.org/10.1155/2017/8391230

Ferrante, A., Beard, L. J., & Feldman, R. G. (1990). IgG subclass distribution of antibodies to bacterial and viral antigens. *Pediatric Infectious Disease Journal*, *9*(8 SUPPL.).

Galeotti, C., Kaveri, S. V., & Bayry, J. (2017). IVIG-mediated effector functions in autoimmune and inflammatory diseases. *International Immunology*. https://doi.org/10.1093/intimm/dxx039

Galli, S. J., & Tsai, M. (2012). IgE and mast cells in allergic disease. *Nature Medicine*, *18*(5), 693–704. https://doi.org/10.1038/nm.2755

Garcia-Lloret, M., McGhee, S., & Chatila, T. A. (2008). Immunoglobulin Replacement Therapy in Children. *Immunology and Allergy Clinics of North America*. https://doi.org/10.1016/j.iac.2008.07.001

Geisberger, R., Lamers, M., & Achatz, G. (2006). The riddle of the dual expression of IgM and IgD. *Immunology*, *118*(4), 429–437. https://doi.org/10.1111/j.1365-2567.2006.02386.x

Gelfand, E. W., Ochs, H. D., & Shearer, W. T. (2013). Controversies in IgG replacement therapy in patients with antibody deficiency diseases. *Journal of Allergy and Clinical Immunology*. https://doi.org/10.1016/j.jaci.2013.02.028

Gould, H. J., & Sutton, B. J. (2008). IgE in allergy and asthma today. *Nature Reviews Immunology*, *8*(3), 205–217. https://doi.org/10.1038/nri2273

Grönwall, C., Vas, J., & Silverman, G. J. (2012). Protective roles of natural IgM antibodies. *Frontiers in Immunology*, *3*(APR). https://doi.org/10.3389/fimmu.2012.00066

Gupta, M., Noel, G. J., Schaefer, M., Friedman, D., Bussel, J., & Johann-Liang, R. (2001). Cytokine modulation with immune γ-globulin in peripheral blood of normal children and its implications in Kawasaki disease treatment. *Journal of Clinical Immunology*. https://doi.org/10.1023/A:1011039216251

Jang, J. E., Hidalgo, A., & Frenette, P. S. (2012). Intravenous immunoglobulins modulate neutrophil activation and vascular injury through fcγRIII and SHP-1. *Circulation Research*. https://doi.org/10.1161/CIRCRESAHA.112.266411

JEFFERIS, R., & KUMARARATNE, D. S. (2008). Selective IgG subclass deficiency: quantification and clinical relevance. *Clinical & Experimental Immunology*, *81*(3), 357–367. https://doi.org/10.1111/j.1365-2249.1990.tb05339.x

Kaneko, Y., Nimmerjahn, F., & Ravetch, J. V. (2006). Anti-inflammatory activity of immunoglobulin G resulting from Fc sialylation. *Science*. https://doi.org/10.1126/science.1129594

Kantha, S. S. (1991). A Centennial Review; the 1890 Tetanus Antitoxin Paper of von Behring and Kitasato and the Related Developments. *The Keio Journal of Medicine*, *40*(1), 35–39. https://doi.org/10.2302/kjm.40.35

Kaplan, M. J., & Radic, M. (2012). Neutrophil Extracellular Traps: Double-Edged Swords of Innate Immunity. *The Journal of Immunology*. https://doi.org/10.4049/jimmunol.1201719

Kerr, J., Quinti, I., Eibl, M., Chapel, H., Späth, P. J., Sewell, W. A. C., … Peter, H. H. (2014). Is dosing of therapeutic immunoglobulins optimal? A review of a three-decade long debate in Europe. *Frontiers in Immunology*. https://doi.org/10.3389/fimmu.2014.00629

Krivan, G., Jolles, S., Granados, E. L., Paolantonacci, P., Ouaja, R., Cissé, O. A., & Bernatowska, E. (2017). New insights in the use of immunoglobulins for the management of immune deficiency (PID) patients. *American Journal of Clinical and Experimental Immunology*.

Lanternier, F., Cypowyj, S., Picard, C., Bustamante, J., Lortholary, O., Casanova, J. L., & Puel, A. (2013). Primary immunodeficiencies underlying fungal infections. *Current Opinion in Pediatrics*.

https://doi.org/10.1097/MOP.0000000000000031

Li, Z., Woo, C. J., Iglesias-Ussel, M. D., Ronai, D., & Scharff, M. D. (2004). The generation of antibody diversity through somatic hypermutation and class switch recombination. *Genes and Development*, *18*(1), 1–11. https://doi.org/10.1101/gad.1161904

Little, A. J., Matthews, A., Oettinger, M., Roth, D. B., & Schatz, D. G. (2014). The Mechanism of V(D)J Recombination. In *Molecular Biology of B Cells: Second Edition* (pp. 13–34). https://doi.org/10.1016/B978-0-12-397933-9.00002-3

Lünemann, J. D., Nimmerjahn, F., & Dalakas, M. C. (2015). Intravenous immunoglobulin in neurology-mode of action and clinical efficacy. *Nature Reviews Neurology*. https://doi.org/10.1038/nrneurol.2014.253

Maizels, N. (2005). Immunoglobulin Gene Diversification. *Annual Review of Genetics*, *39*(1), 23–46. https://doi.org/10.1146/annurev.genet.39.073003.110544

Mawas, F., Wiener, E., Williamson, L. M., & Rodeck, C. H. (2009). Immunoglobulin G subclasses of anti-human platelet antigen la in maternal sera: relation to the severity of neonatal alloimmune thrombocytopenia. *European Journal of Haematology*, *59*(5), 287–292. https://doi.org/10.1111/j.1600-0609.1997.tb01688.x

Netea, M. G., Joosten, L. A. B., Latz, E., Mills, K. H. G., Natoli, G., Stunnenberg, H. G., … Xavier, R. J. (2016). Trained immunity: A program of innate immune memory in health and disease. *Science*. https://doi.org/10.1126/science.aaf1098

Netea, M. G., & Van Der Meer, J. W. M. (2011). Immunodeficiency and genetic defects of pattern-recognition receptors. *New England Journal of Medicine*. https://doi.org/10.1056/NEJMra1001976

Nimmerjahn, F., & Ravetch, J. V. (2008). Anti-Inflammatory Actions of Intravenous Immunoglobulin. *Annual Review of Immunology*. https://doi.org/10.1146/annurev.immunol.26.021607.090232

Nouri-Aria, K. T., Wachholz, P. A., Francis, J. N., Jacobson, M. R., Walker, S. M., Wilcock, L. K., … Durham, S. R. (2004). Grass Pollen Immunotherapy Induces Mucosal and Peripheral IL-10 Responses and Blocking IgG Activity. *The Journal of Immunology*, *172*(5), 3252–3259. https://doi.org/10.4049/jimmunol.172.5.3252

Orange, J. S., Hossny, E. M., Weiler, C. R., Ballow, M., Berger, M., Bonilla, F. A., … Cunningham-Rundles, C. (2006). Use of intravenous immunoglobulin in human disease: A review of evidence by members of the Primary Immunodeficiency Committee of the American Academy of Allergy, Asthma and Immunology. *Journal of Allergy and Clinical Immunology*. https://doi.org/10.1016/j.jaci.2006.01.015

Porter, R. R. (1973). Structural studies of immunoglobulins. *Science (New York, N.Y.)*, *180*(4087), 713–716. https://doi.org/10.1126/science.180.4087.713

Qureshi, O. S., Rowley, T. F., Junker, F., Peters, S. J., Crilly, S., Compson, J., … Humphreys, D. P. (2017). Multivalent Fcγ-receptor engagement by a hexameric Fc-fusion protein triggers Fcγ-receptor internalisation and modulation of Fcγ-receptor functions. *Scientific Reports*. https://doi.org/10.1038/s41598-017-17255-8

Rada, C., Ehrenstein, M. R., Neuberger, M. S., & Milstein, C. (1998). Hot spot focusing of somatic hypermutation in MSH2-deficient mice suggests two stages of mutational targeting. *Immunity*, *9*(1), 135–141. https://doi.org/10.1016/S1074-7613(00)80595-6

Riesbeck, K., & Nordström, T. (2006). Structure and immunological action of the human pathogen Moraxella catarrhalis IgD-binding protein. *Critical Reviews in Immunology*, *26*(4), 353–376.

Savva, A., & Roger, T. (2013). Targeting Toll-like receptors: Promising therapeutic strategies for the management of sepsis-associated pathology and infectious diseases. *Frontiers in Immunology*. https://doi.org/10.3389/fimmu.2013.00387

Schroeder, H. W. J., & Cavacini, L. (2010). Structure and Function of Immunoglobulins (author manuscript). *Journal of Allergy and Clinical Immunology*. https://doi.org/10.1016/j.jaci.2009.09.046.Structure

Schwab, I., & Nimmerjahn, F. (2013). Intravenous immunoglobulin therapy: How does IgG modulate the immune system? *Nature Reviews Immunology*. https://doi.org/10.1038/nri3401

Shimoni, Z., Bulvik, S., & Froom, P. (2013). Intravenous immune globulin in autoimmune and inflammatory diseases. *New England Journal of Medicine*. https://doi.org/10.1056/NEJMc1215489

Sondermann, P., Pincetic, A., Maamary, J., Lammens, K., & Ravetch, J. V. (2013).

General mechanism for modulating immunoglobulin effector function. *Proceedings of the National Academy of Sciences of the United States of America*, *110*(24), 9868–9872. https://doi.org/10.1073/pnas.1307864110

Stavnezer, J., & Schrader, C. E. (2014). IgH Chain Class Switch Recombination: Mechanism and Regulation. *The Journal of Immunology*, *193*(11), 5370–5378. https://doi.org/10.4049/jimmunol.1401849

Stewart, J. (2012). Immunological principles: Antigens and antigen recognition. In *Medical Microbiology: Eighteenth Edition* (pp. 98–108). https://doi.org/10.1016/B978-0-7020-4089-4.00023-8

Stubbe, H., Berdoz, J., Kraehenbuhl, J.-P., & Corthésy, B. (2000). Polymeric IgA Is Superior to Monomeric IgA and IgG Carrying the Same Variable Domain in Preventing Clostridium difficile Toxin A Damaging of T84 Monolayers . *The Journal of Immunology*, *164*(4), 1952–1960. https://doi.org/10.4049/jimmunol.164.4.1952

The Nobel Prize in Physiology or Medicine 1901 - NobelPrize.org. (n.d.).

The Nobel Prize in Physiology or Medicine 1972. (n.d.).

Tiselius, A., & Kabat, E. A. (1939). An electrophoretic study of immune sera and purified antibody preparations. *Journal of Experimental Medicine*, *69*(1), 119–132. https://doi.org/10.1084/jem.69.1.119

Tonegawa, S. (1983). Somatic generation of antibody diversity. *Nature*, *302*(5909), 575–581. https://doi.org/10.1038/302575a0

Vidarsson, G., Dekkers, G., & Rispens, T. (2014). IgG subclasses and allotypes: From structure to effector functions. *Frontiers in Immunology*, *5*(OCT). https://doi.org/10.3389/fimmu.2014.00520

Vidarsson, G., Sigurdardottir, S. T., Gudnason, T., Kjartansson, S., Kristinsson, K. G., Ingolfsdottir, G., … Jonsdottir, I. (1998). Isotypes and opsonophagocytosis of pneumococcus type 6B antibodies elicited in infants and adults by an experimental pneumococcus type 6B- tetanus toxoid vaccine. *Infection and Immunity*, *66*(6), 2866–2870.

Williams, A. F., & Barclay, A. N. (1988). The immunoglobulin superfamily - Domains for cell surface recognition. *Annual Review of Immunology*, *6*, 381–405.

Woof, J. M., & Mestecky, J. (2015). Mucosal Immunoglobulins. In *Mucosal Immunology: Fourth Edition* (Vol. 1–2, pp. 287–324). https://doi.org/10.1016/B978-0-12-415847-4.00017-3

A. Cell Culture Media, Buffers and Solutions

RPMI 1640 cell culture medium

10% (regular complete medium): 50 ml heat inactivated FBS

2% (wash medium): 10 ml heat inactivated FBS

2% (medium for NETosis assay): 10 ml DNase inactivated FBS (at 65°)

500 ml RPMI 1640

5 ml Penicillin/Streptomycin

5 ml Sodium Pyruvate

5 ml HEPES

5 ml non-essential amino acid

2% FBS Containing RPMI 1640 (Wash medium)

500 ml of RPMI 1640

10 ml heat inactivated FBS

5 ml Penicillin/Streptomycin

5 ml Sodium Pyruvate

5 ml HEPES

5ml non-essential amino acid

Ammonium-Chloride-Potassium (ACK) Lysis Buffer

154.4 mM ammonium chloride (8.26 g)

10 mM potassium bicarbonate (1.0 g)

97.3 μM EDTA tetrasodium salt (0.037 g EDTA in 1 L of ultrapure water)

Sodium Bicarbonate Coating Buffer (pH=9.5)

8.4 g $NaHCO_3$

3.56 g Na_2CO_3

Deionized water to 1.0 L

10X PBS

80 g NaCl

2 g KCl

8,01 g $Na_2HPO_4.2H_2O$

2 g KH_2PO_4

Complete to 1L with dH_2O (pH=6.8)

Blocking Buffer

5 g BSA (1%)

250 µl Tween20

500 ml 1X PBS (pH=7.2)

Wash Buffer (ELISA)

500 ml 10X PBS

2.5 ml Tween20

4.5 L dH_2O

T-cell Buffer (ELISA)

25 ml FBS

250 µl Tween20

500 ml 1X PBS

B. Flow Cytometric Analysis of ROS Production in Neutrophils and in Trained THP1-Dual Cells

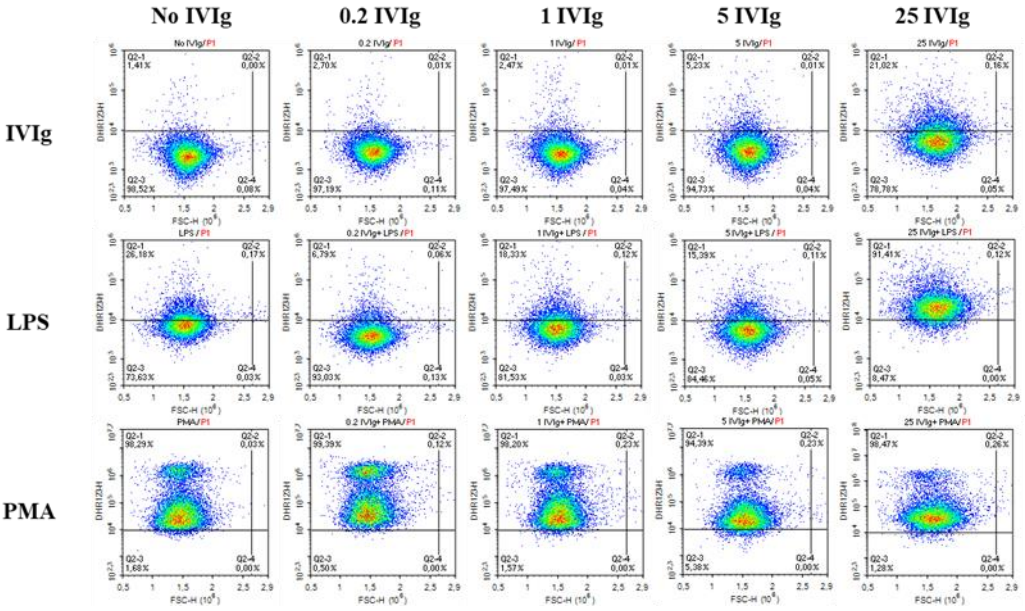

Figure B.1. Representative density plots showing ROS production of neutrophils following stimulation in the presence of different IVIg concentrations.

DHR123 straining was performed and the cells were analyzed by flow cytometer. Density plots show $DHR123^{+}$ cell percentages.

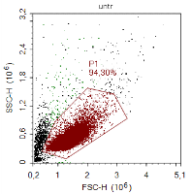

Untreated

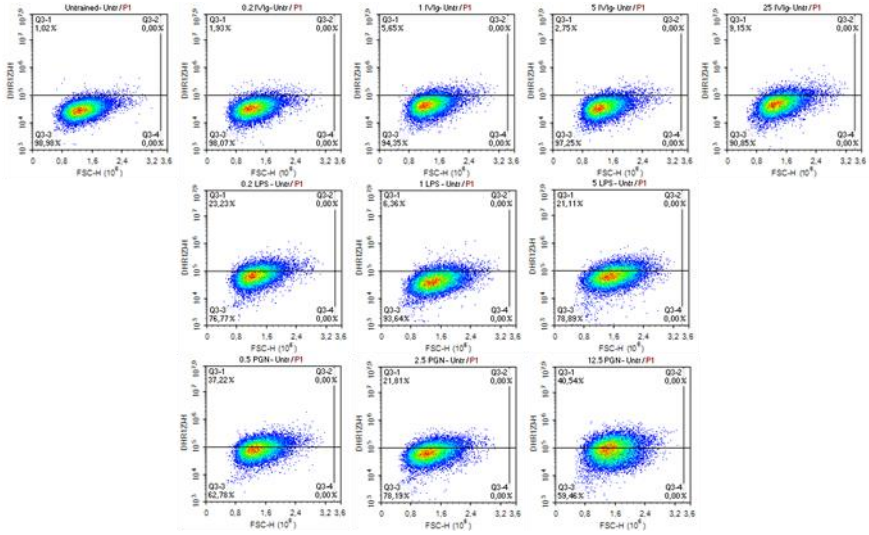

LPS

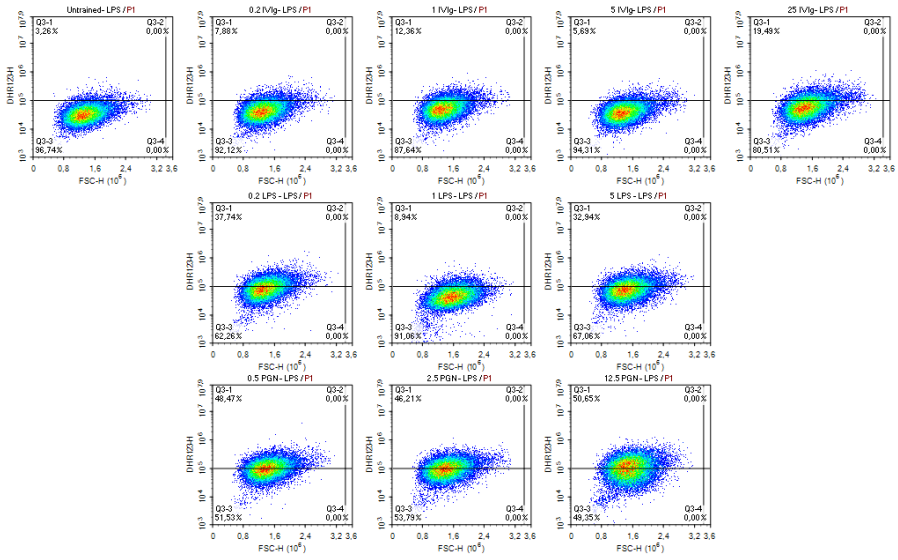

Zymosan

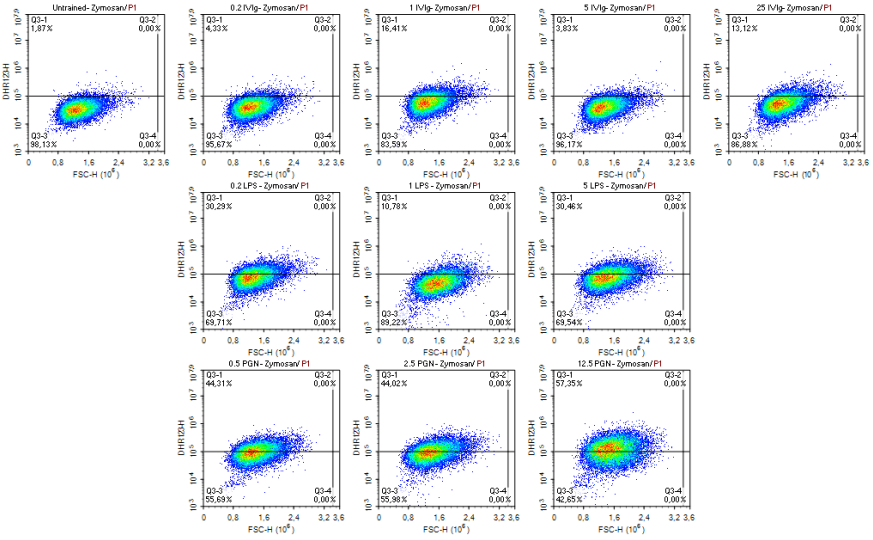

Opsonized HKCA

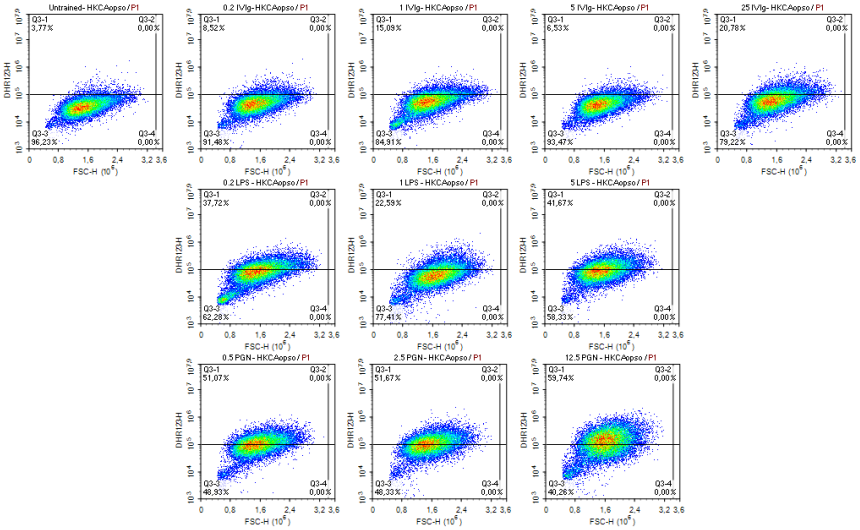

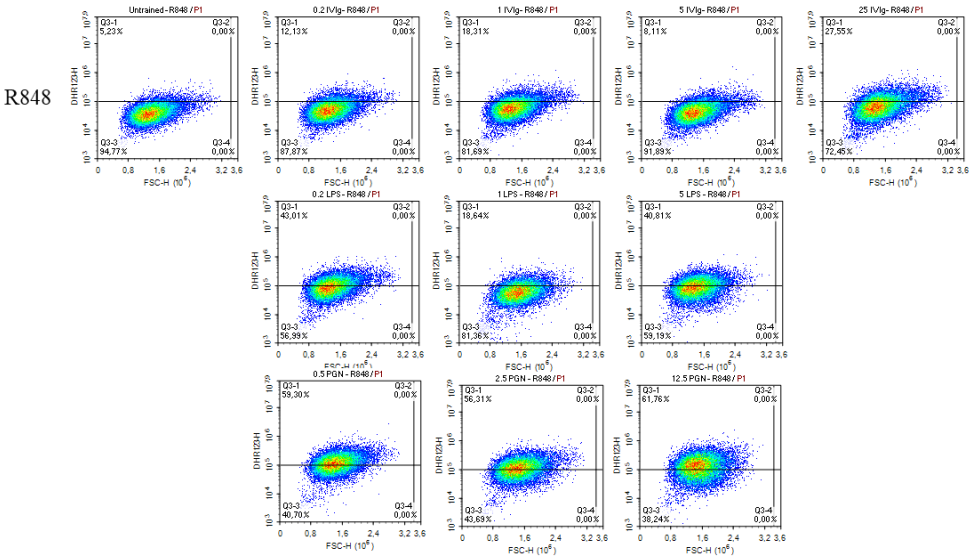

Figure B.2. Density plots representing ROS levels ($DHR123^+$ cell percentages) upon TLR ligand stimulation of trained and untrained cells.

DHR123 straining was performed and the cells were analyzed by flow cytometery. Density plots show $DHR123^+$ cell percentages.

C. Neutrophil Viability

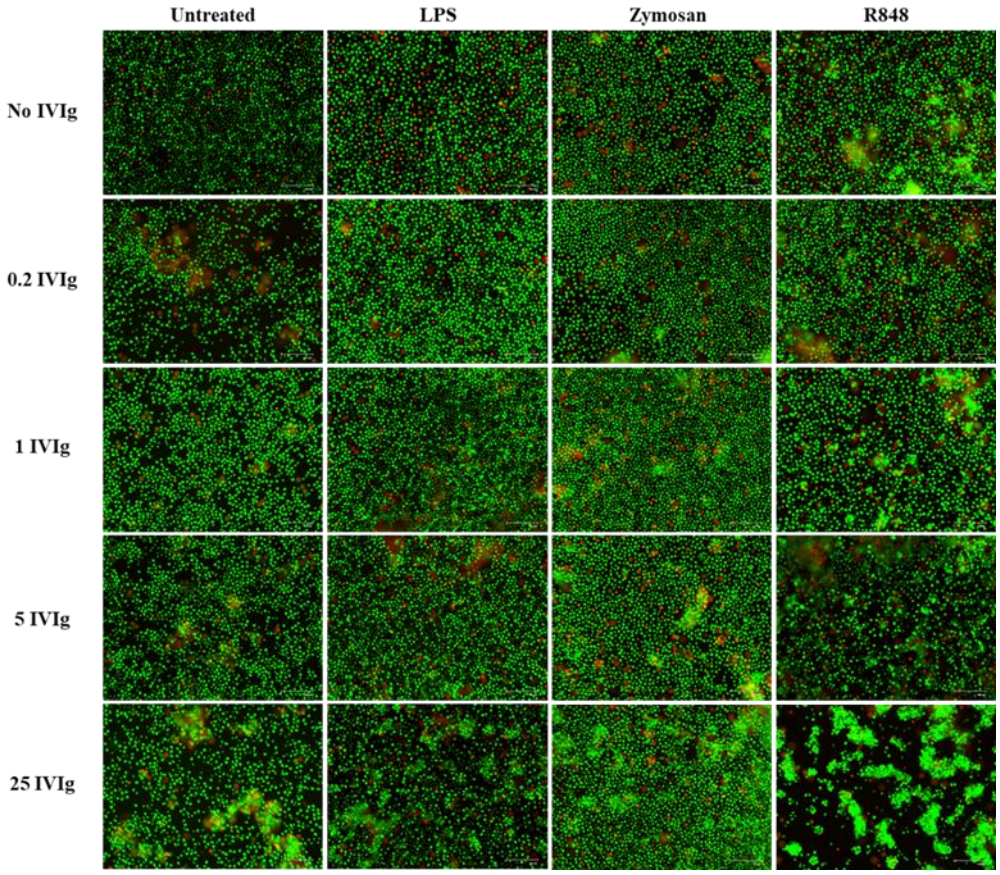

Figure C.1. Fluorescent microscopy images of viable neutrophils.

Nucleic acid probes Syto16 Green and Sytox Orange were used to stain the cells. Live cells are stained green, whereas dead cells appear orange/yellow. Magnification is 20x.

D. Light Microscopy Images of Trained THP1-Dual Cells

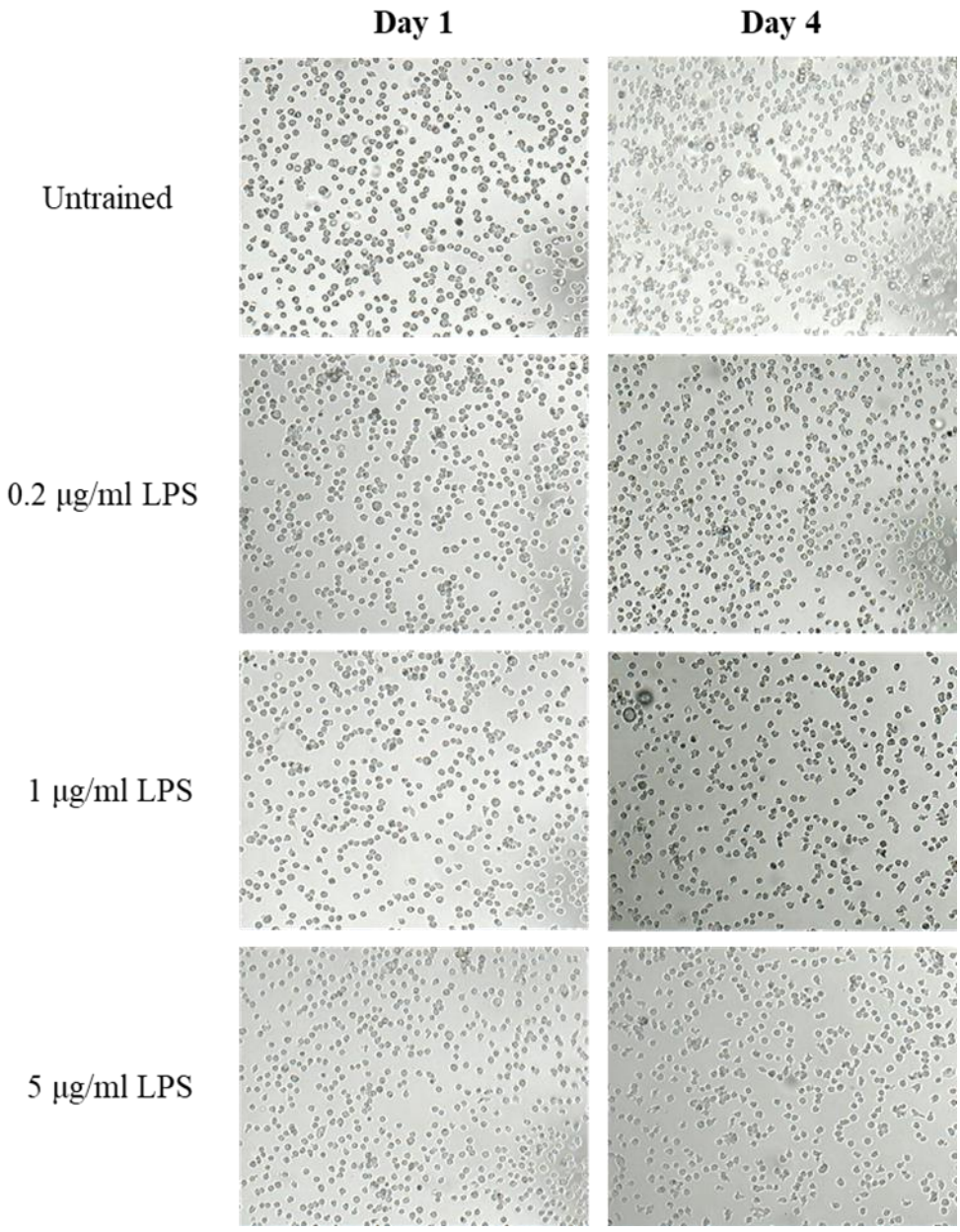

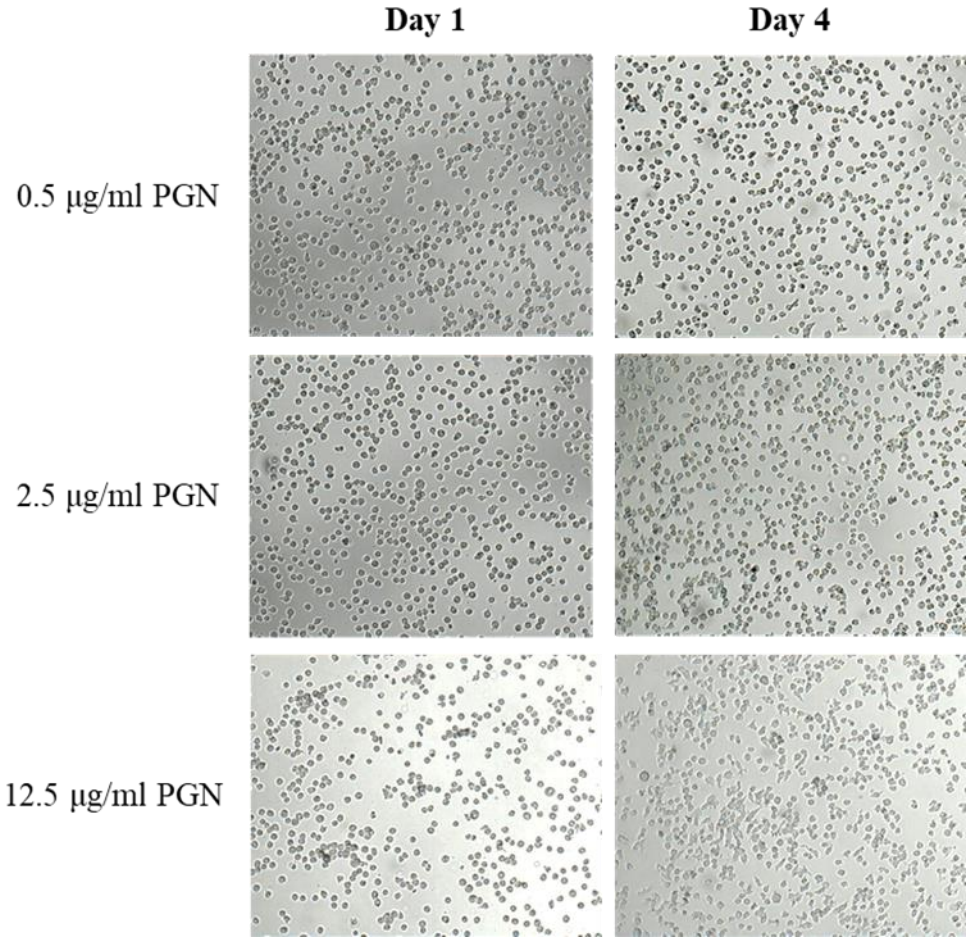
Day 1
Day 4
0.5 µg/ml PGN
2.5 µg/ml PGN
12.5 µg/ml PGN

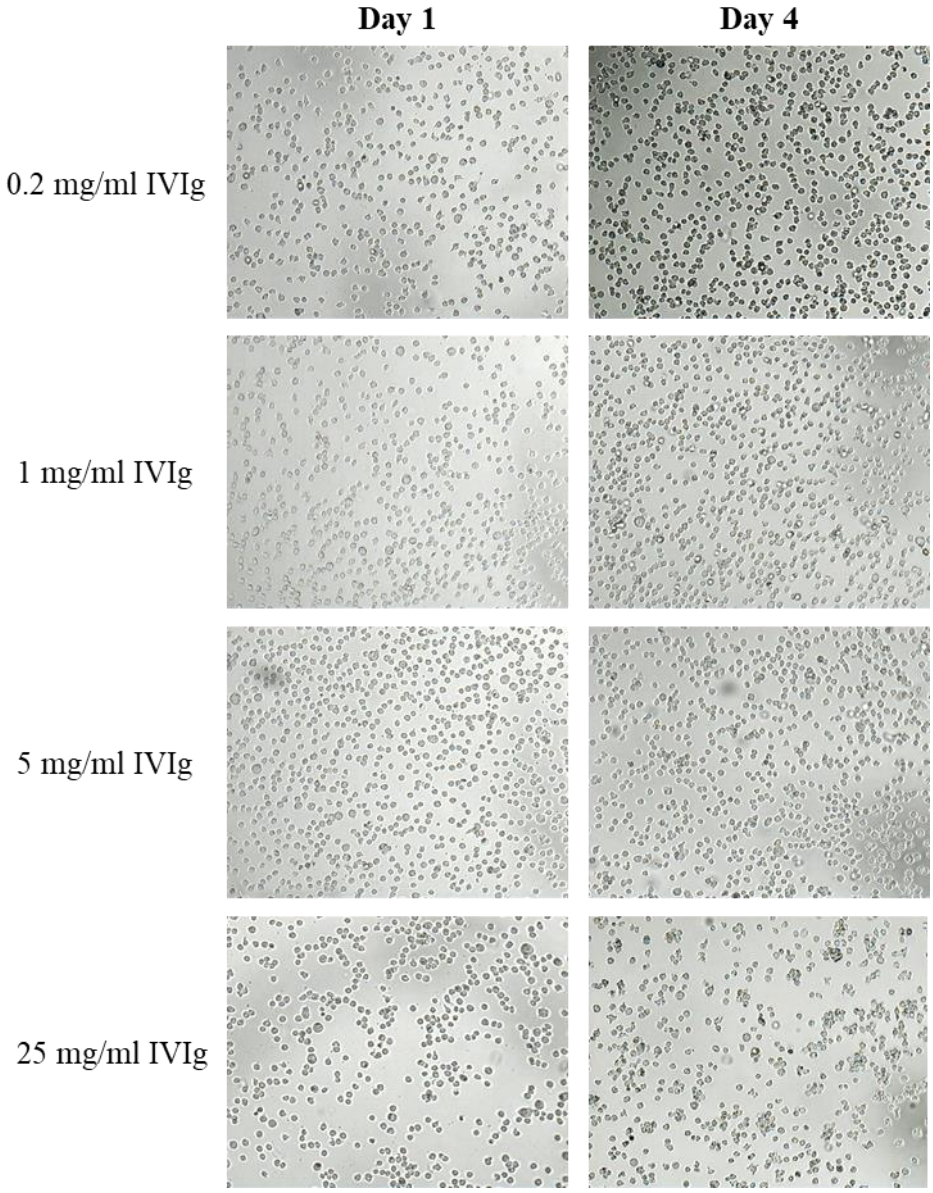

Figure D.1. Light microcopy images of trained cells.

Images were taken on Day 1 and Day 4. Magnification 4x.

Copyright Clearance Center

Note: Copyright.com supplies permissions but not the copyrighted content itself.

1 PAYMENT 2 REVIEW 3 CONFIRMATION

Step 3: Order Confirmation

Thank you for your order! A confirmation for your order will be sent to your account email address. If you have questions about your order, you can call us 24 hrs/day, M-F at +1.855.239.3415 Toll Free, or write to us at info@copyright.com. This is not an invoice.

Confirmation Number: 11849593
Order Date: 09/10/2019

If you paid by credit card, your order will be finalized and your card will be charged within 24 hours. If you choose to be invoiced, you can change or cancel your order until the invoice is generated.

Payment Information

Busranur Geckin
bsrnrgckn@gmail.com
+90 (530)4730513
Payment Method: n/a

Order Details

Nature Reviews Immunology

Order detail ID:	72005041
Order License Id:	4665270057380
ISSN:	1474-1741
Publication Type:	e-Journal
Volume:	
Issue:	
Start page:	
Publisher:	NATURE PUBLISHING GROUP

Permission Status: Granted
Permission type: Republish or display content
Type of use: Thesis/Dissertation

Requestor type	Academic institution
Format	Print, Electronic
Portion	chart/graph/table/figure
Number of charts/graphs/tables/figures	2
The requesting person/organization	Busranur Geckin
Title or numeric reference of the portion(s)	Figure 2, Figure 4
Title of the article or chapter the portion is from	Discriminating self from non-self in nucleic acid sensing
Editor of portion(s)	N/A
Author of portion(s)	N/A
Volume of serial or monograph	N/A

Title:	Structure and function of immunoglobulins
Author:	Harry W. Schroeder,Lisa Cavacini
Publication:	Journal of Allergy and Clinical Immunology
Publisher:	Elsevier
Date:	February 2010

Order Completed

Thank you for your order.

This Agreement between Busranur Geckin ("You") and Elsevier ("Elsevier") consists of your license details and the terms and conditions provided by Elsevier and Copyright Clearance Center.

Your confirmation email will contain your order number for future reference.

printable details

License Number	4665290049469
License date	Sep 10, 2019
Licensed Content Publisher	Elsevier
Licensed Content Publication	Journal of Allergy and Clinical Immunology
Licensed Content Title	Structure and function of immunoglobulins
Licensed Content Author	Harry W. Schroeder,Lisa Cavacini
Licensed Content Date	Feb 1, 2010
Licensed Content Volume	125
Licensed Content Issue	2
Licensed Content Pages	12
Type of Use	reuse in a thesis/dissertation
Portion	figures/tables/illustrations
Number of figures/tables/illustrations	1
Format	both print and electronic
Are you the author of this Elsevier article?	No
Will you be translating?	No
Original figure numbers	Figure 1
Title of your thesis/dissertation	CHARACTERIZATION OF INTRAVENOUS IMMUNOGLOBULIN-MEDIATED FUNCTIONAL CHANGES IN INNATE IMMUNE CELLS
Publisher of new work	Middle East Technical University
Expected completion date	Sep 2019
Estimated size (number of pages)	1
Requestor Location	Busranur Geckin METU, Department of Biological Sciences, Lab B-58 Ankara, other Turkey Attn:
Publisher Tax ID	GB 494 6272 12
Total	0.00 USD

ORDER MORE CLOSE WINDOW